Review of medium to long term coastal risks associated with British Energy sites: Climate Change Effects - Final Report

Prepared for British Energy Generation Ltd

Authors:	Mark L Gallani
Reviewed by:	Rob Harrison and Mo Mylne
Authorised for issue by:	Nick Roberts, Business Development

22 February 2007

Met Office ref.: CPM/2006/C001C/P176/1

Met Office FitzRoy Road Exeter Devon EX1 3PB
Tel 0870 900 0100 Fax 0870 900 5050 www.metoffice.gov.uk

Contents

1. Executive Summary

1.1 This report is designed to give an overview of UK climate change, and fulfils the requirements for the project "Review of medium to long term coastal risks associated with British Energy sites: Climate Change Effects", contract number 40199260. It covers the magnitude of predicted change in the UK's climate for several variables for the next 100 years, for four British Energy sites in addition to the four British Energy sites selected for Stage 3 of the project "Major Effects of Global Warming on UK Nuclear Sites", ref. EE/GNSR/5039, contract number BWD/40069464.

1.2 The Met Office Regional Climate Model predicts that seasonal average temperatures will increase significantly for all the sites, with the greatest increases seen in the summer and for sites in the south of the UK. Daily maximum temperatures will also increase significantly, generally in both the mean and at the extreme (warm) tail of the distribution, although some sites see little change in the distribution about the mean in winter. In summer for all sites the mean and extreme temperatures increase. Consequently unprecedented maximum temperatures will be experienced in the 2080s. Conversely, frosts will diminish in frequency.

1.3 Seasonal average precipitation amounts are predicted to increase in winter and to decrease in summer for all the sites examined. In general, extreme precipitation amounts are predicted to increase for events of duration from one hour up to twelve hours, and for return periods from two years up to very rare events with return periods of one hundred years and more.

1.4 In general the seasonal average wind speeds are predicted to increase during winter and decrease during summer, but with some exceptions, e.g. Dungeness where wind speeds are predicted to increase in both winter and summer. The Met Office's HadRM3 Regional Climate Model predicts that extreme hourly winds and extreme gusts will be slightly higher in future for all the sites studied, but the increases only range from just under 2% for Torness to 6% for Hinkley Point.

1.5 Mean sea level increases in themselves are not thought to be a major future hazard, but contribute to increases in future surge heights of potentially as much as 1.7 metres in places.

2. Introduction

2.1 The reports for stages 1, 2 and 3 of project "Major Effects of Global Warming on UK Nuclear Sites", ref. EE/GNSR/5039, contract number BWD/40069464 covered observed and predicted climate change both for the globe as a whole and for the UK, and predicted climate change for the following sites: Calder Hall, Dungeness, Hartlepool, Hunterston and Sizewell. This new report is intended to give similar information (but without consideration of the site specific flood defence and coastal geohazard implications, which are being dealt with by a separate study) for British Energy's other nuclear power station sites, i.e. Heysham, Hinkley Point, Bradwell and Torness, in addition to the sites previously covered (excluding Calder Hall).

2.2 Figure 2.1 shows the location of all the UK's civilian nuclear power stations, both in operation and in decommissioning, so that the local climatic changes shown later can be interpreted more easily. Note that Calder Hall is on the same site as Sellafield.

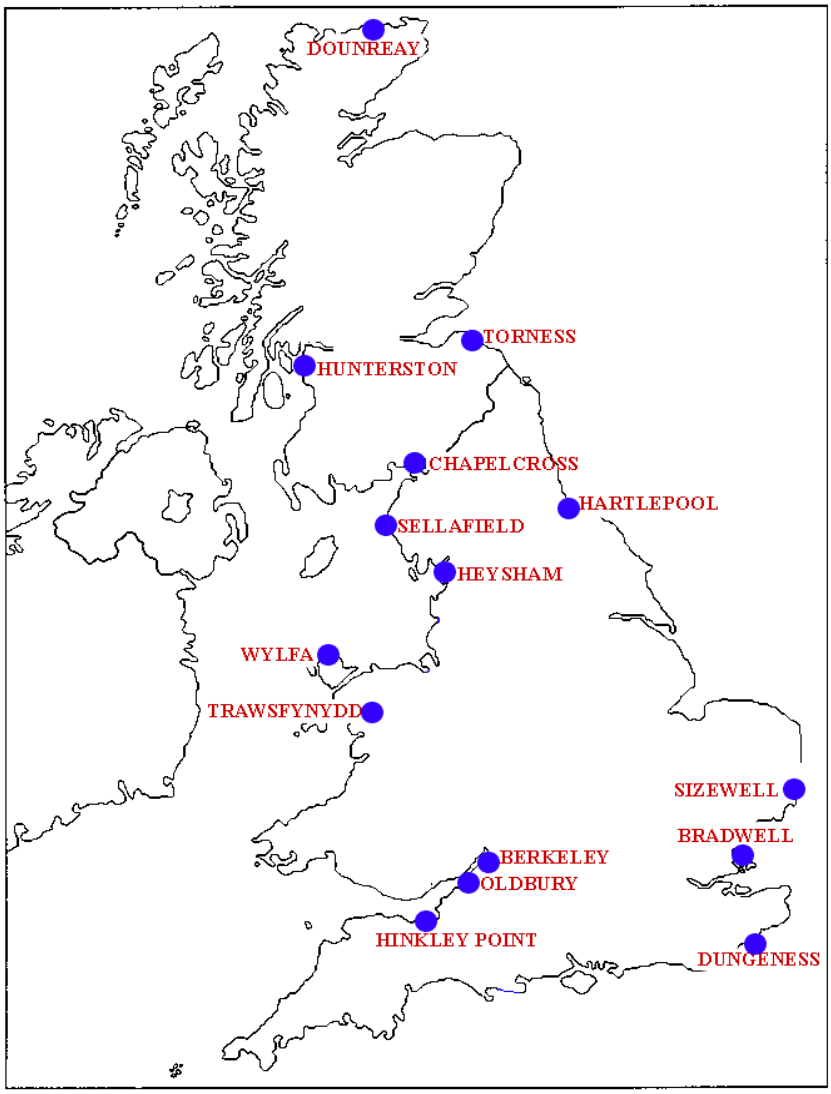

Figure 2.1. Location of UK civilian nuclear power stations and other nuclear facilities.

2.3 Where possible, predicted changes are shown for the 2020s, 2050s and 2080s, (each 'timeslice' representing the mean of a period of three decades) and for

several scenarios of future changes. These scenarios are known as low, medium-low, medium-high and high. They correspond to IPCC emissions scenarios (IPCC 2000) B1, B2, A2 and A1FI (respectively) referred to in the stage 1 report of the previous project. None of these scenarios is judged to be any more or less likely than the others.

2.4 Most of the climate change diagrams in this report are derived from the Met Office's Hadley Centre climate change simulations that used the HadRM3 Regional Climate Model. It has a resolution of about 50km in both the north-south and east-west directions. Figure 2.2 shows how the 50km gridboxes correspond to the geography of the British Isles. Areas shown with a black outline box are treated as land points by the climate model while those not outlined in black are sea. Changes in temperature, precipitation and wind speed are presented in this report as a panel of images. In each case the figures are arranged with the low to high scenario predictions in columns from left to right while the three timeslices are presented with the 2020s as the upper row, the 2050s in the middle row and the 2080s in the lower row. Thus, the top left image in these panels depicts the predicted change for the 2020s under the Low emissions scenario while the lower right image shows predicted changes for the 2080s under the High emission scenario. The mapped images of climate change in this report show the changes expected for the sea gridboxes near the sites as well as for the land gridboxes. They also show a detailed coastline, much more detailed than the coastline represented in the HadRM3 model.

Figure 2.2: the 50km resolution grid of land points in the HadRM3 regional climate model, overlaid on a map of the British Isles.

Climate change modelling and Uncertainty

2.5 The climate change information assessed in this study comes mainly from one climate model, the Hadley Centre regional climate model HadRM3. There are uncertainties in the predictions of future climate due to unknown future greenhouse gas emissions, uncertainties in the models used to simulate climate

change, and because of natural variability. The effect of different emissions scenarios is simulated by HadRM3 and included in this study. Natural climate variations occur on a range of timescales. For a given future period, the natural variability may either add to or subtract from any anthropogenic climate change. Consequently, climate model simulations made with the same climate model and set of emissions, but different plausible initial conditions, will predict a range of future climates. Climate model uncertainty arises from choices made when models are designed, such as the spatial scales that they can represent and the manner in which physical processes of the atmosphere, ocean and land surface are represented. Modelling uncertainty results in differing projections of future climate even if the same global emissions scenario is used to 'force' the models. Modelling uncertainty can be qualitatively assessed by comparing the projections from a range of climate models that have been designed and built by different climate modelling centres.

Future work

2.6 Many of the problems regarding uncertainty in climate model projections are being addressed as part of UKCIP08, which is the Defra-funded project to make climate projections for the UK available to a wide community of climate impacts data users. The climate projections will be created by the Hadley Centre, and access and communication will be facilitated by the UK Climate Impacts Programme (UKCIP). The new UKCIP08 climate projections (containing results at 25km resolution) will be available for a range of emissions scenarios and will include an assessment of model uncertainty and natural variability. It is recommended that a similar study should be carried out after the UKCIP08 scenarios become available in 2008. It is also recommended that future studies should build on the probability estimates planned for UKCIP08, and should be aimed at providing the information required for risk-based planning calculations. Similar studies should be carried out periodically after subsequent improvements in regional climate model predictions, which generally occur every 5 to 6 years or so.

3. Predicted Temperature Changes

3.1 Daily maximum temperature changes for Heysham are presented in figures 3.1 and 3.2. As previously described, figure 3.1 shows the predicted changes in average summer (June-August) daily maximum temperature corresponding to low, medium-low, medium-high and high emissions scenarios (columns, left to right), for three periods centred on the 2020s, 2050s and 2080s (rows, top to bottom), relative to the simulated 1961-90 climate. It can be seen that, in the Heysham region, by the **2020s** for the Low scenario the summer average daily maximum temperature will have risen by between 0.5 and 1 °C. For the High scenario, the summer average daily maximum temperature is predicted to rise by between 4.5 and 5.0 °C by the 2080s.

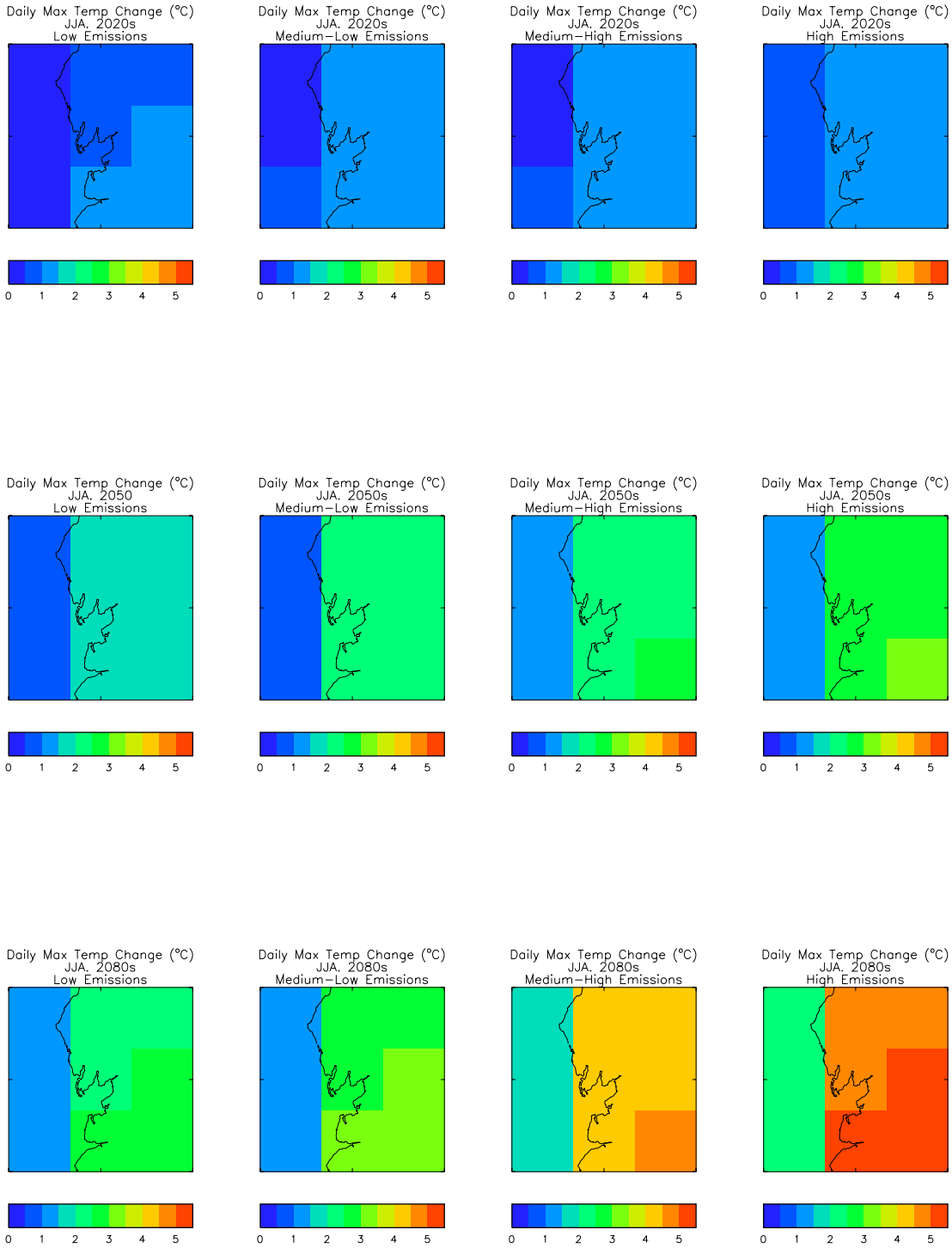

Figure 3.1. Predicted changes (°C), in Heysham summer (June-August) average maximum temperatures (relative to the simulated 1961-90 climate) for four emissions scenarios (Low - left column, High – right column), for thirty-year periods centred on the 2020s, 2050s and 2080s (rows, top to bottom).

3.2 While average summer maximum temperatures are predicted to increase by up to 4.5 °C by the 2080s under the Medium-High emissions scenario, figure 3.2 illustrates the change for that scenario in the distribution of temperatures for the Heysham region. The lower panel shows that the range of temperatures which

may be experienced in a summer season also increases, as do the extremes of the distribution. In the model control climate in this region, summer temperatures rarely exceed 26 °C (and never exceed 38 °C) but under this scenario of change, a temperature of 24 °C or greater is experienced on a quarter of all days during the season (see figure A2.1 in Appendix 2), and modelled 2080s temperatures occasionally reach 47 °C. During the other seasons daily maximum temperature increases are predicted to be more modest with an increase in average daily maximum temperatures for winter (December to February) of no more than 2.5°C by the 2080s under the High scenario of forcing (see Appendix 3). Again the extreme daily maxima increase although the distribution of temperatures about the contemporary average during the season remains similar to present day climate (see figure 3.2). Days are still likely to occur when temperatures do not rise above 0°C in the Heysham region but this will become increasingly rare.

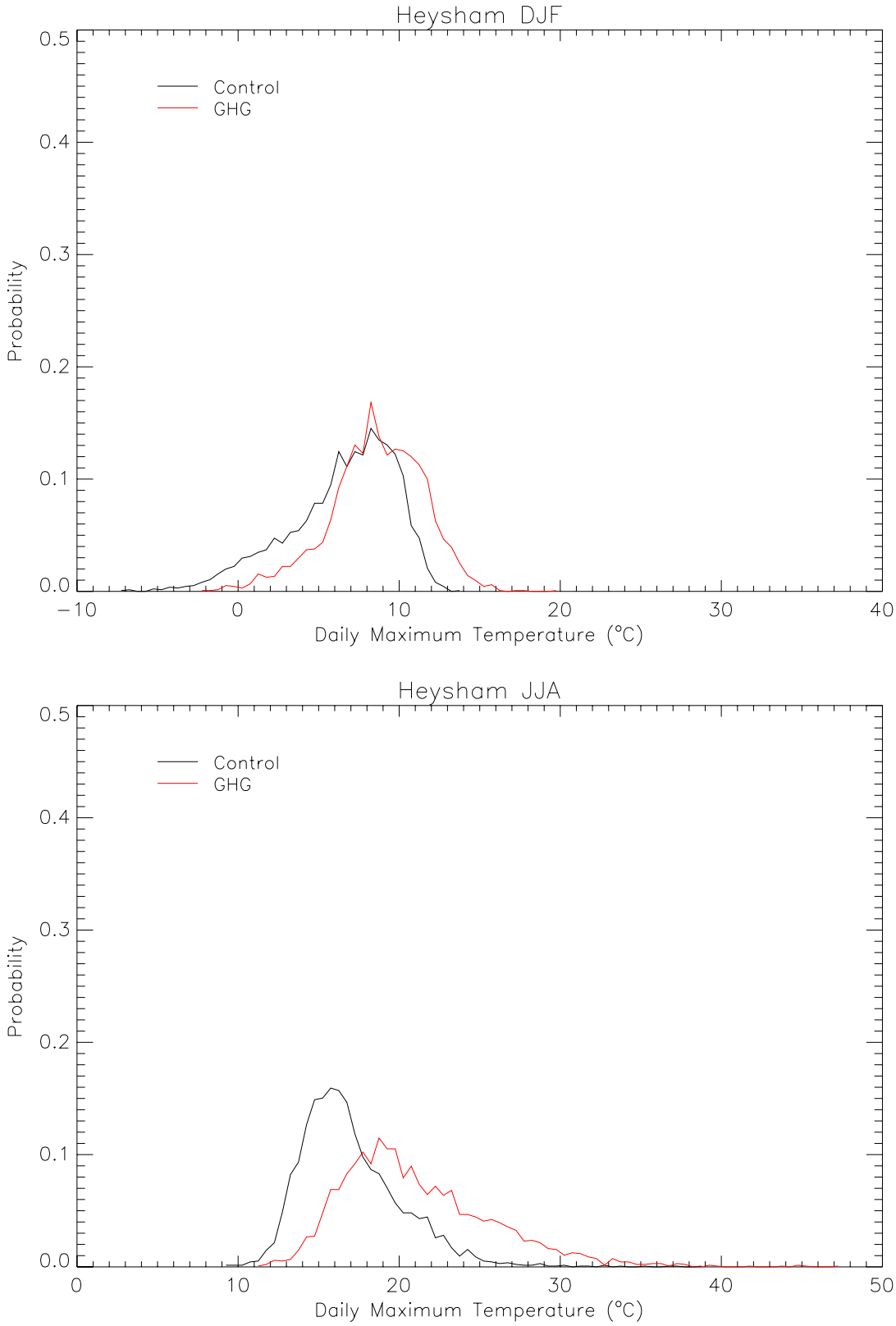

Figure 3.2: Frequency distribution for daily maximum temperature thresholds for Heysham in winter (December – February, upper panel) and summer (June – August, lower panel), for the control (1961-1990, black line) and Medium-High 2080s (red line) climates.

3.3 It can be seen in figure 3.3 that, in the Hinkley Point region, by the **2020s** for the Low scenario the summer average daily maximum temperature will have risen by between 1.0 and 1.5 °C. For the High scenario, the summer average daily maximum temperature is predicted to rise by over 5.0 °C by the 2080s. Figure 3.4 shows the frequency distribution of daily maximum temperatures attained

during the summer season (lower panel) in both the modelled present day and future (2080s under the medium-high scenario) climates. As the average daily maximum temperature increases the shape of the distribution of maximum temperatures also changes with the range of probable daily maximums experienced in a summer season tending to increase. Under present day climate (modelled) it is rare that a summertime daily maximum temperature of more than 30 °C is experienced in the Hinkley Point region, less than five days per year on average. By the 2080s such daily maximum temperatures will be exceeded much more frequently, more than twenty percent of summer days will be warmer than this threshold, and an average year will see at least one day when temperatures rise to over 40 °C, see Appendix 2, figure A2.2.

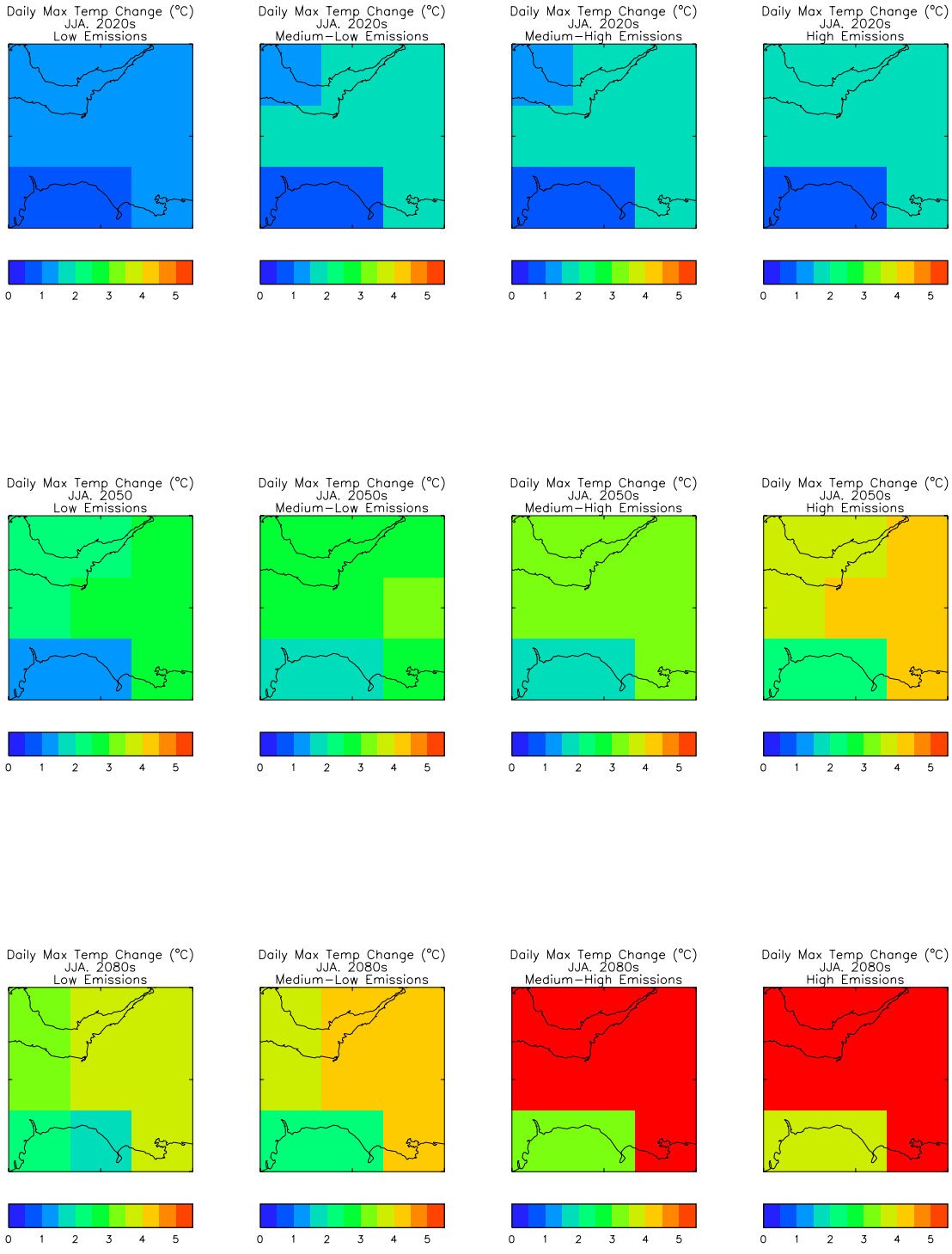

Figure 3.3. Predicted changes (°C), in Hinkley Point summer (June-August) average maximum temperatures (relative to the simulated 1961-90 climate) for four emissions scenarios (Low - left column, High – right column), for thirty-year periods centred on the 2020s, 2050s and 2080s (rows, top to bottom).

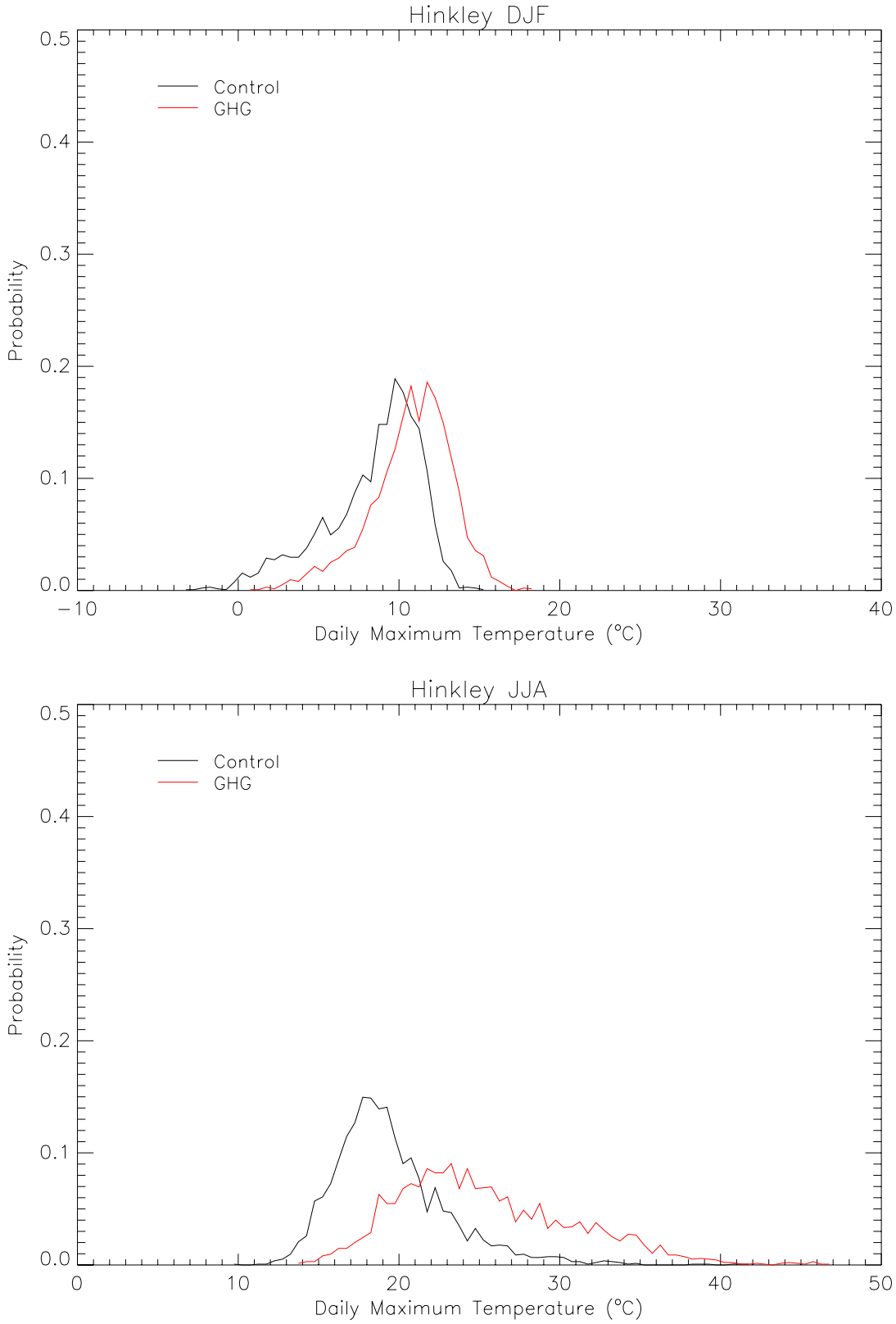

Figure 3.4: Frequency distribution for daily maximum temperature thresholds for Hinkley Point in winter (December – February, upper panel) and summer (June – August, lower panel), for the control (1961-1990, black line) and Medium-High 2080s (red line) climates.

3.4 During winter months temperature increases in the Hinkley Point area will be less extreme than the summer months with daily maximum temperatures predicted to increase by less than 3.5 °C (high scenario) by the 2080s (see Appendix 3). As for the Heysham region, although daily maximum temperatures during winter months increase, the distribution of temperatures about the mean

value stays similar to present day (figure 3.4, upper panel). The modelled present day climate includes a small number of days in an average winter when maximum daily temperatures in the Hinkley Point region do not rise above freezing however this is highly unlikely to be true as climate changes. In fact, analysis of the medium high 2080s climate shows that this threshold is likely to be exceeded on every day of the model integration (Appendix 2, figure A2.2).

3.5 Figure 3.5 shows predicted changes in summertime daily maximum temperature (in degrees Celsius) for the Bradwell region. By the 2020s with the low scenario of forcing, average maximum temperatures are predicted to increase by between 0.5 and 1.0 °C. By the 2080s, with the high emissions scenario of forcing, average daily maximum summertime temperatures rise by 4.5 to 5.0 °C above present day climate. The distribution of temperatures about the mean value also increases (see figure 3.6) and very warm days become increasingly common. Currently it is quite rare (probability=0.01, i.e. 1%) for temperatures to be experienced over approximately 33 °C in the Bradwell area (figure A2.3, Appendix 2) however by the 2080s this temperature will be exceeded for approximately nine percent of days during summer (taking the medium-high forcing scenario).

3.6 As has been noted for the other sites daily maximum temperatures also increase in winter in the Bradwell region, although to a lesser degree than the increases predicted for summer time. Even in the high emissions climate of the 2080s, average maximum temperatures in winter months are expected to increase by no more at 3 °C (figure A3.3 of appendix 3). Again the distribution of temperatures about the mean retains similar characteristics to present day climate (upper panel, figure 3.6) although the range of the most probable daily maximum decreases. Bradwell occasionally experiences days in the current average winter season when the daily maximum temperature does not rise above freezing. This will become increasingly rare as climate changes, and by the 2080s it is predicted to be a highly unlikely occurrence (medium-high scenario).

3.7 Daily maximum temperature changes for the Torness area are presented in figures 3.7 and 3.8. As previously described, figure 3.7 shows the predicted changes in average summer (June-August) daily maximum temperature corresponding to low, medium-low, medium-high and high emissions scenarios (columns, left to right), for three periods centred on the 2020s, 2050s and 2080s (rows, top to bottom), relative to the simulated 1961-90 climate. It can be seen that, in the Torness region, by the **2020s** for the Low scenario the summer average daily maximum temperature will have risen by between 0.5 and 1 °C. For the High scenario, the summer average daily maximum temperature is predicted to rise by between 3.5 and 4.0 °C by the 2080s. The shift in distribution of daily maximum temperatures for summer months (June – August) is shown in figure 3.8. It can be seen that while the shape of the future distribution remains similar to present day, the range of values increase about the mean. Currently, days with maximum temperatures over 23 °C account for less than five percent of the entire summer season, however this will increase to approximately one in every five days exceeding this threshold by the 2080s (medium high scenario)

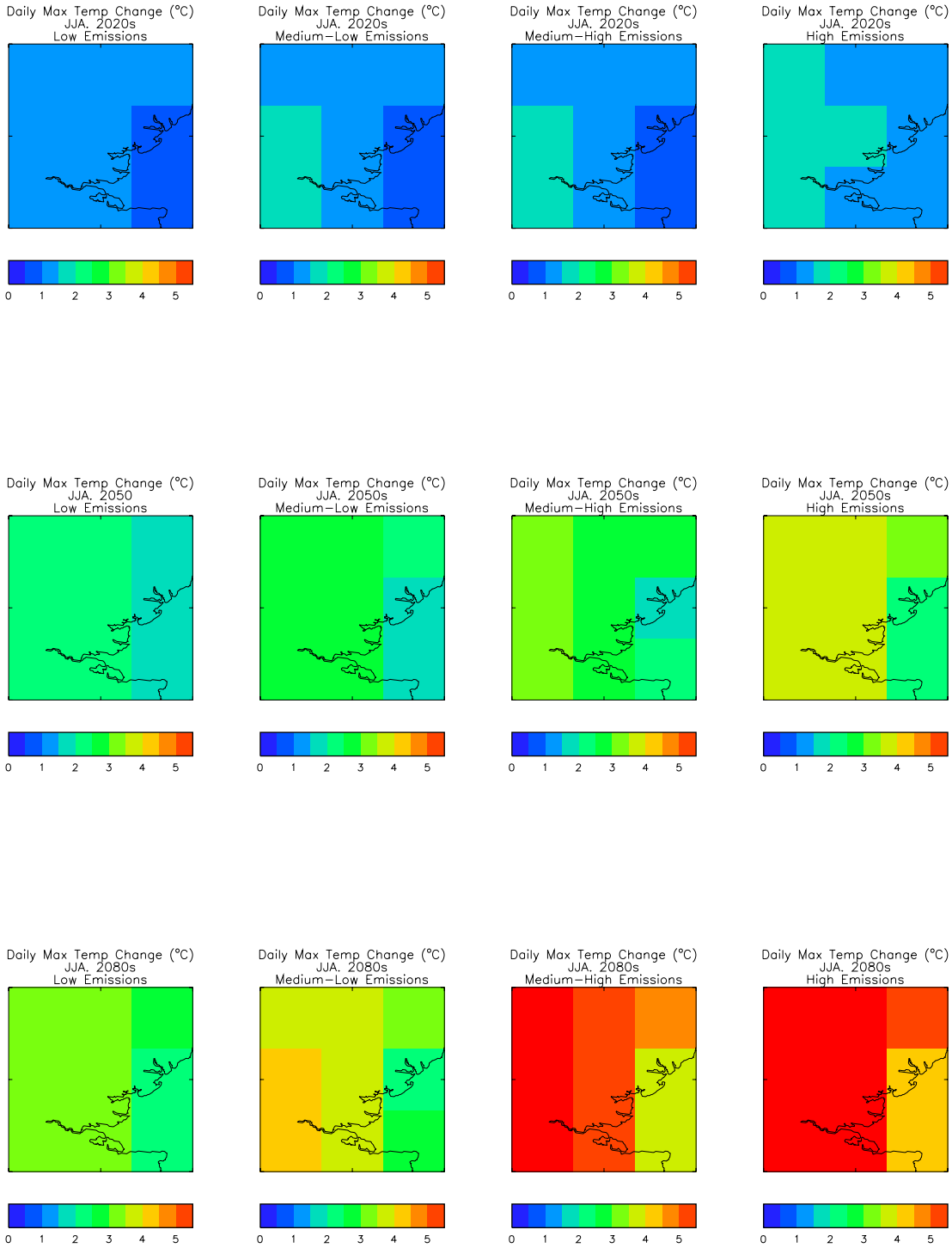

Figure 3.5. Predicted changes (°C), in Bradwell summer (June-August) average maximum temperatures (relative to the simulated 1961-90 climate) for four emissions scenarios (Low - left column, High – right column), for thirty-year periods centred on the 2020s, 2050s and 2080s (rows, top to bottom).

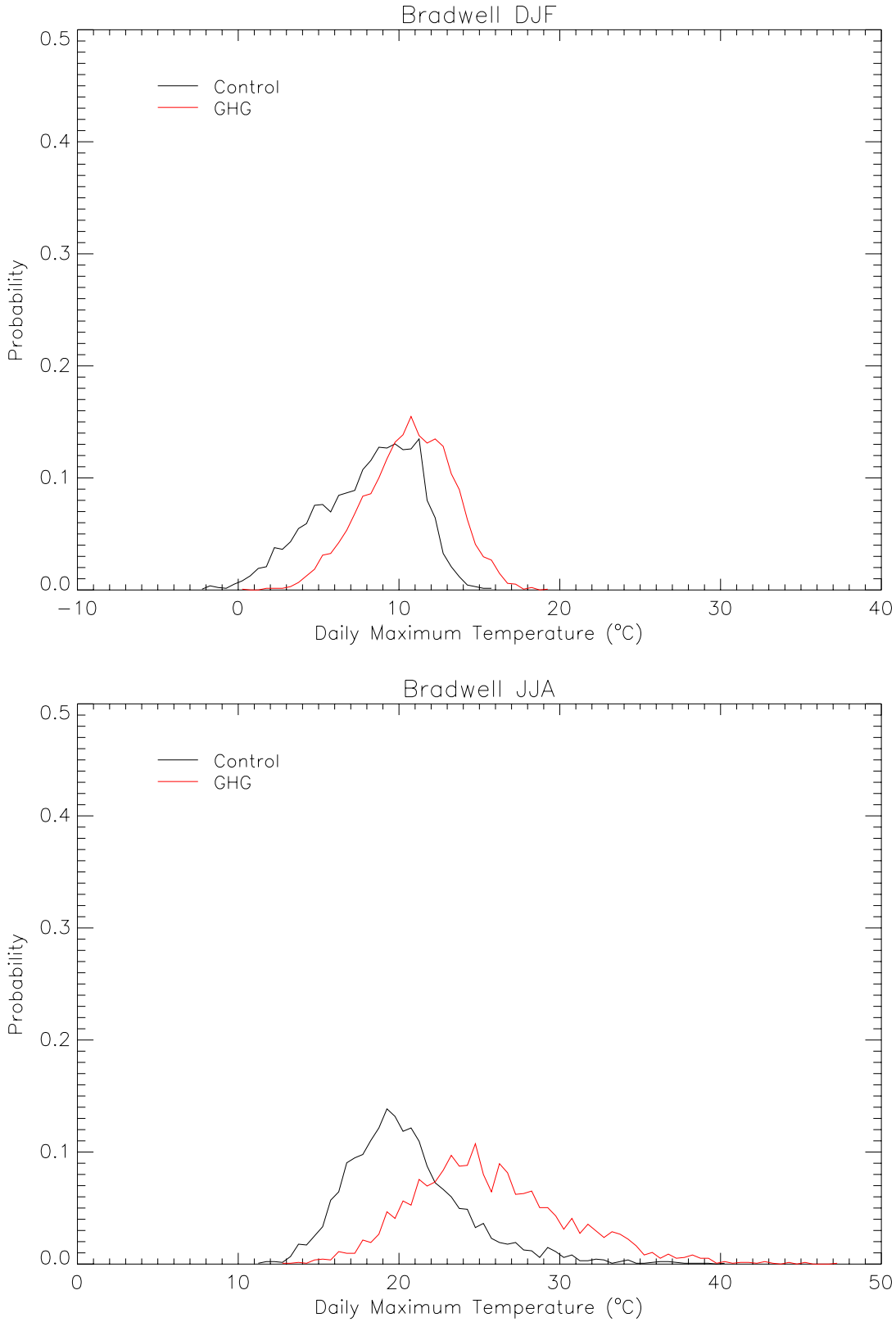

Figure 3.6: Frequency distribution for daily maximum temperature thresholds for Bradwell in winter (December – February, upper panel) and summer (June – August, lower panel), for the control (1961-1990, black line) and Medium-High 2080s (red line) climates.

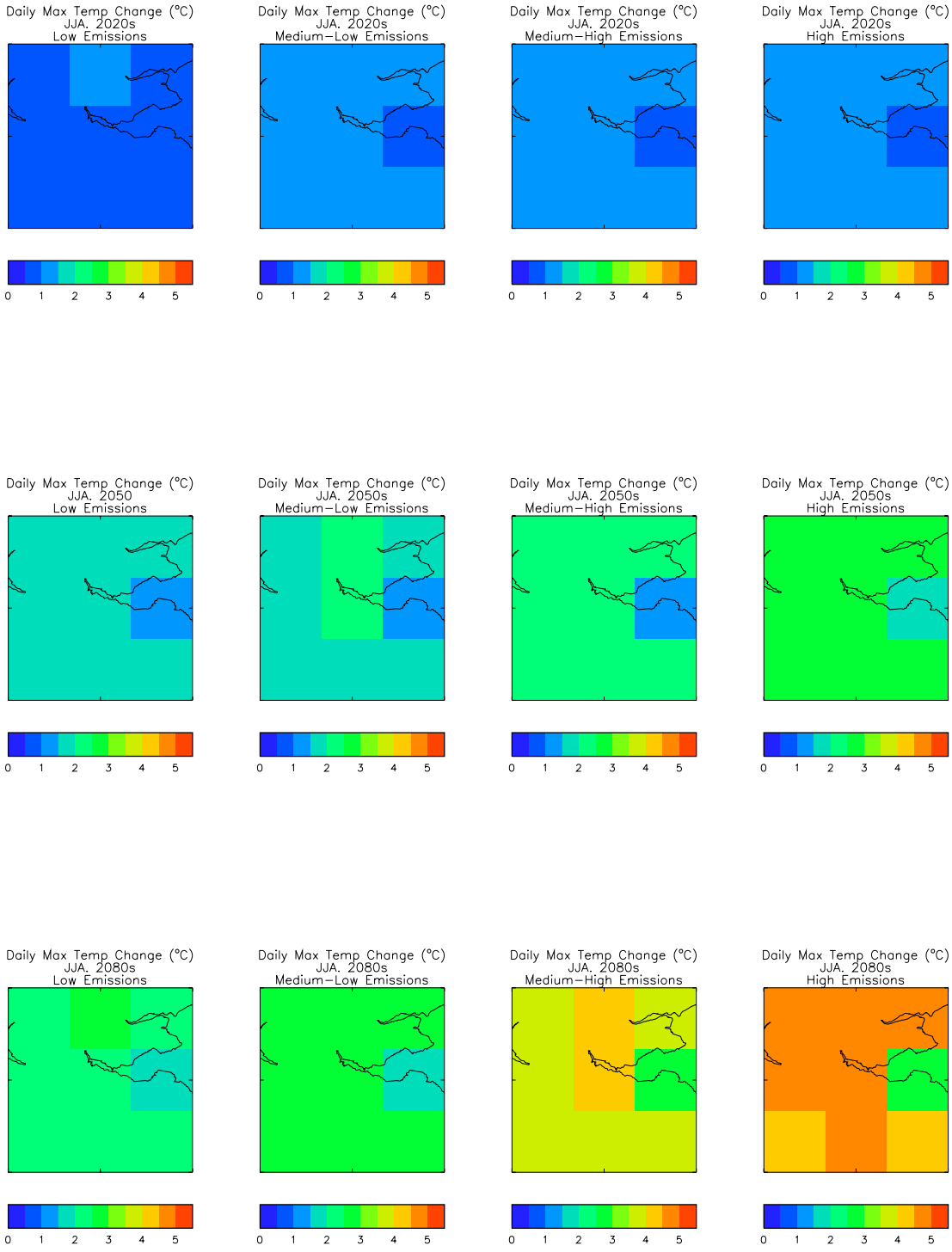

Figure 3.7. Predicted changes (°C), in Torness summer (June-August) average maximum temperatures (relative to the simulated 1961-90 climate) for four emissions scenarios (Low - left column, High – right column), for thirty-year periods centred on the 2020s, 2050s and 2080s (rows, top to bottom).

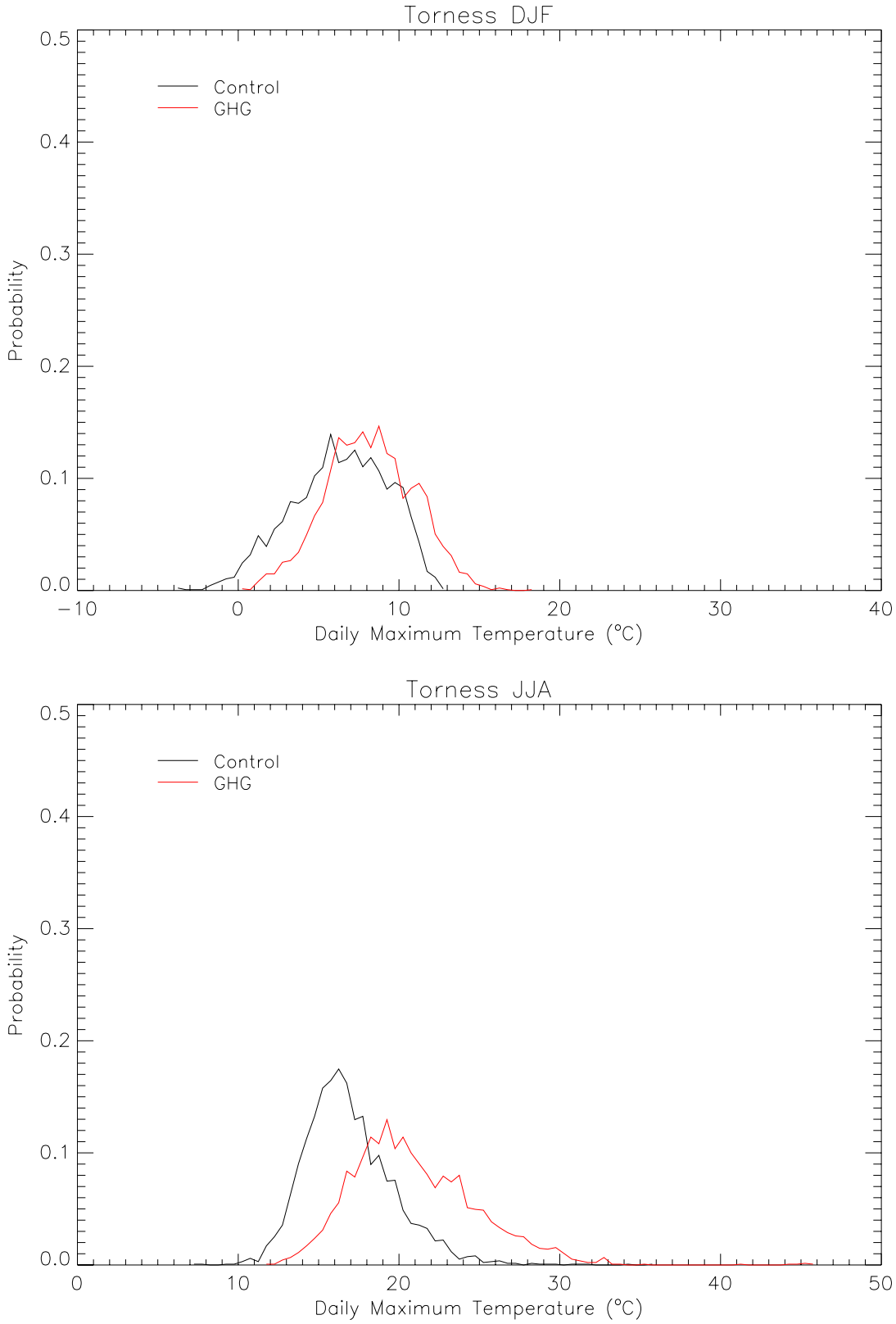

Figure 3.8: Frequency distribution for daily maximum temperature thresholds for Torness in winter (December – February, upper panel) and summer (June – August, lower panel), for the control (1961-1990, black line) and Medium-High 2080s (red line) climates.

3.8 Maximum daily temperatures also increase in winter months in the Torness region (see figure A3.4 of appendix 3). By the 2020s, under the Low scenario, winter daily maximum temperatures are predicted to be comparable with the present day, however by the 2080s (high scenario) winter maximum daily temperatures are predicted to be approximately 2.5 °C warmer than in the

current climate. The distribution of probable temperatures about the mean value remains similar and it can be seen in figure 3.8 that days when maximum temperatures do not rise about freezing will still occur in the 2080s, although with decreasing frequency.

3.9 Figure 3.9 shows predicted summer time daily maximum temperature changes for the Sizewell area. It can be seen that by the 2020s, with the Low scenario of change, that temperatures are predicted to increase by up to 1.5 °C above the control (1961 to 1990) climate. By the 2080s temperature increases exceed 5 °C in the High scenario. The distribution of summer time daily maximum temperatures broadens by the 2080s (Medium High scenario), illustrated in figure 3.10. A threshold value of 30 °C is rarely exceeded in the control climate in the vicinity of Sizewell, however almost fifteen percent of all days in an average summer season for this region will be warmer than 30 °C by the 2080s (Medium – High) and a day or more with maximum temperatures over 40 °C are likely in most years.

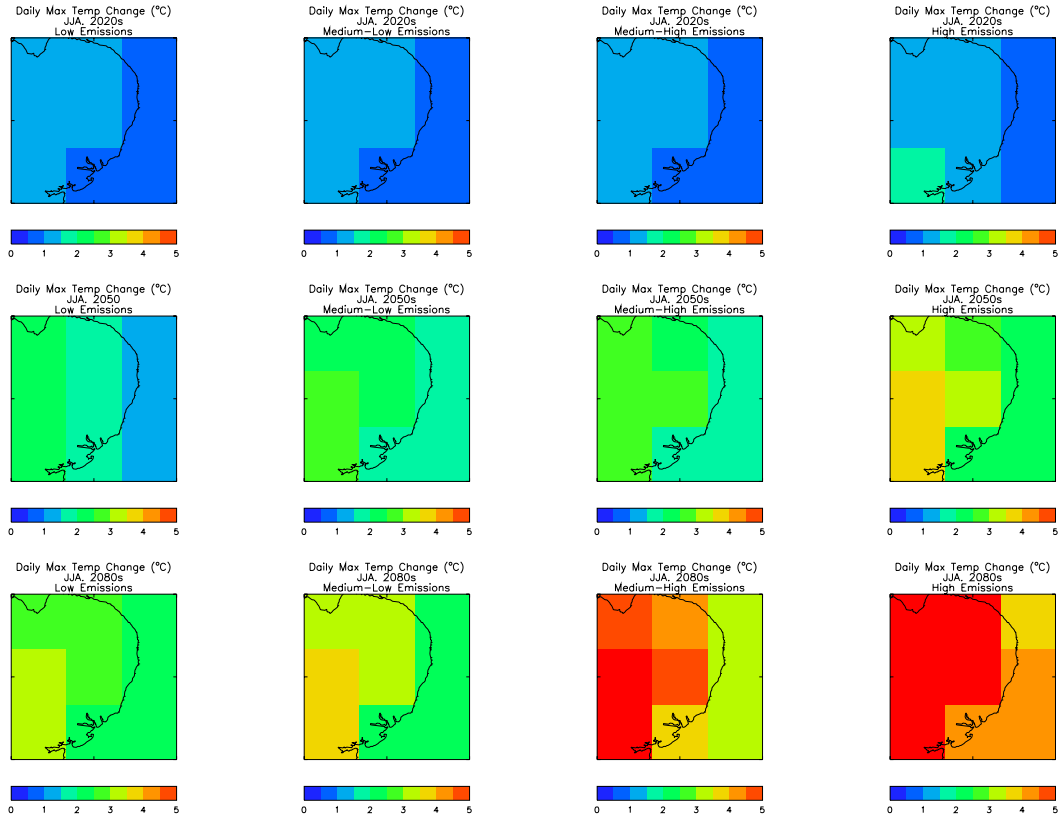

Figure 3.9. Predicted changes (°C), in Sizewell summer (June-August) average maximum temperatures (relative to the simulated 1961-90 climate) for four emissions scenarios (Low - left column, High – right column), for thirty-year periods centred on the 2020s, 2050s and 2080s (rows, top to bottom).

3.10 Maximum daily temperatures also increase in winter months in the Sizewell region (see figure A3.8 of appendix 3). By the 2080s, under the High scenario, winter daily maximum temperature increases are predicted to be approximately 3.5 °C warmer than current climate. The distribution of probable temperatures about the mean value remains similar although shifted by a few degrees. Figure 3.10 illustrates that although there are occasions in a typical winter currently when temperatures in the Sizewell area do not rise above 0 °C that this will become increasingly rare until by the 2080s (medium – High scenario) such an occurrence will be highly unlikely.

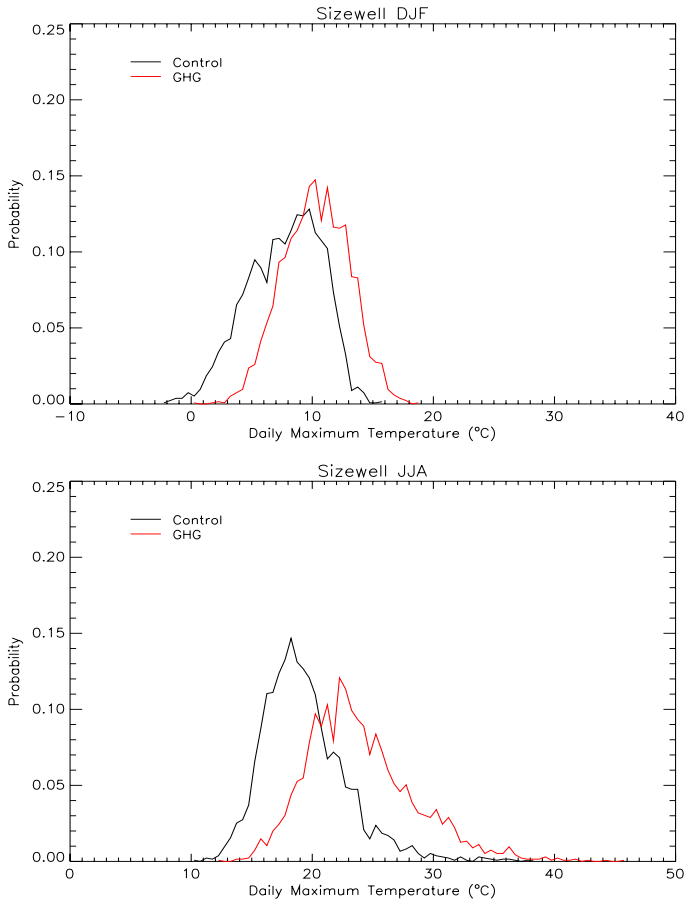

Figure 3.10: Frequency distribution for daily maximum temperature thresholds for Sizewell in winter (December – February, upper panel) and summer (June – August, lower panel), for the control (1961-1990, black line) and Medium-High 2080s (red line) climates.

3.11 It can be seen in figure 3.11 that, in the Dungeness region, by the **2020s** for the Low scenario the summer average daily maximum temperature will have risen by between 1.0 and 1.5 °C. For the High scenario, the summer average daily maximum temperature is predicted to rise by over 5.0 °C by the 2080s. Figure 3.12 shows the frequency distribution of daily maximum temperatures attained during the summer season (lower panel) in both the modelled present day and future (2080s under the medium-high scenario) climates. As the average daily maximum temperature increases the shape of the distribution of maximum temperatures also changes with the range of probable daily maximums experienced in a summer season tending to increase. Under present day climate (modelled) it is rare that a summertime daily maximum temperature of more than 30 °C is experienced in the Dungeness region, less than five days per year on average. By the 2080s such daily maximum temperatures will be exceeded much more frequently, more than twenty percent of summer days will be warmer than this threshold, and an average year will see at least one day when temperatures rise to over 40 °C, see Appendix 2, figure A2.5.

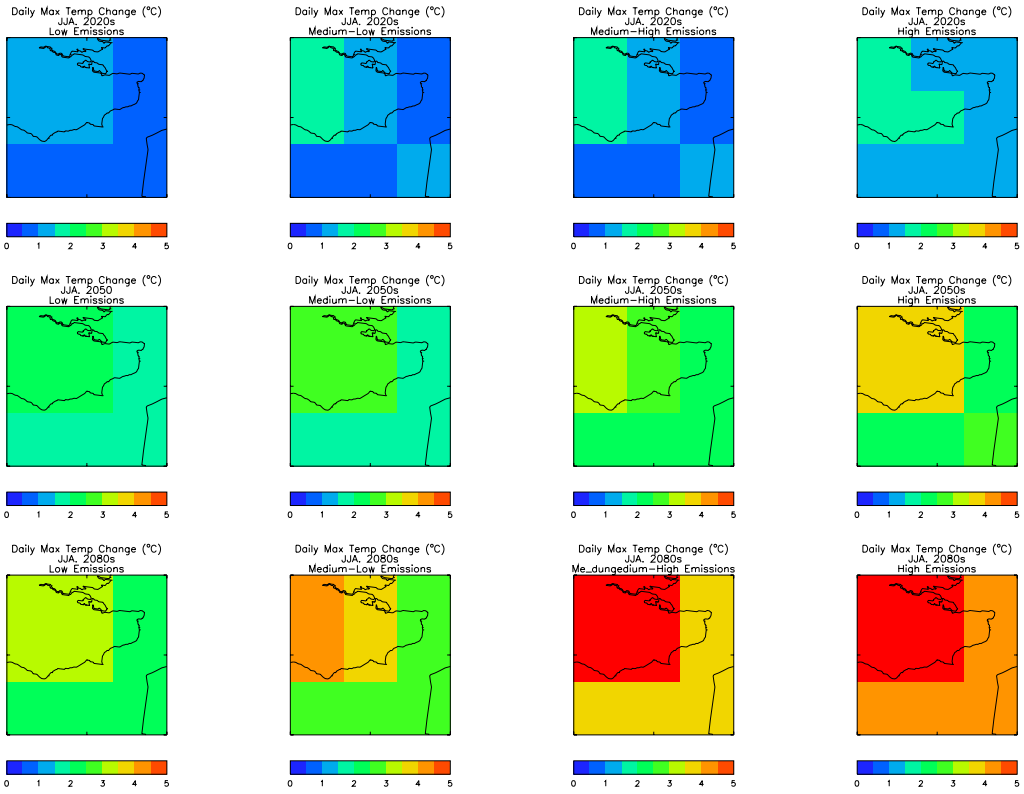

Figure 3.11. Predicted changes (°C), in Dungeness summer (June-August) average maximum temperatures (relative to the simulated 1961-90 climate) for four emissions scenarios (Low - left column, High – right column), for thirty-year periods centred on the 2020s, 2050s and 2080s (rows, top to bottom).

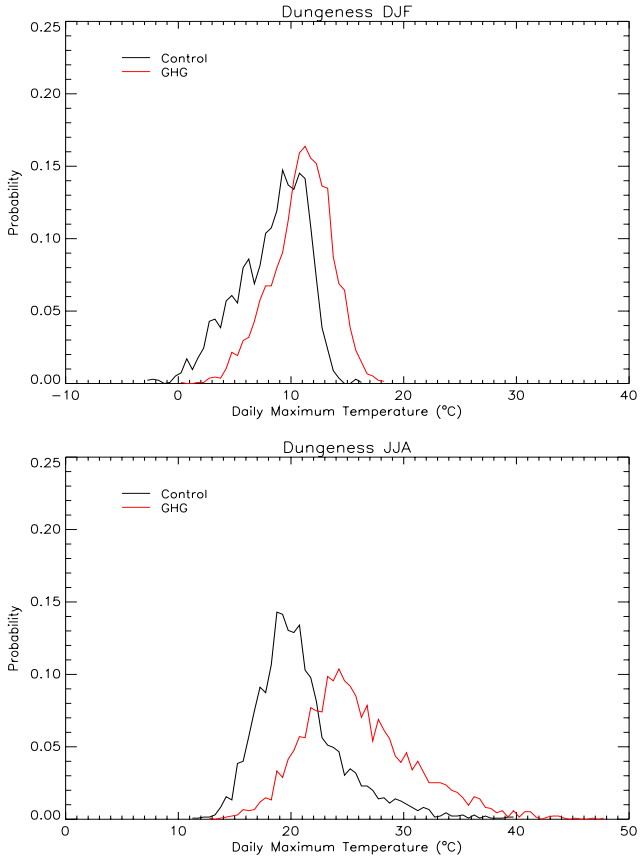

Figure 3.12: Frequency distribution for daily maximum temperature thresholds for Dungeness in winter (December – February, upper panel) and summer (June – August, lower panel), for the control (1961-1990, black line) and Medium-High 2080s (red line) climates.

3.12 During winter months temperature increases in the Dungeness area will be less extreme than the summer months with daily maximum temperatures predicted to increase by less than 3.5 °C (high scenario) by the 2080s (see Appendix 3). Although daily maximum temperatures during winter months increase, the distribution of temperatures about the mean value stays similar to present day (figure 3.12, upper panel). The modelled present day climate includes a small number of days in an average winter when maximum daily temperatures in the Dungeness region do not rise above freezing however this is highly unlikely to be true as climate changes. In fact, analysis of the medium high 2080s climate shows that this threshold is exceeded on every day of the model integration (Appendix 2, figure A2.5).

3.13 Figure 3.13 shows predicted changes in summertime daily maximum temperature (in degrees Celsius) for the Hartlepool region. By the 2020s with the low scenario of forcing, average maximum temperatures are predicted to increase by between 0.5 and 1.0 °C. By the 2080s, with the high emissions scenario of forcing, average daily maximum summertime temperatures rise by 4.5 to 5.0 °C above present day climate. The distribution of temperatures about the mean value also increases (see figure 3.14) and very warm days become increasingly common. Currently it is extremely rare for temperatures to be experienced over 30 °C in the Hartlepool area (figure A2.6, Appendix 2) however by the 2080s this temperature will be exceeded for approximately five percent of days during summer (taking the medium-high forcing scenario).

3.14 As has been noted for the other sites daily maximum temperatures also increase in winter in the Hartlepool region, although to a lesser degree than the increases predicted for summer time. Even in the high emissions climate of the 2080s, average maximum temperatures in winter months are expected to increase by no more at 3 °C (figure A3.6 of appendix 3). Again the distribution of temperatures about the mean retains similar characteristics to present day climate (upper panel, figure 3.14) although the range of the most probable daily maximum decreases. Hartlepool occasionally experiences days in the current average winter season when the daily maximum temperature does not rise above freezing. This will become increasingly rare as climate changes, and by the 2080s it is predicted to be a highly unlikely occurrence (medium-high scenario).

3.15 Daily maximum temperature changes for the Hunterston area are presented in figures 3.15 and 3.16. As previously described, figure 3.15 shows the predicted changes in average summer (June-August) daily maximum temperature corresponding to low, medium-low, medium-high and high emissions scenarios (columns, left to right), for three periods centred on the 2020s, 2050s and 2080s (rows, top to bottom), relative to the simulated 1961-90 climate. It can be seen that, in the Hunterston region, by the **2020s** for the Low scenario the summer average daily maximum temperature will have risen by between 0.5 and 1 °C. For the High scenario, the summer average daily maximum temperature is predicted to rise by between 3.5 and 4.0 °C by the 2080s. The shift in distribution of daily maximum temperatures for summer months (June – August) is shown in figure 3.16. It can be seen that while the shape of the future distribution remains similar to present day, the range of values increase about the mean. Currently, days with maximum temperatures over 23 °C account for less than five percent of the entire summer season, however this will increase to approximately one in every five days exceeding this threshold by the 2080s (medium high scenario)

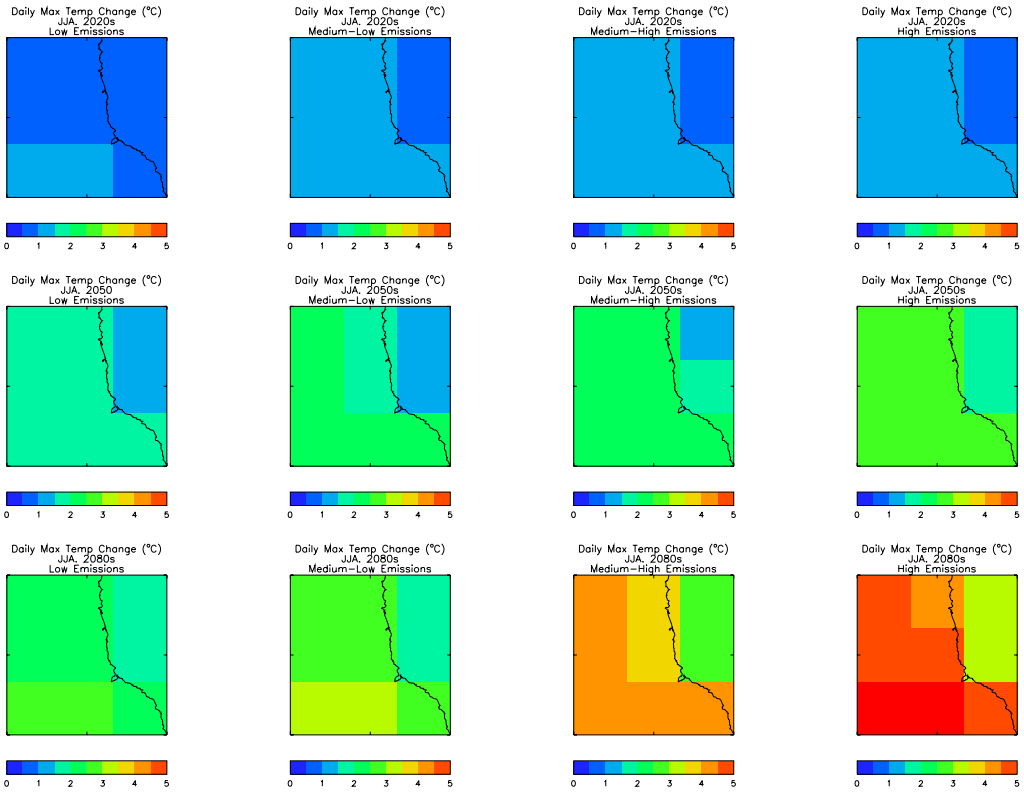

Figure 3.13. Predicted changes (°C), in Hartlepool summer (June-August) average maximum temperatures (relative to the simulated 1961-90 climate) for four emissions scenarios (Low - left column, High – right column), for thirty-year periods centred on the 2020s, 2050s and 2080s (rows, top to bottom).

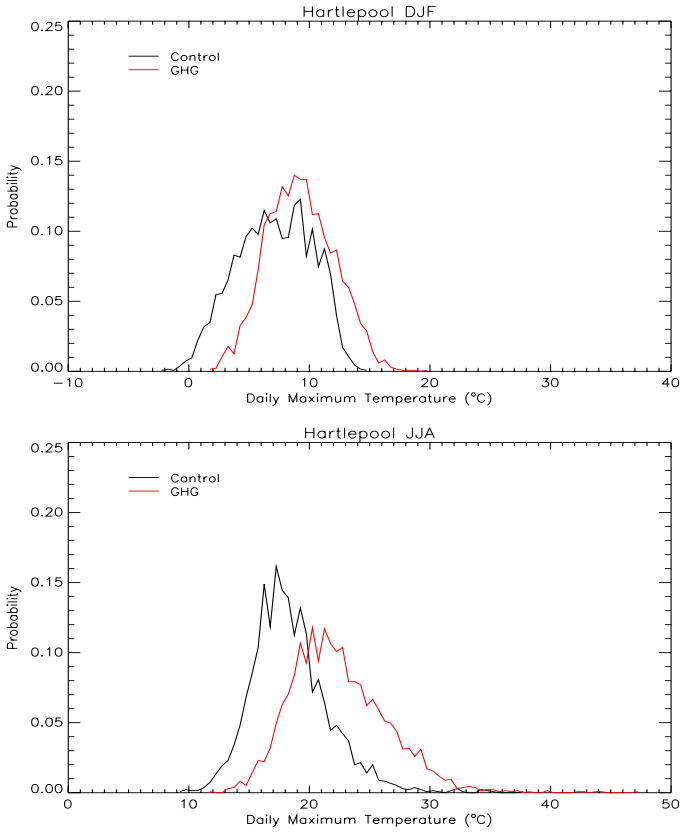

Figure 3.14: Frequency distribution for daily maximum temperature thresholds for Hartlepool in winter (December – February, upper panel) and summer (June – August, lower panel), for the control (1961-1990, black line) and Medium-High 2080s (red line) climates.

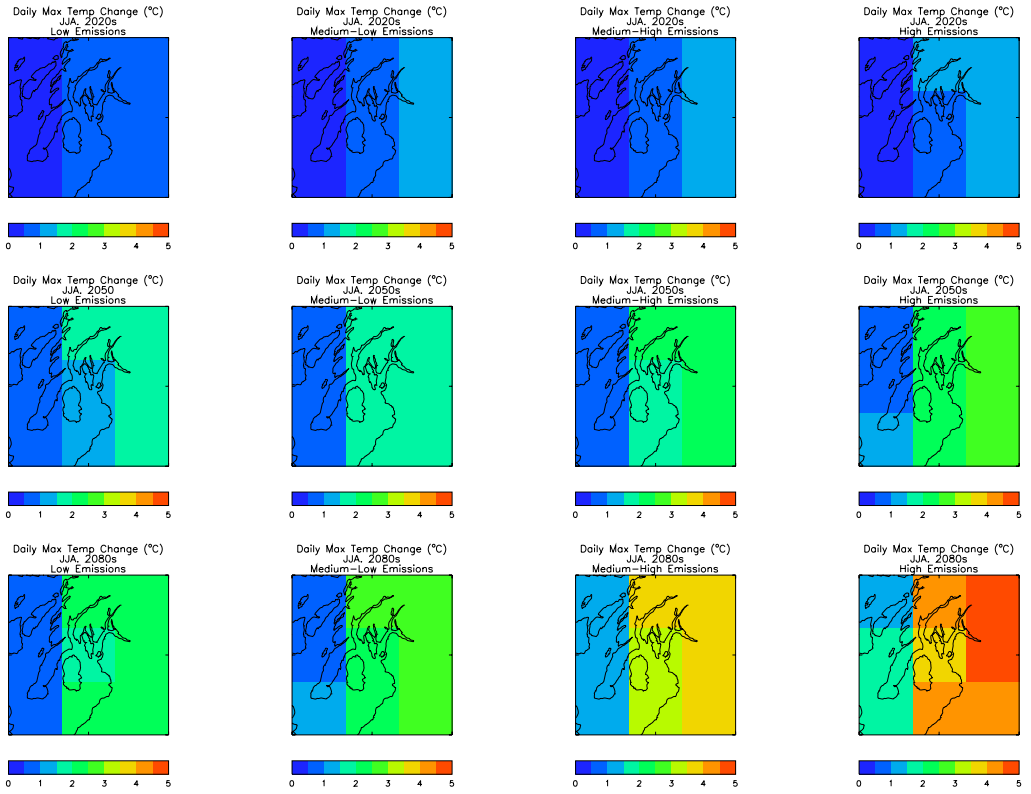

Figure 3.15. Predicted changes (°C), in Hunterston summer (June-August) average maximum temperatures (relative to the simulated 1961-90 climate) for four emissions scenarios (Low - left column, High – right column), for thirty-year periods centred on the 2020s, 2050s and 2080s (rows, top to bottom).

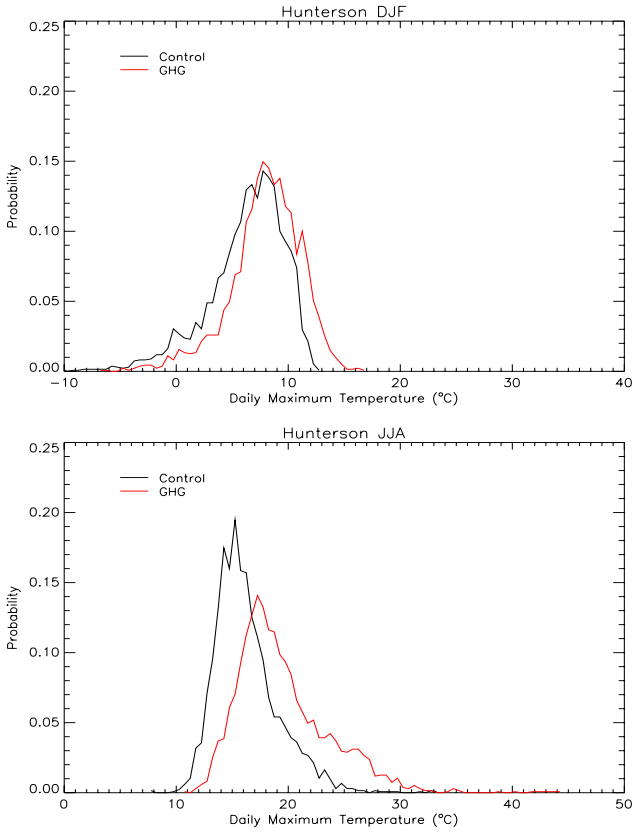

Figure 3.16: Frequency distribution for daily maximum temperature thresholds for Hunterston in winter (December – February, upper panel) and summer (June – August, lower panel), for the control (1961-1990, black line) and Medium-High 2080s (red line) climates.

3.16 Maximum daily temperatures also increase in winter months in the Hunterston region (see figure A3.7 of appendix 3). By the 2020s, under the Low scenario, winter daily maximum temperatures are predicted to be comparable with the present day, however by the 2080s (high scenario) winter maximum daily temperatures are predicted to be approximately 2.5 °C warmer than in the current climate. The distribution of probable temperatures about the mean value remains similar and it can be seen in figure 3.16 that days when maximum temperatures do not rise about freezing will still occur in the 2080s, although with decreasing frequency.

3.17 It is apparent in each of the timeslices, scenarios and locations that while summer maximum temperature increases everywhere, the rise in temperature is not uniform. Over the ocean increases are moderated during summer months but temperatures rise with increasing distance inland from the coast. The same is not true during winter months when the ocean to land temperature gradient is greatly reduced.

3.18 Figures 3.17 to 3.24 show the predicted changes from the control climate to the 2080s in the distributions of daily minimum temperatures for the eight sites. It can be seen that the distribution of daily minimum temperature at most of the sites is extended to higher temperature regimes more in summer than in winter. Although minimum temperatures in each scenario increase everywhere by the 2080s, all increases are smaller than seen in maximum temperatures. Distributions of minimum temperatures within an average season remain very similar in the future, although at slightly higher temperature values. The important factor to note is the reduction in the number of days of very cold nights. Presently the RCM grid box in which each every site is located experiences minimum, or night time, temperatures of well below freezing for a significant part of the winter season. Although each site (or equivalent grid box) continues to see winter minimum temperatures below freezing in the Medium High scenario 2080s, the frequency of occurrence is greatly reduced for most sites. For Hunterston the shift in the distribution of winter minimum temperatures below freezing is not as great as at other sites, although there is a warm shift of more than 7 °C in the absolute coldest winter temperatures in the model simulation.

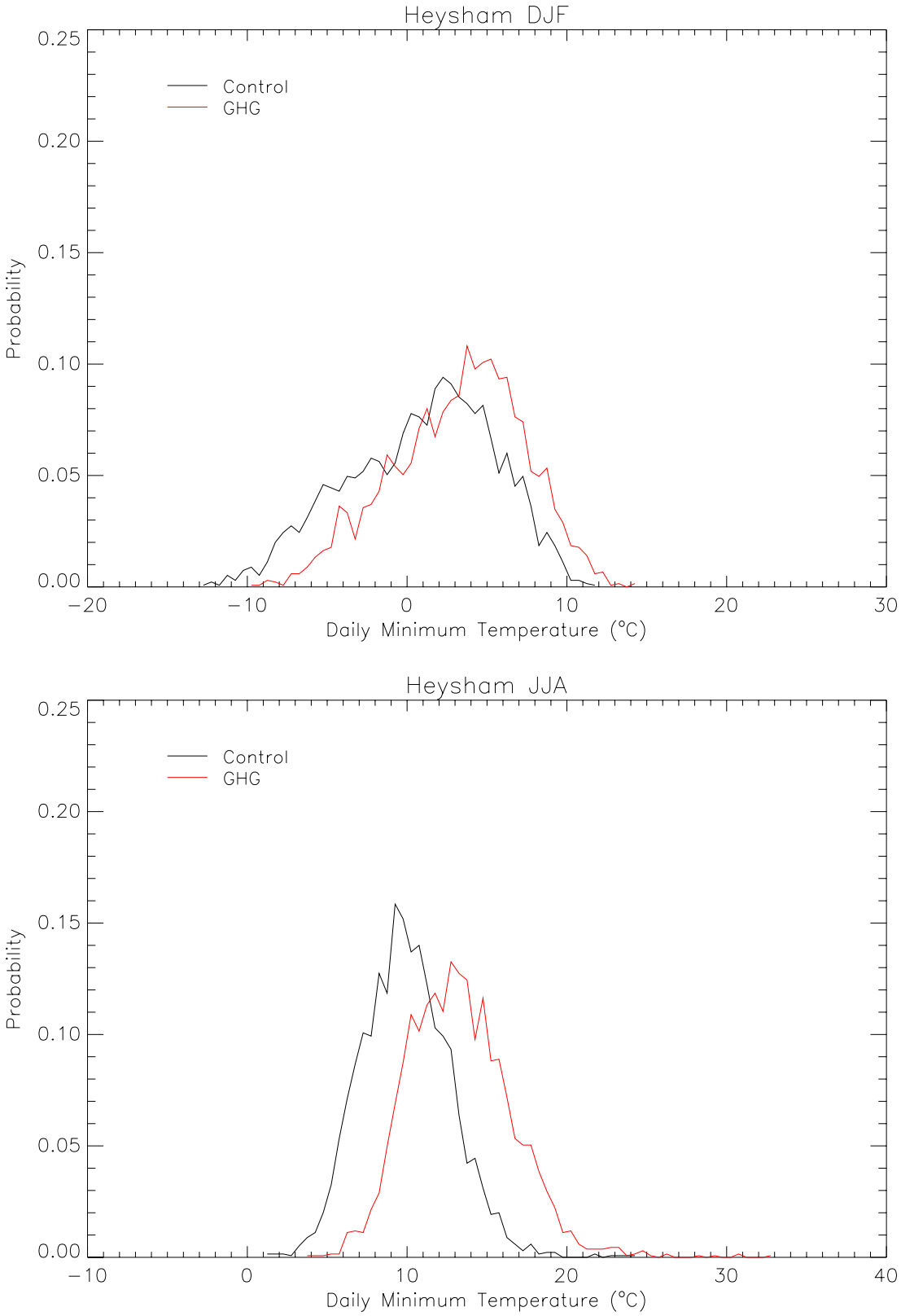

Figure 3.17: Frequency distribution for daily minimum temperature thresholds for Heysham in winter (December – February, upper panel) and summer (June – August, lower panel), for the control (1961-1990, black line) and Medium-High 2080s (red line) climates.

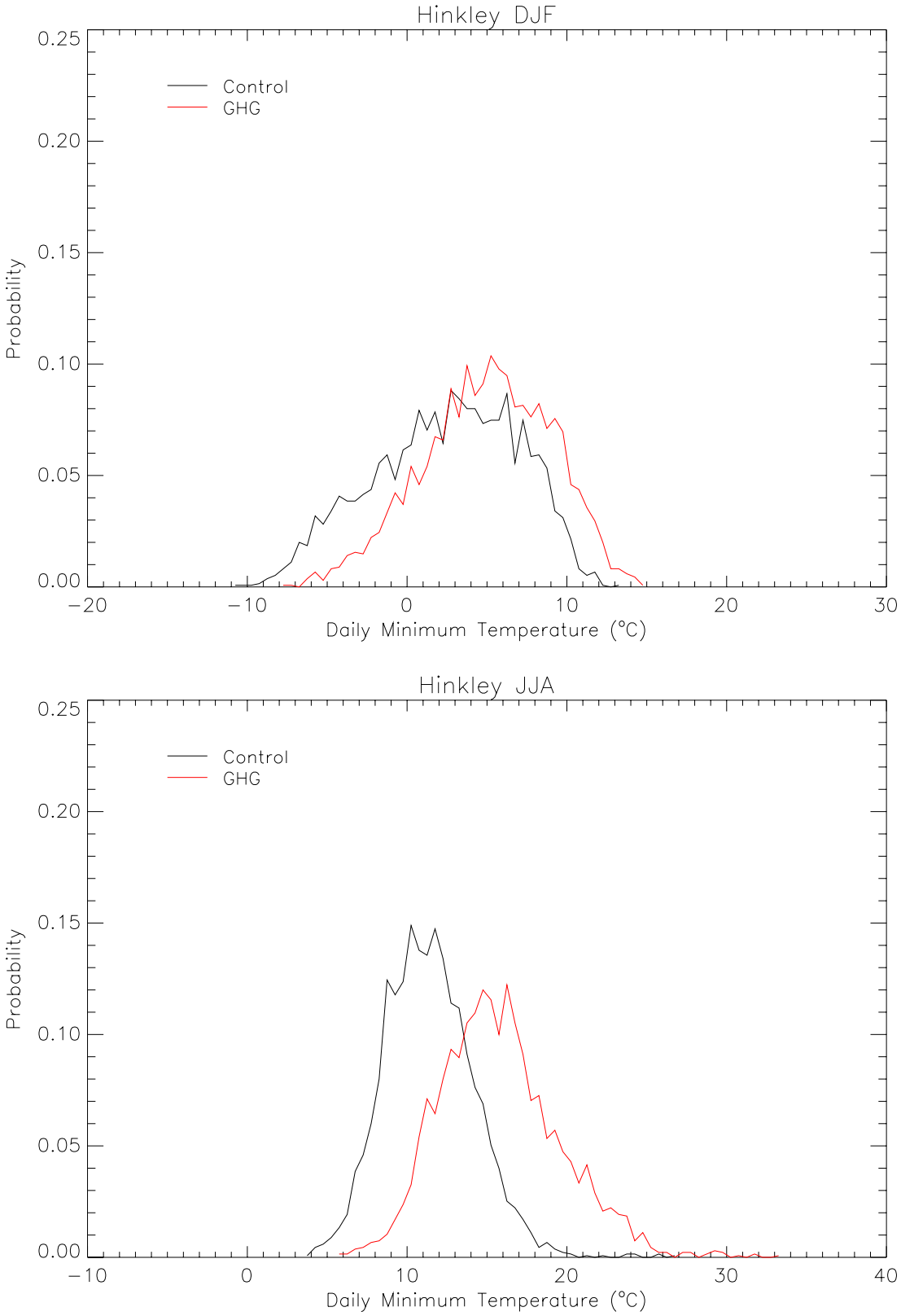

Figure 3.18: Frequency distribution for daily minimum temperature thresholds for Hinkley Point in winter (December – February, upper panel) and summer (June – August, lower panel), for the control (1961-1990, black line) and Medium-High 2080s (red line) climates.

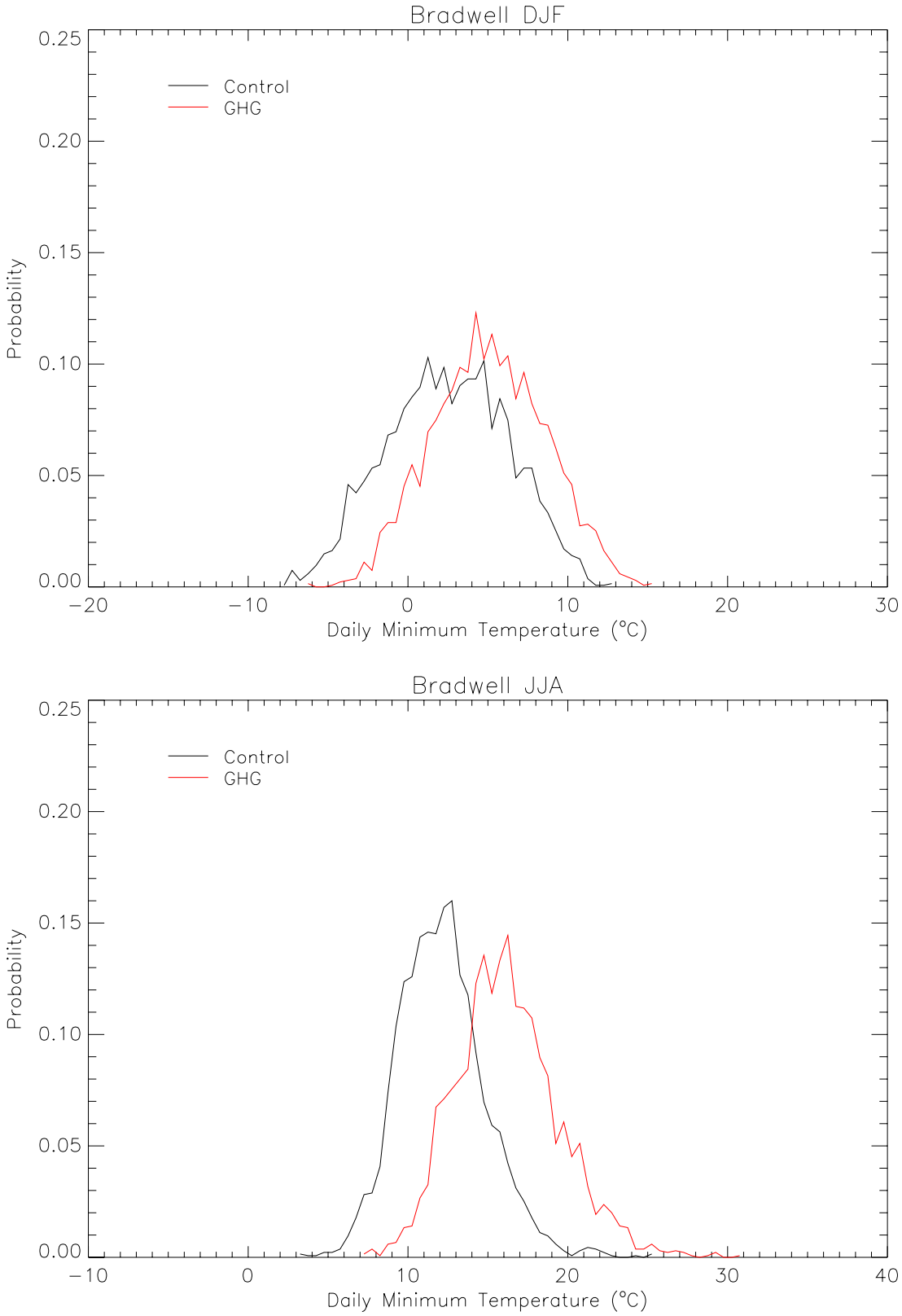

Figure 3.19: Frequency distribution for daily minimum temperature thresholds for Bradwell in winter (December – February, upper panel) and summer (June – August, lower panel), for the control (1961-1990, black line) and Medium-High 2080s (red line) climates.

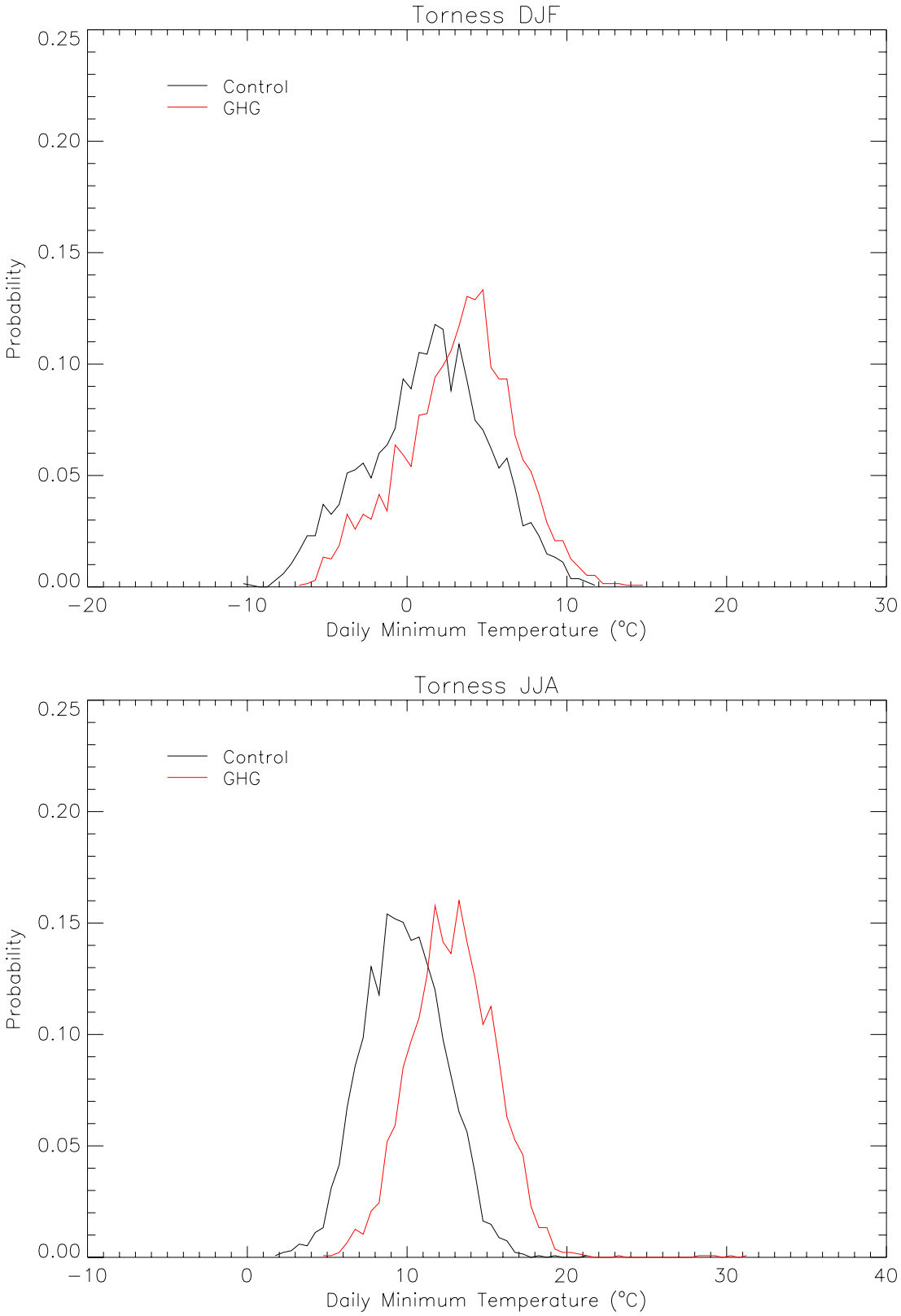

Figure 3.20: Frequency distribution for daily minimum temperature thresholds for Torness in winter (December – February, upper panel) and summer (June – August, lower panel), for the control (1961-1990, black line) and Medium-High 2080s (red line) climates.

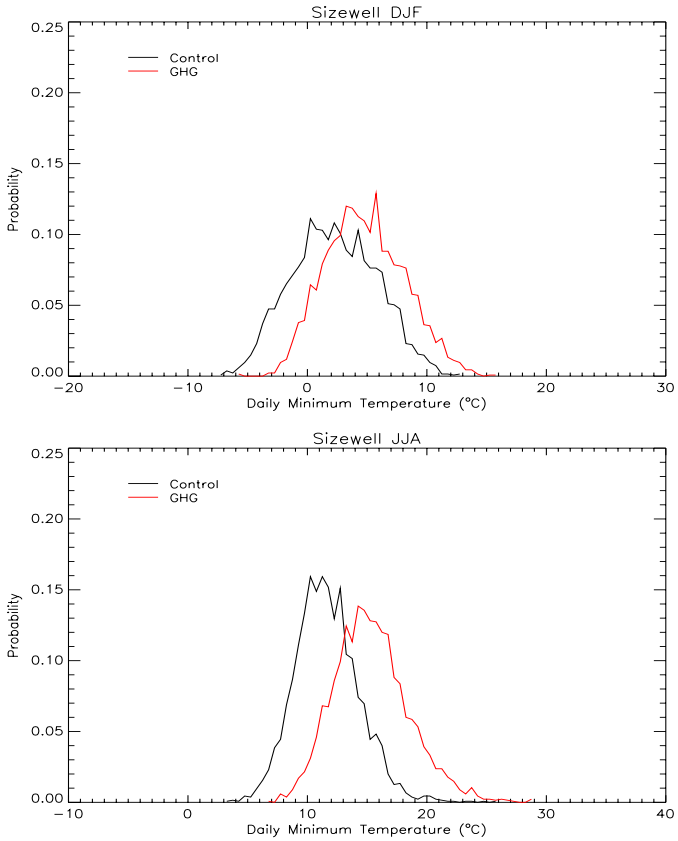

Figure 3.21: Frequency distribution for daily minimum temperature thresholds for Sizewell in winter (December – February, upper panel) and summer (June – August, lower panel), for the control (1961-1990, black line) and Medium-High 2080s (red line) climates.

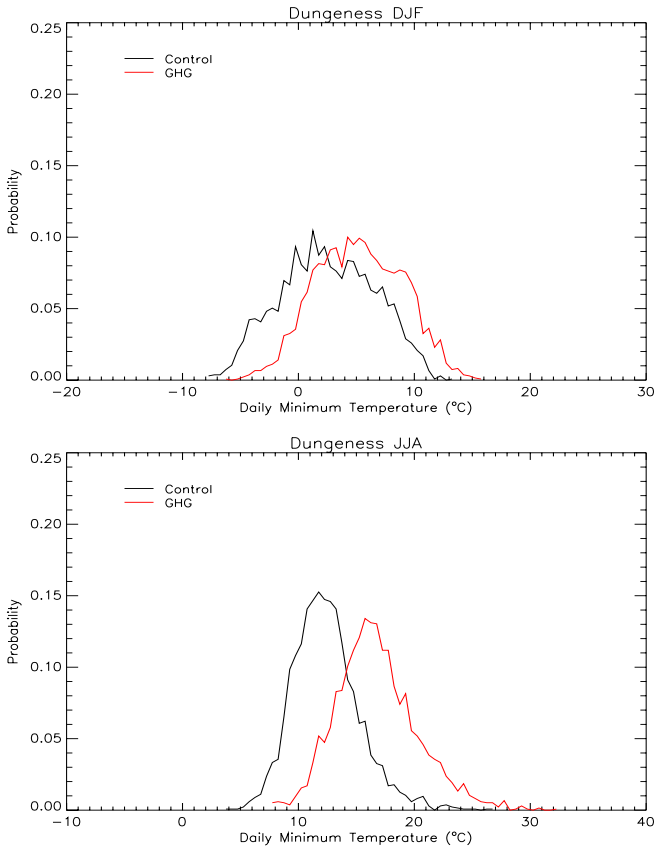

Figure 3.22: Frequency distribution for daily minimum temperature thresholds for Dungeness in winter (December – February, upper panel) and summer (June – August, lower panel), for the control (1961-1990, black line) and Medium-High 2080s (red line) climates.

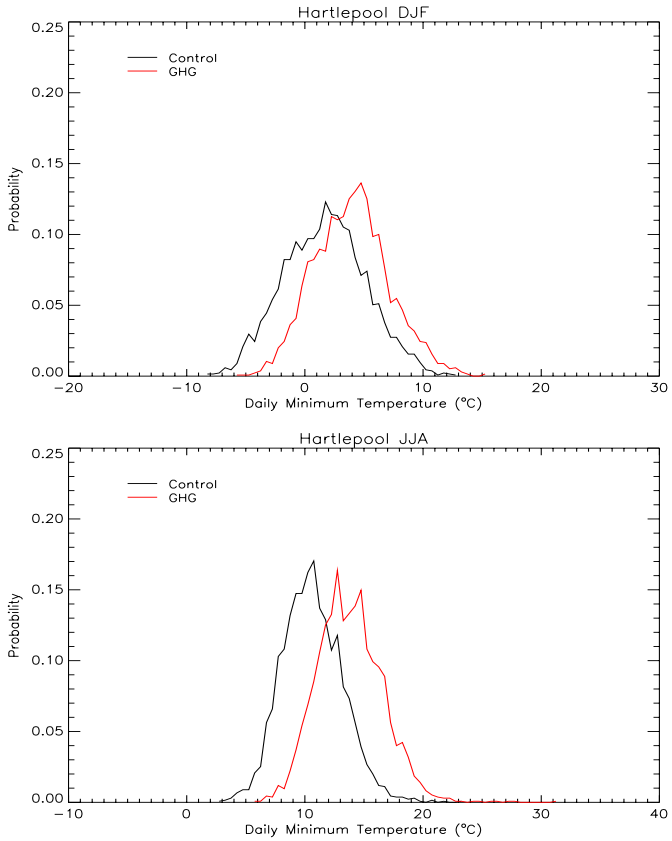

Figure 3.23: Frequency distribution for daily minimum temperature thresholds for Hartlepool in winter (December – February, upper panel) and summer (June – August, lower panel), for the control (1961-1990, black line) and Medium-High 2080s (red line) climates.

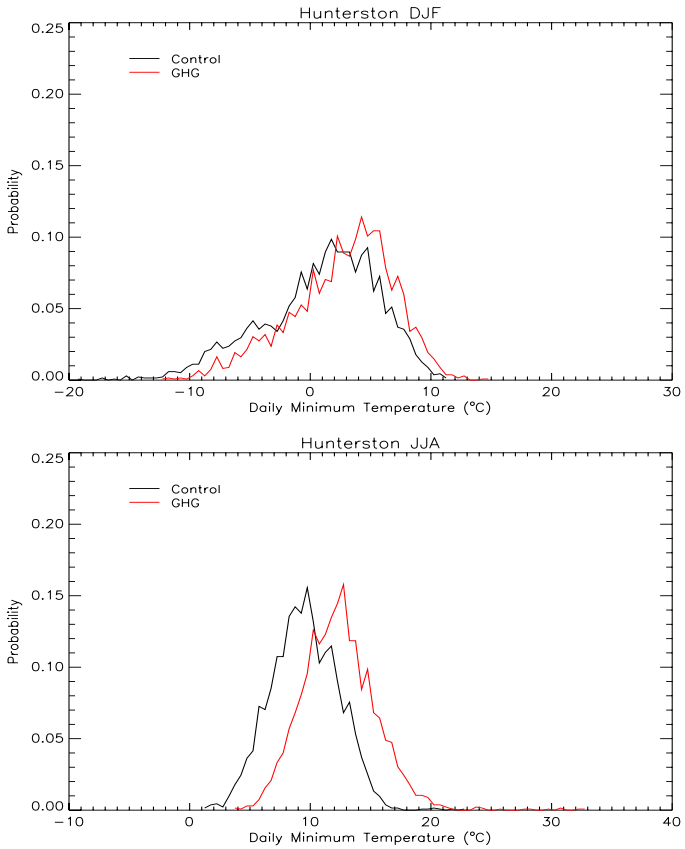

Figure 3.24: Frequency distribution for daily minimum temperature thresholds for Hunterston in winter (December – February, upper panel) and summer (June – August, lower panel), for the control (1961-1990, black line) and Medium-High 2080s (red line) climates.

3.19 The following series of tables shows the extreme daily maximum temperatures derived from the control and anomaly (2071-2100 Medium High) runs of the HadRM3 RCM, for all eight sites. The method of Tabony (1996) based on median annual maximum temperatures (from the 30-year model simulations) was used to derive the extreme values. The important aspect of the tables is the change from the control to the future climates (in degrees), rather than the absolute temperature values. Note that because the climate model simulations were 30 years in length, estimation of return period quantities for greater than 30 years is highly uncertain, so the lines for return periods of 50 years and more are italicised to show that they are indicative. To obtain more accurate figures for long return periods, longer climate model simulations would be needed.

Return Period (Years)	Control climate		Anomaly climate	
	Maximum Temperature	Standard Error Max Temp	Maximum Temperature	Standard Error Max Temp
2	25.5	0.4	34.2	0.4
5	27.4	0.4	36.0	0.4
10	28.5	0.5	37.1	0.5
20	29.3	0.6	37.9	0.6
50	*30.3*	*0.7*	*38.9*	*0.7*
100	*30.8*	*0.8*	*39.5*	*0.8*
200	*31.4*	*0.9*	*40.0*	*0.9*
500	*31.9*	*1.1*	*40.6*	*1.1*
1000	*32.3*	*1.2*	*40.9*	*1.2*
10000	*33.2*	*1.5*	*41.9*	*1.5*
100000	*33.8*	*1.8*	*42.4*	*1.8*
1000000	*34.2*	*2.1*	*42.8*	*2.1*
Limit	*34.7*	*2.5*	*43.3*	*2.5*

Table 3.1 Heysham. Modelled extremes of temperature (deg C)

Return Period (Years)	Control Climate		Anomaly Climate	
	Maximum Temperature	Standard Error Max Temp	Maximum Temperature	Standard Error Max Temp
2	28.4	0.4	38.9	0.4
5	30.4	0.5	40.9	0.5
10	31.5	0.5	42.0	0.5
20	32.4	0.6	42.9	0.6
50	*33.4*	*0.7*	*43.9*	*0.7*
100	*34.1*	*0.8*	*44.5*	*0.8*
200	*34.6*	*1.0*	*45.1*	*1.0*
500	*35.3*	*1.1*	*45.7*	*1.1*
1000	*35.7*	*1.3*	*46.1*	*1.3*
10000	*36.6*	*1.6*	*47.1*	*1.6*
100000	*37.3*	*2.0*	*47.7*	*2.0*
1000000	*37.7*	*2.2*	*48.1*	*2.2*
Limit	*38.2*	*2.7*	*48.6*	*2.7*

Table 3.2 Hinkley Point. Modelled extremes of temperature (deg C)

Return Period (Years)	Control Climate		Anomaly Climate	
	Maximum Temperature	Standard Error Max Temp	Maximum Temperature	Standard Error Max Temp
2	30.9	0.4	39.2	0.4
5	32.9	0.4	41.2	0.4
10	34.0	0.5	42.3	0.5
20	34.9	0.6	43.2	0.6
50	*35.9*	*0.7*	*44.2*	*0.7*
100	*36.5*	*0.8*	*44.8*	*0.8*
200	*37.0*	*1.0*	*45.3*	*1.0*
500	*37.7*	*1.1*	*45.9*	*1.1*
1000	*38.1*	*1.2*	*46.3*	*1.2*
10000	*39.0*	*1.6*	*47.3*	*1.6*
100000	*39.6*	*1.9*	*47.9*	*1.9*
1000000	*40.0*	*2.2*	*48.3*	*2.2*
Limit	*40.5*	*2.6*	*48.8*	*2.6*

Table 3.3 Bradwell. Modelled extremes of temperature (deg C)

Return Period (Years)	Control Climate		Anomaly Climate	
	Maximum Temperature	Standard Error Max Temp	Maximum Temperature	Standard Error Max Temp
2	24.3	0.4	29.6	0.4
5	26.1	0.4	31.4	0.4
10	27.1	0.5	32.4	0.5
20	27.9	0.5	33.2	0.5
50	*28.8*	*0.7*	*34.1*	*0.7*
100	*29.4*	*0.8*	*34.7*	*0.8*
200	*29.9*	*0.9*	*35.1*	*0.9*
500	*30.4*	*1.0*	*35.7*	*1.0*
1000	*30.8*	*1.1*	*36.1*	*1.1*
10000	*31.7*	*1.5*	*36.9*	*1.5*
100000	*32.2*	*1.8*	*37.5*	*1.8*
1000000	*32.6*	*2.0*	*37.8*	*2.0*
Limit	*33.0*	*2.4*	*38.3*	*2.4*

Table 3.4 Torness. Modelled extremes of temperature (deg C)

Return Period (Years)	Control Climate		Anomaly Climate	
	Maximum Temperature	Standard Error Max Temp	Maximum Temperature	Standard Error Max Temp
2	28.5	0.4	36.9	0.4
5	30.4	0.4	38.8	0.4
10	31.5	0.5	39.9	0.5
20	32.4	0.6	40.8	0.6
50	*33.4*	*0.7*	*41.8*	*0.7*
100	*34.0*	*0.8*	*42.4*	*0.8*
200	*34.5*	*0.9*	*42.9*	*0.9*
500	*35.1*	*1.1*	*43.5*	*1.1*
1000	*35.5*	*1.2*	*43.9*	*1.2*
10000	*36.5*	*1.6*	*44.9*	*1.6*
100000	*37.1*	*1.9*	*45.5*	*1.9*
1000000	*37.5*	*2.2*	*45.9*	*2.2*
Limit	*38.0*	*2.6*	*49.4*	*2.6*

Table 3.5 Sizewell. Modelled extremes of temperature (deg C)

Return Period (Years)	Control Climate		Anomaly Climate	
	Maximum Temperature	Standard Error Max Temp	Maximum Temperature	Standard Error Max Temp
2	32.4	0.4	39.2	0.4
5	34.4	0.5	41.2	0.5
10	35.5	0.5	42.3	0.5
20	36.4	0.6	43.2	0.6
50	*37.4*	*0.7*	*44.2*	*0.7*
100	*38.1*	*0.9*	*44.9*	*0.9*
200	*38.6*	*1.0*	*45.4*	*1.0*
500	*39.3*	*1.1*	*46.1*	*1.1*
1000	*39.7*	*1.3*	*46.5*	*1.3*
10000	*40.7*	*1.6*	*47.5*	*1.6*
100000	*41.3*	*2.0*	*48.1*	*2.0*
1000000	*41.7*	*2.2*	*48.5*	*2.2*
Limit	*42.2*	*2.7*	*49.0*	*2.7*

Table 3.6 Dungeness. Modelled extremes of temperature (deg C)

Return Period (Years)	Control Climate		Anomaly Climate	
	Maximum Temperature	Standard Error Max Temp	Maximum Temperature	Standard Error Max Temp
2	27.4	0.4	33.6	0.4
5	29.2	0.4	35.4	0.4
10	30.2	0.5	36.4	0.5
20	31.1	0.6	37.3	0.6
50	*32.0*	*0.7*	*38.2*	*0.7*
100	*32.6*	*0.8*	*38.8*	*0.8*
200	*33.1*	*0.9*	*39.3*	*0.9*
500	*33.7*	*1.1*	*39.9*	*1.1*
1000	*34.0*	*1.2*	*40.2*	*1.2*
10000	*35.0*	*1.5*	*41.2*	*1.5*
100000	*35.5*	*1.8*	*41.7*	*1.8*
1000000	*35.9*	*2.1*	*42.1*	*2.1*
Limit	*36.4*	*2.5*	*42.6*	*2.5*

Table 3.7 Hartlepool. Modelled extremes of temperature (deg C)

Return Period (Years)	Control Climate		Anomaly Climate	
	Maximum Temperature	Standard Error Max Temp	Maximum Temperature	Standard Error Max Temp
2	23.7	0.4	29.3	0.4
5	25.5	0.4	31.3	0.4
10	26.5	0.5	32.1	0.5
20	27.3	0.5	32.9	0.5
50	*28.2*	*0.7*	*33.8*	*0.7*
100	*28.8*	*0.8*	*34.4*	*0.8*
200	*29.2*	*0.9*	*34.8*	*0.9*
500	*29.8*	*1.0*	*35.4*	*1.0*
1000	*30.2*	*1.1*	*35.8*	*1.1*
10000	*31.0*	*1.5*	*36.6*	*1.5*
100000	*31.6*	*1.8*	*37.2*	*1.8*
1000000	*32.0*	*2.0*	*37.6*	*2.0*
Limit	*32.4*	*2.4*	*38.0*	*2.4*

Table 3.8 Hunterston. Modelled extremes of temperature (deg C)

3.20 It is apparent that (for example) the daily maximum temperature with a return period of 10,000 years is predicted to increase by several degrees Celsius for all sites, with the increase ranging from 5.2 degrees at Torness to 10.5 degrees at Hinkley Point. The intermediate predicted increases are 8.7 degrees at Heysham, 8.3 degrees at Bradwell, 6.8 degrees at Dungeness, 6.2 degrees at Hartlepool, 5.6 degrees at Hunterston and 8.4 degrees at Sizewell.

3.21 In summary, the climate model predicts that both daily maximum and minimum temperatures will increase in all seasons. Maximum daily temperatures will increase most during summer with increases being slightly less during winter. Extremely warm days will occur more frequently in summer although, as noted in the supplementary report by Arup (Appendix 6) of the 2004 report, temperatures will not approach the operating temperature of the cores of the decommissioned stations. Minimum, or night time, temperatures also increase at all locations resulting in fewer nights with freezing conditions and less severe temperatures for each of the decommissioned power station sites.

4. Predicted Precipitation Changes

4.1 Figures 4.1 to 4.2 show the predicted seasonal changes in precipitation amounts, for Heysham, relative to the 1961-90 control period, for thirty-year periods centred on the 2020s, 2050s and 2080s (rows, top to bottom respectively). The predicted changes are shown for the low, medium-low, medium-high and high emissions scenarios (columns, left to right). For all the maps in this chapter, the colour bars in the key are not symmetric around zero, because typically the magnitude of the greatest reductions is greater than the magnitude of the greatest increases.

4.2 Figure 4.1 shows the predicted changes in winter (December-January) average of the daily precipitation for the Low to High emissions scenarios for the Heysham area. It shows that for the 2080s, even in the Low scenario, significant increases (of between 15 and 20%) are predicted, and in the High scenario it is predicted that the seasonal average of the daily precipitation could increase by more than 30%.

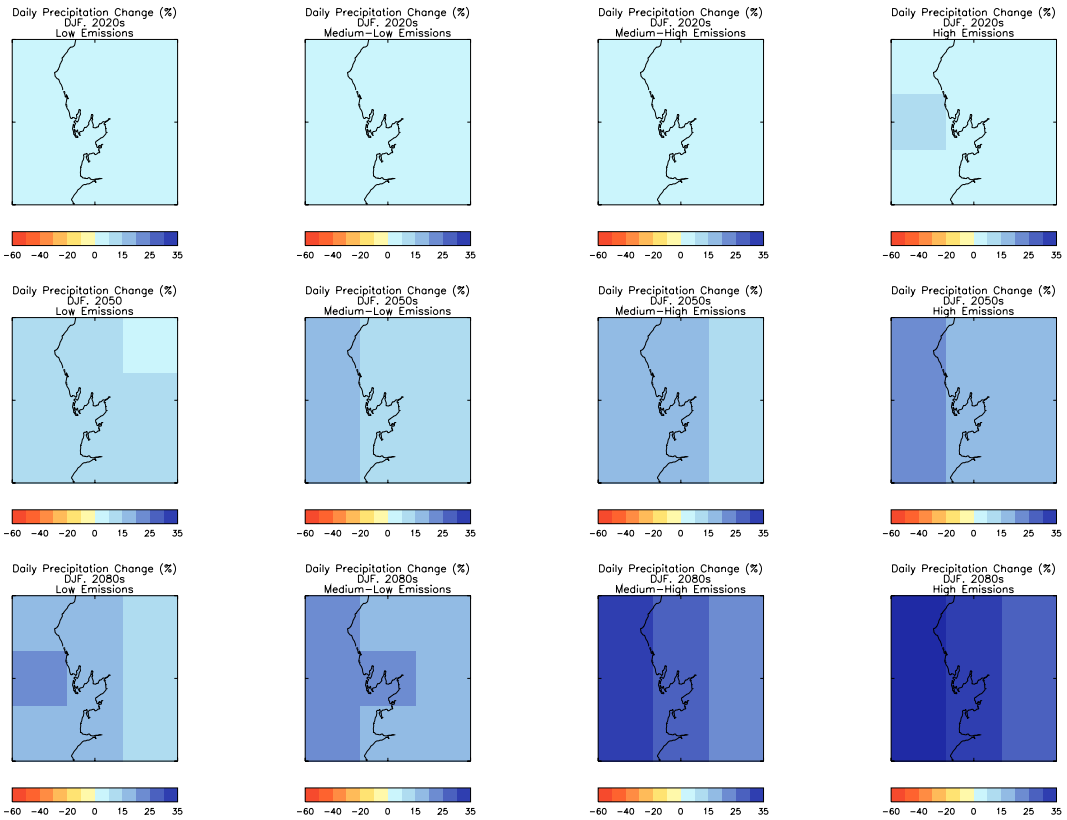

Figure 4.1. Predicted percentage change in wintertime (December- February) mean precipitation for the Heysham region. Low (left hand column), Medium Low (second column), Medium High (third column) and High (right hand column) emissions scenarios, for thirty-year periods centred on the 2020s (top row), 2050s (middle row) and 2080s (bottom row).

4.3 Figure 4.2 shows the precipitation changes predicted in summer for the Heysham area. By the 2080s it is predicted that there will be between 20 and 30% less precipitation falling in the summer, even in the Low emissions scenario. In the High emissions scenario, the predicted reductions are even greater, at between 40 and 50% over most of the land gridboxes in the region shown (the three leftmost gridboxes are treated as sea in the HadRM3 model).

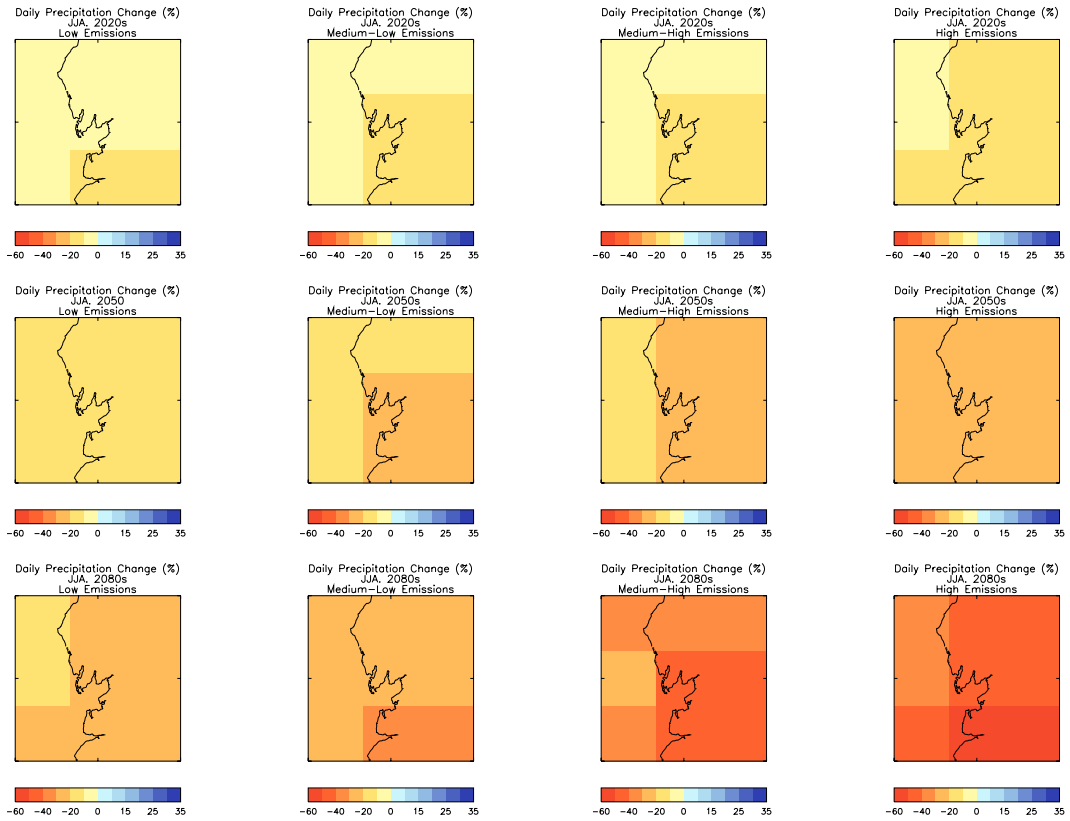

Figure 4.2. Predicted percentage change in summertime (June – August) mean precipitation for the Heysham region. Low (left hand column), Medium Low (second column), Medium High (third column) and High (right hand column) emissions scenarios, for thirty-year periods centred on the 2020s (top row), 2050s (middle row) and 2080s (bottom row).

4.4 Figures 4.3 and 4.4 show the predicted changes in the seasonal precipitation at Hinkley Point. It can be seen in Figure 4.3 that by the 2080s the mean winter precipitation around Hinkley Point is predicted to increase by 10 to 15% for the Low scenario, and to increase by more than 25% for the High scenario. Figure 4.4 shows that the model predicts that the mean summer precipitation around Hinkley Point will decrease by 30 to 40% for the Low scenario, and decrease by 50 to 60% for the High scenario by the 2080s.

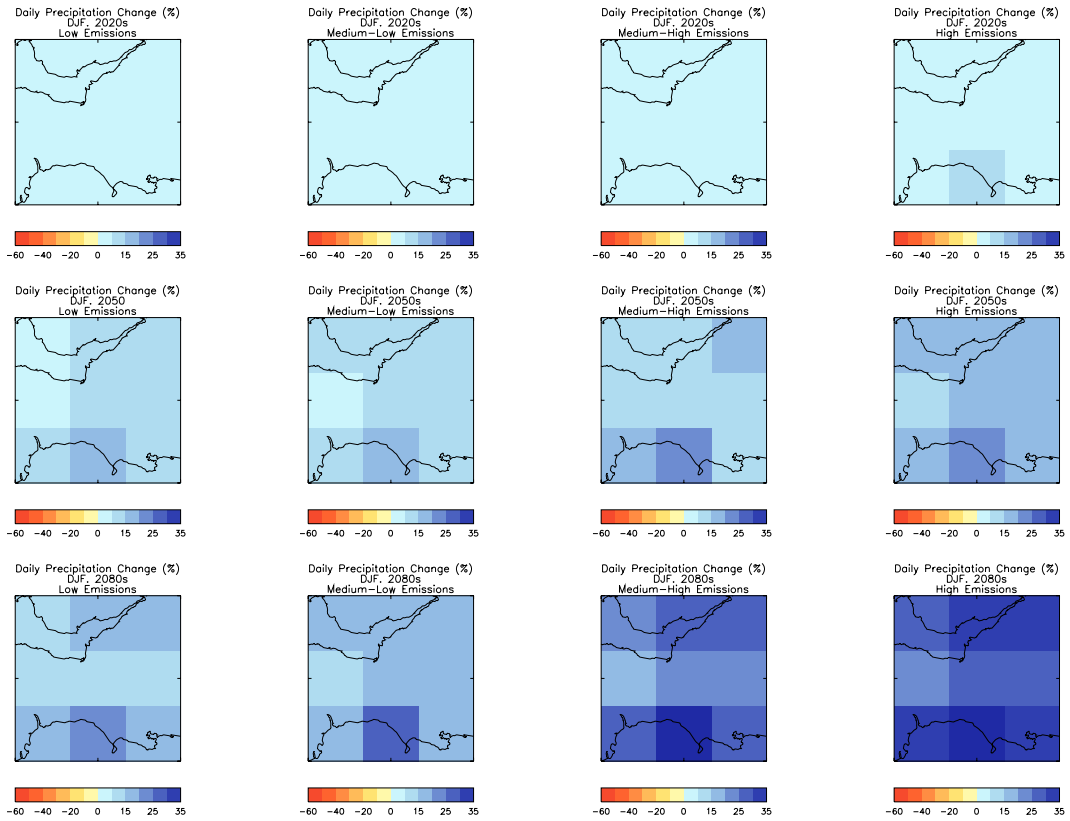

Figure 4.3. Predicted percentage change in winter (DJF) mean precipitation for the Hinkley Point region. Low (left hand column), Medium Low (second column), Medium High (third column) and High (right hand column) emissions scenarios, for thirty-year periods centred on the 2020s (top row), 2050s (middle row) and 2080s (bottom row).

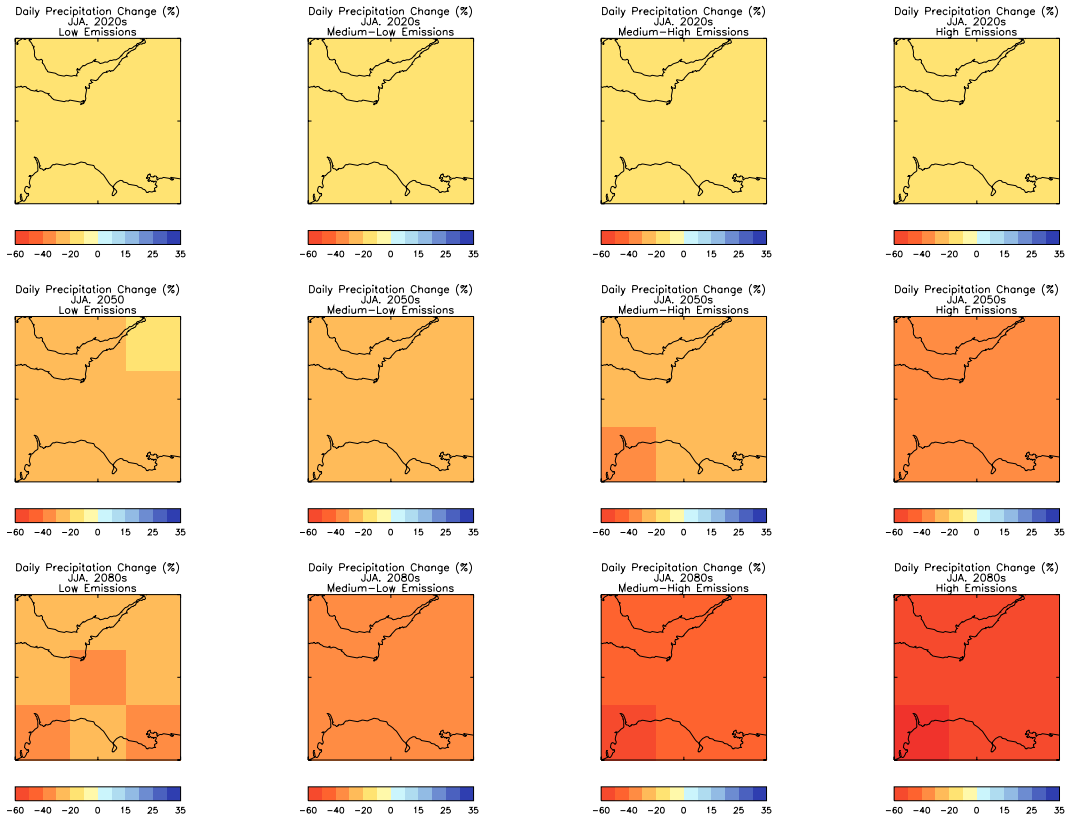

Figure 4.4 Predicted percentage change in summertime (June – August) mean precipitation for the Hinkley Point region. Low (left hand column), Medium Low (second column), Medium High (third column) and High (right hand column) emissions scenarios, for thirty-year periods centred on the 2020s (top row), 2050s (middle row) and 2080s (bottom row).

4.5 Figures 4.5 and 4.6 show the predicted changes in winter and summer precipitation in the Bradwell area. Figure 4.5 shows the predicted changes for winter, and shows a trend for the predicted precipitation increases to diminish as one moves inland from the east coast. In the Low scenario, by the 2080s the amount of winter precipitation is predicted to increase by 15 to 20% in most of the region shown, including the gridbox containing Bradwell power station itself. For the High scenario by the 2080s, the winter precipitation is predicted to increase by more than 30% over most of the area shown. Figure 4.6 shows the predicted changes for summer, and shows that the model predicts there will be reductions in summer precipitation for all timeslices and scenarios. By the 2080s even the Low scenario shows reductions of 20 to 30% over all gridboxes in the region. In the High scenario the predicted reductions are 40 to 60% for most of the land gridboxes in the area.

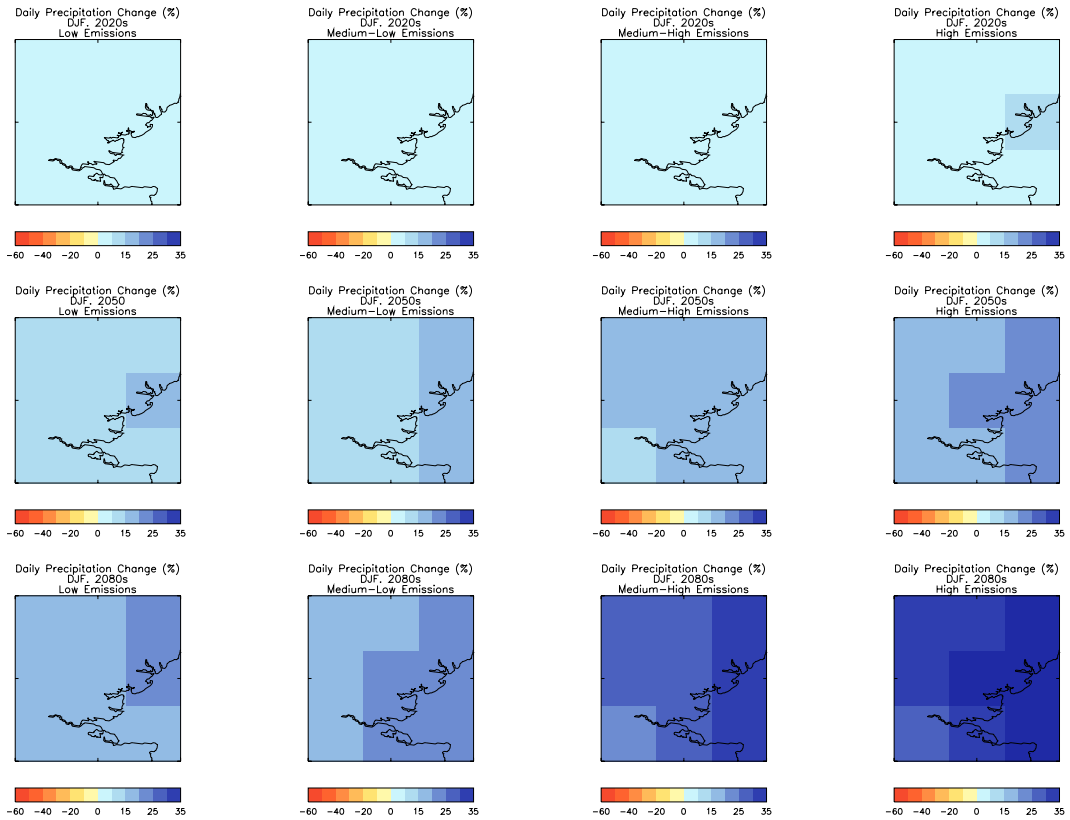

Figure 4.5 Predicted percentage change in winter (DJF) mean precipitation for the Bradwell region. Low (left hand column), Medium Low (second column), Medium High (third column) and High (right hand column) emissions scenarios, for thirty-year periods centred on the 2020s (top row), 2050s (middle row) and 2080s (bottom row).

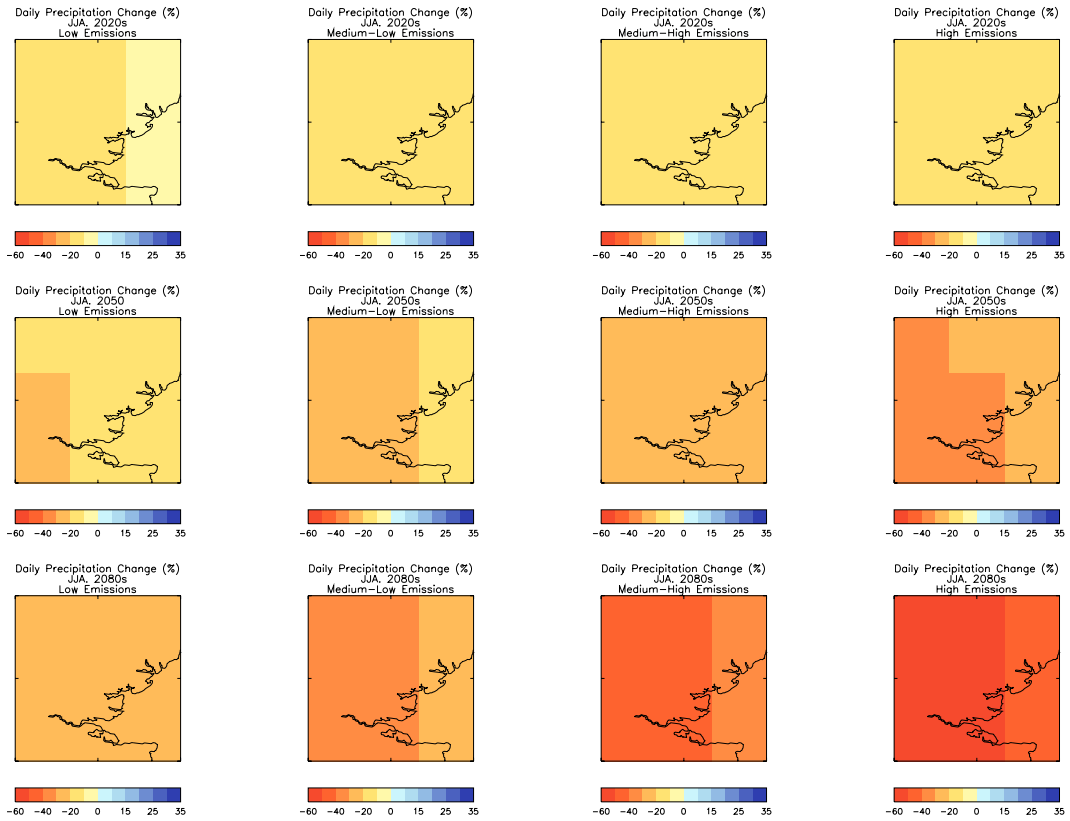

Figure 4.6 Predicted percentage change in summertime (June – August) mean precipitation for the Bradwell region. Low (left hand column), Medium Low (second column), Medium High (third column) and High (right hand column) emissions scenarios, for thirty-year periods centred on the 2020s (top row), 2050s (middle row) and 2080s (bottom row).

4.6 Figures 4.7 and 4.8 show the predicted changes in mean seasonal precipitation for the Torness region, for winter and summer respectively. Figure 4.7 shows that the model predicts that precipitation will increase in winter for all scenarios and timeslices. By the 2080s the Low scenario predicts that winter precipitation will have increased by 10-15% for most of the land gridboxes in the region, and by 25-30% for the sea gridbox containing the power station itself. In the High scenario the model predicts that by the 2080s, winter precipitation will have increased by more than 20% over most of the region, with increases of more than 30% in places. Figure 4.8 shows a predicted reduction in summer precipitation in the Torness region, as with all the regions being examined. The changes predicted for the 2080s range from decreases of 20 to 30% for all of the gridboxes in the Low scenario, to decreases of 40 to 50% for all of the land gridboxes in the High scenario.

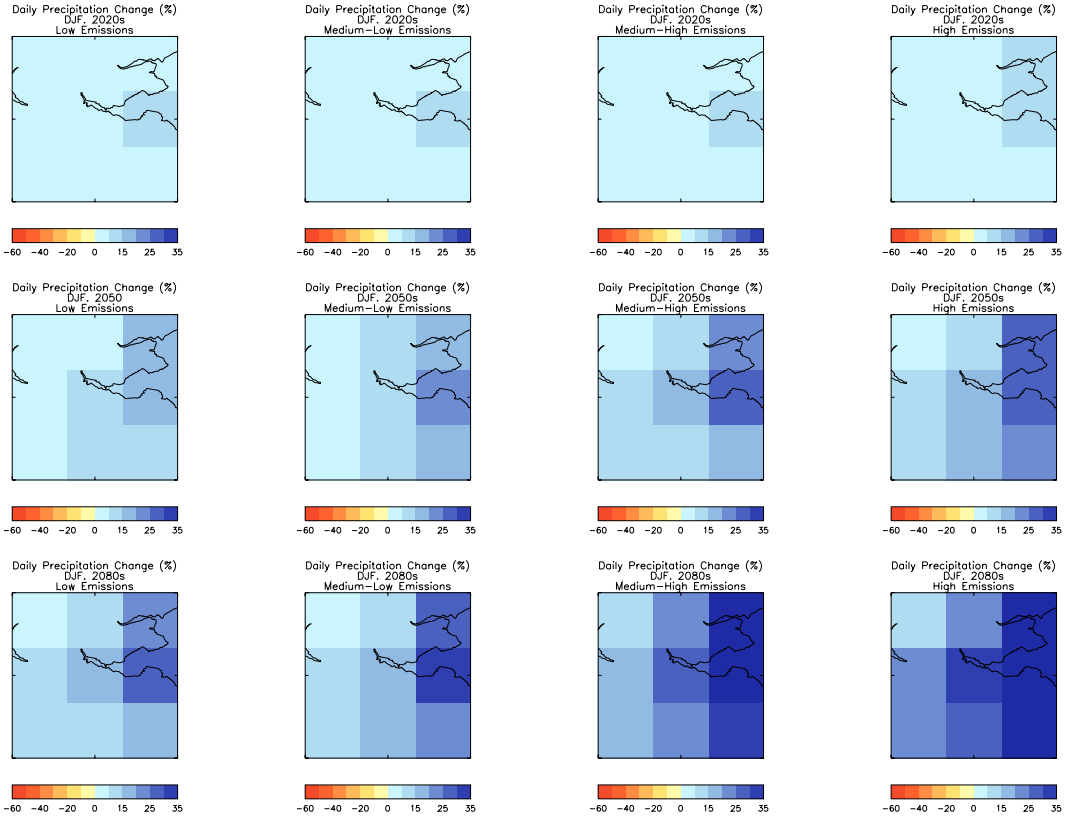

Figure 4.7 Predicted percentage change in winter (DJF) mean precipitation for the Torness region. Low (left hand column), Medium Low (second column), Medium High (third column) and High (right hand column) emissions scenarios, for thirty-year periods centred on the 2020s (top row), 2050s (middle row) and 2080s (bottom row).

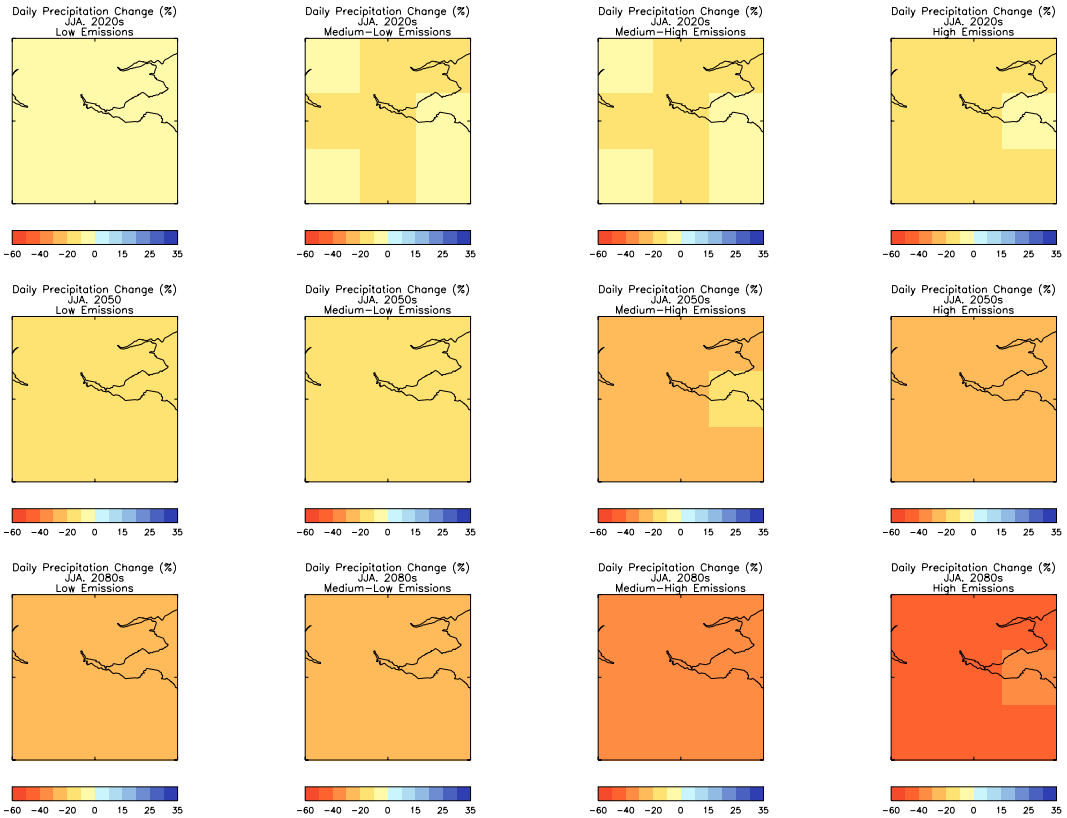

Figure 4.8 Predicted percentage change in summertime (June – August) mean precipitation for the Torness region. Low (left hand column), Medium Low (second column), Medium High (third column) and High (right hand column) emissions scenarios, for thirty-year periods centred on the 2020s (top row), 2050s (middle row) and 2080s (bottom row).

4.7 Figures 4.9 and 4.10 show the predicted changes in seasonal precipitation for the Sizewell region, for winter and summer respectively. From Figure 4.9 it can be seen that by the 2080s, the model predicts that for the Low scenario the winter precipitation will increase by 15 to 20% over most of the land gridboxes in the region (with increases of 20 to 25% over all of the sea gridboxes and the nearest land gridbox to the actual location of Sizewell). For the High scenario the model predicts increases of more than 30% over almost all of the region. Figure 4.10 shows that the model predicts that for the Low scenario the summer precipitation amount in the 2080s will be 20 to 30% smaller over all the land gridboxes in the region, whilst in the High scenario the model predicts there will be reductions of 40 to 60% over the land portion of the region.

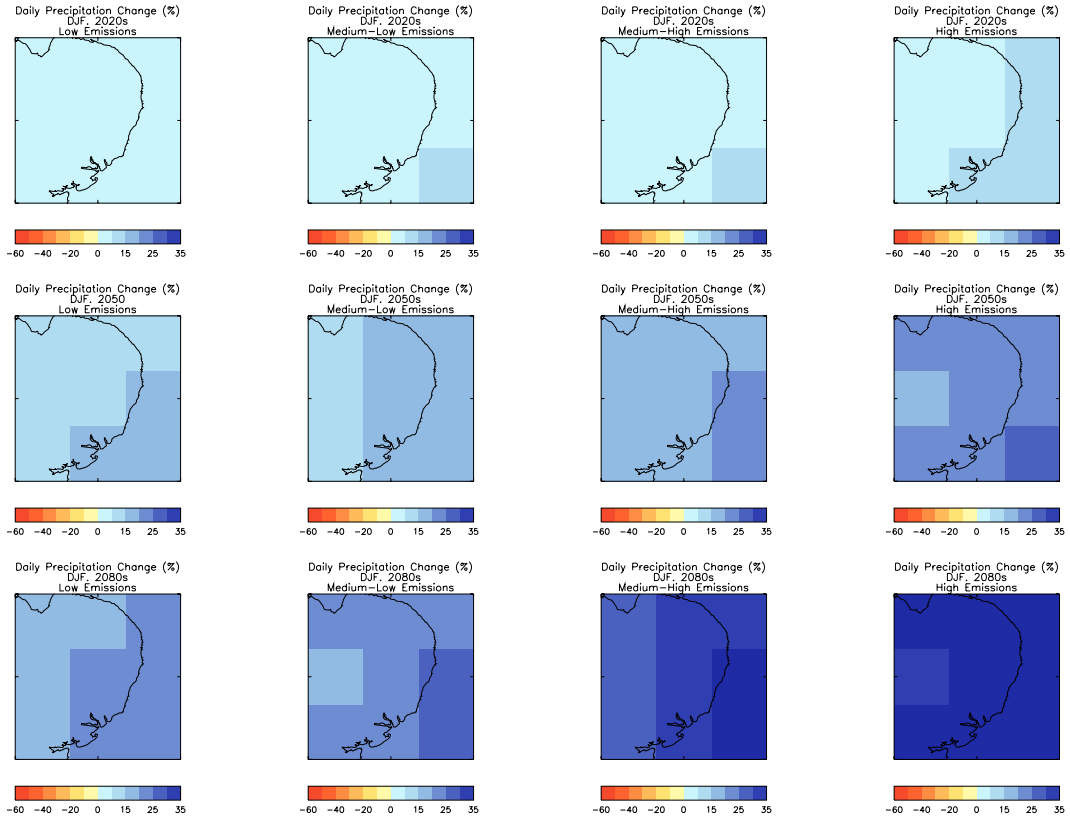

Figure 4.9 Predicted percentage change in winter (DJF) mean precipitation for the Sizewell region. Low (left hand column), Medium Low (second column), Medium High (third column) and High (right hand column) emissions scenarios, for thirty-year periods centred on the 2020s (top row), 2050s (middle row) and 2080s (bottom row).

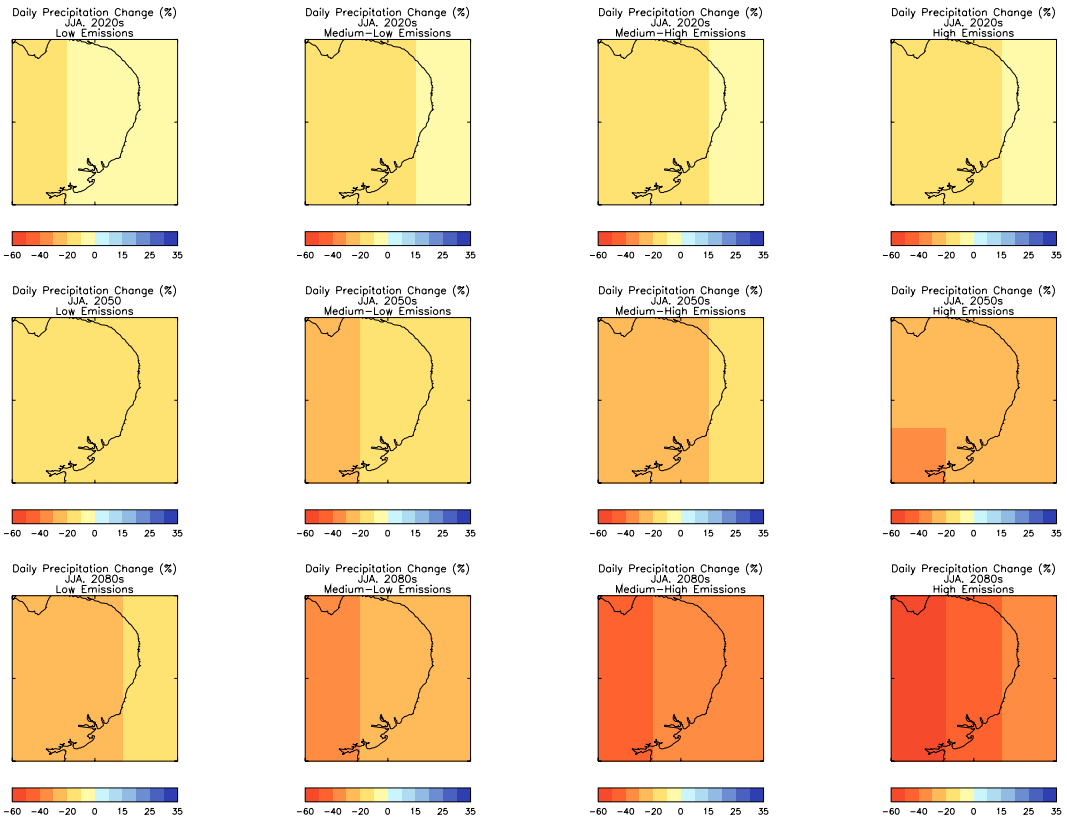

Figure 4.10 Predicted percentage change in summertime (June – August) mean precipitation for the Sizewell region. Low (left hand column), Medium Low (second column), Medium High (third column) and High (right hand column) emissions scenarios, for thirty-year periods centred on the 2020s (top row), 2050s (middle row) and 2080s (bottom row).

4.8 Figures 4.11 and 4.12 show the predicted changes in the seasonal precipitation at Dungeness. It can be seen in Figure 4.3 that by the 2080s the mean winter precipitation around Dungeness is predicted to increase by 15 to 20% for the Low scenario, and to increase by more than 30% for the High scenario. Figure 4.4 shows that the model predicts that the mean summer precipitation around Dungeness will decrease by 20 to 30% for the Low scenario, and decrease by 50 to 60% for the High scenario.

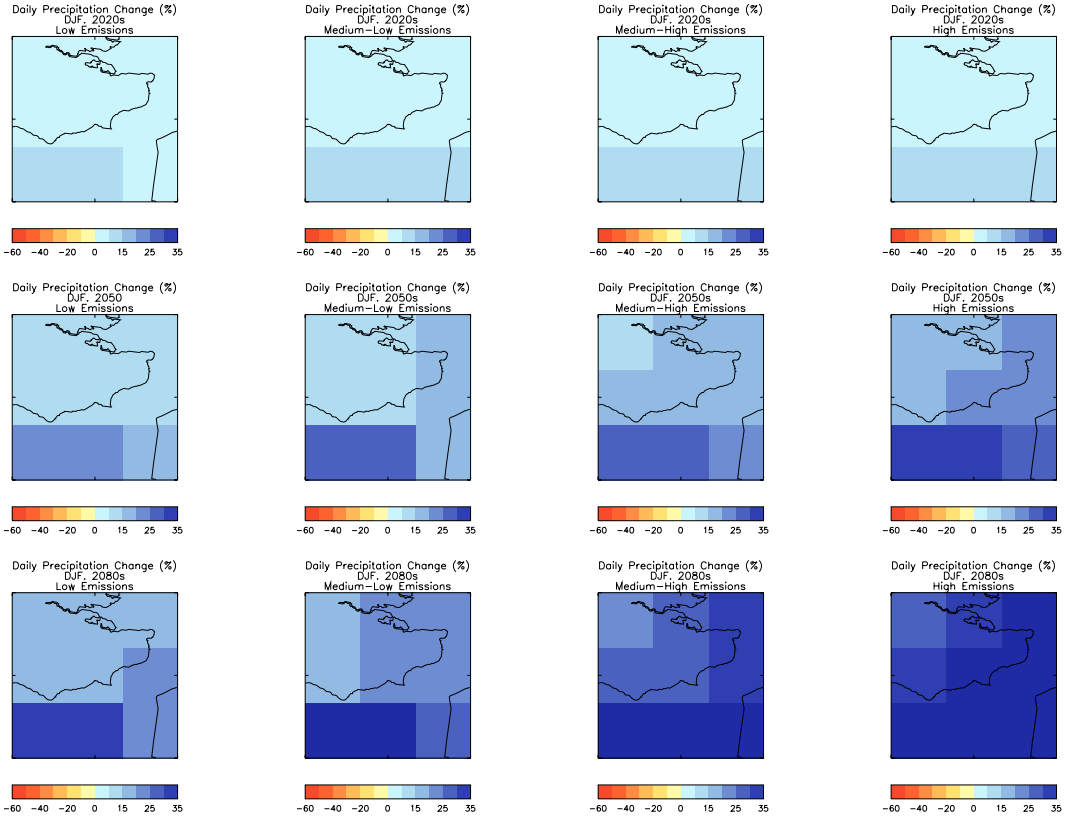

Figure 4.11. Predicted percentage change in winter (DJF) mean precipitation for the Dungeness region. Low (left hand column), Medium Low (second column), Medium High (third column) and High (right hand column) emissions scenarios, for thirty-year periods centred on the 2020s (top row), 2050s (middle row) and 2080s (bottom row).

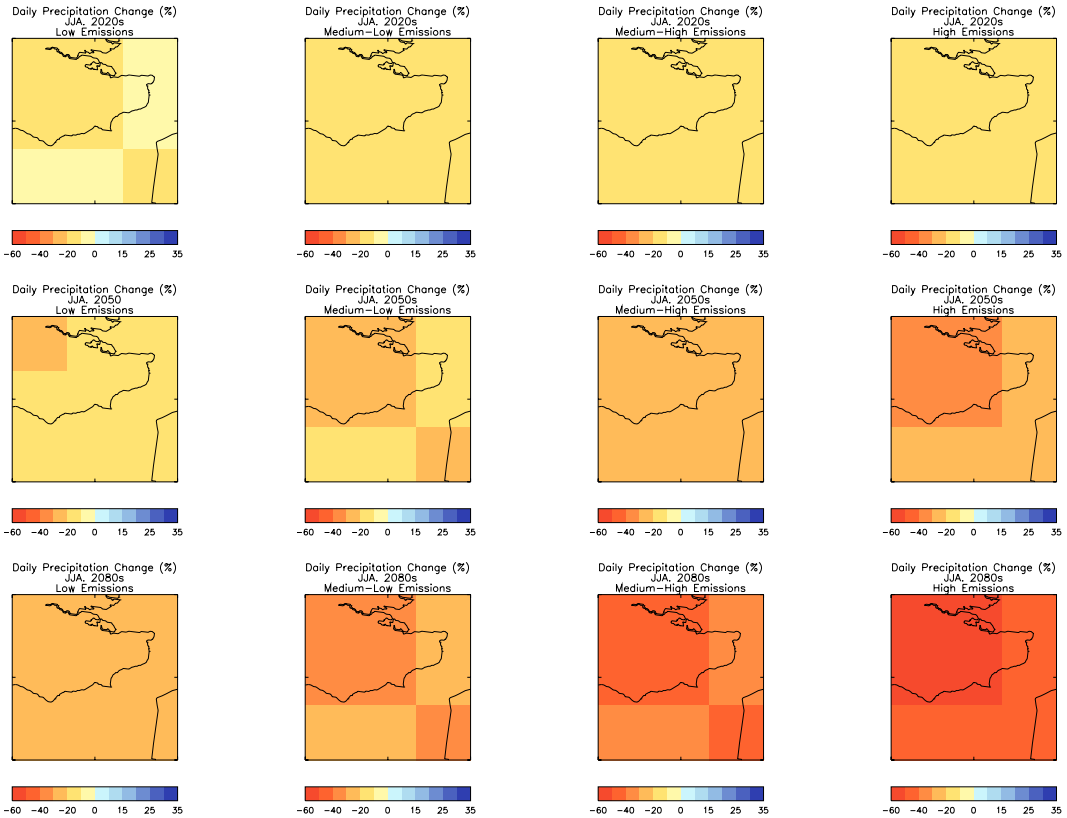

Figure 4.12 Predicted percentage change in summertime (June – August) mean precipitation for the Dungeness region. Low (left hand column), Medium Low (second column), Medium High (third column) and High (right hand column) emissions scenarios, for thirty-year periods centred on the 2020s (top row), 2050s (middle row) and 2080s (bottom row).

4.9 Figures 4.13 and 4.14 show the predicted changes in winter and summer precipitation in the Hartlepool area. Figure 4.13 shows the predicted changes for winter, and shows a trend for the predicted precipitation increases to diminish as one moves inland from the east coast. However, even in the Low scenario, by the 2080s the amount of winter precipitation is predicted to increase by 10 to 15% in the west of the region shown, and by 20 to 25% for the gridbox containing Hartlepool power station itself. For the High scenario by the 2080s, the winter precipitation is predicted to increase by more than 25% over most of the area shown. Figure 4.14 shows the predicted changes for summer, and shows that the model predicts there will be reductions in summer precipitation for all timeslices and scenarios. By the 2080s even the Low scenario shows reductions of 20 to 30% over all land gridboxes in the region. In the High scenario the predicted reductions are 40 to 60% for most of the land gridboxes in the area.

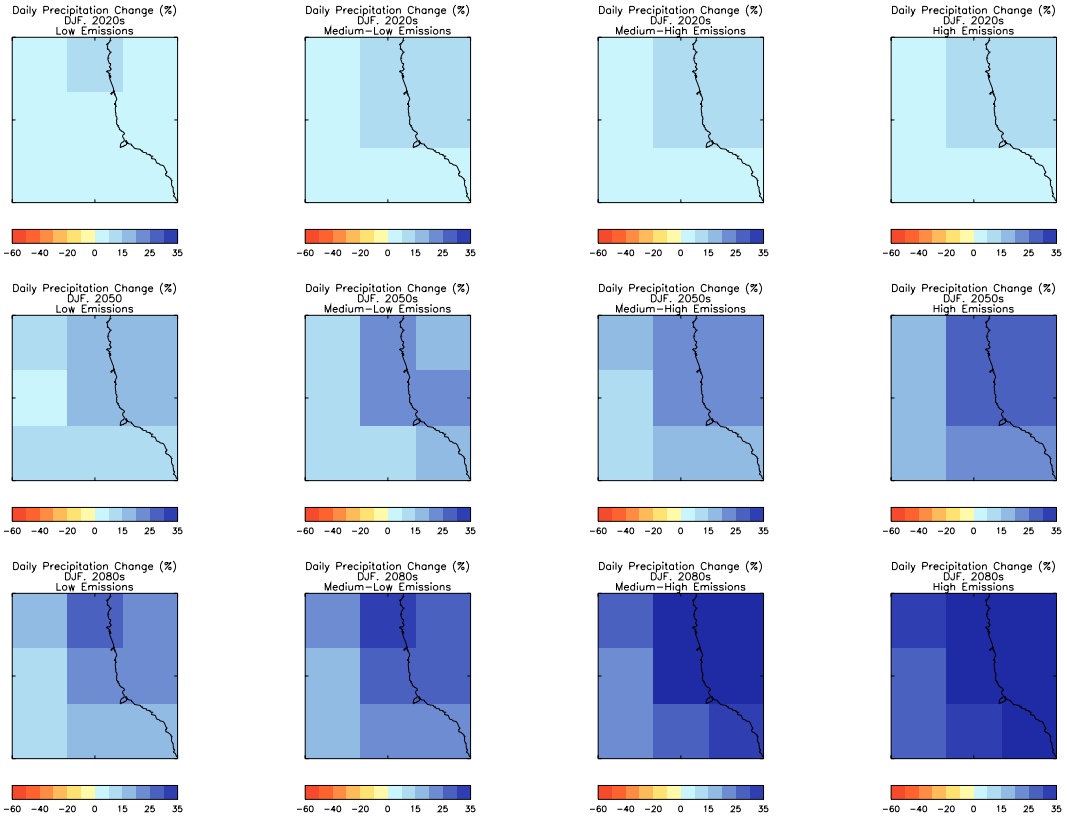

Figure 4.13 Predicted percentage change in winter (DJF) mean precipitation for the Hartlepool region. Low (left hand column), Medium Low (second column), Medium High (third column) and High (right hand column) emissions scenarios, for thirty-year periods centred on the 2020s (top row), 2050s (middle row) and 2080s (bottom row).

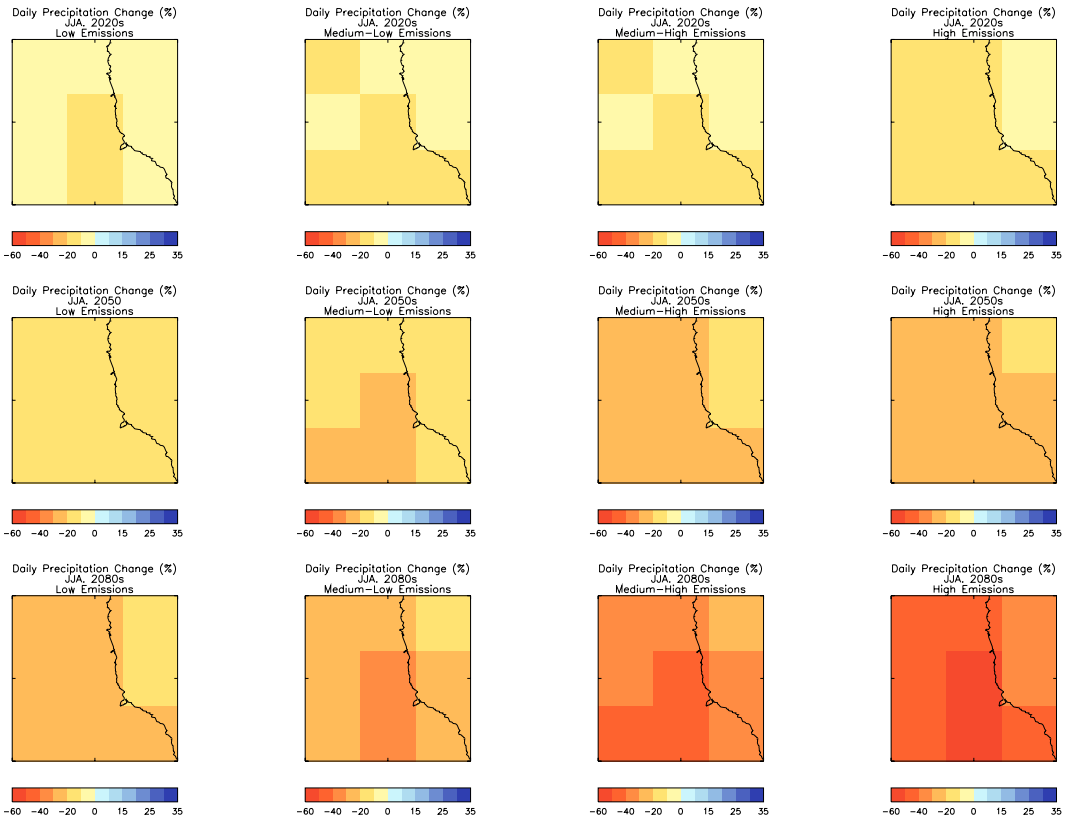

Figure 4.14 Predicted percentage change in summertime (June – August) mean precipitation for the Hartlepool region. Low (left hand column), Medium Low (second column), Medium High (third column) and High (right hand column) emissions scenarios, for thirty-year periods centred on the 2020s (top row), 2050s (middle row) and 2080s (bottom row).

4.10 Figures 4.15 and 4.16 show the predicted changes in mean seasonal precipitation for the Hunterston region, for winter and summer respectively. Figure 4.15 shows that although the model predicts that precipitation will increase in winter for all scenarios and timeslices, the increases are smaller than for the other sites examined, and it is only for the more severe emissions scenarios and the later timeslices that all of the predicted changes in the area shown exceed 10%. By the 2080s the Low scenario predicts that winter precipitation will have increased by up to 10% for some of the region, and by 10-15% for the rest of the region. In the High scenario the model predicts that by the 2080s, winter precipitation will have increased by more than 15% over most of the region, with increases of 20 to 25% in places. Figure 4.16 shows a predicted reduction in summer precipitation in the Hunterston region, as with all the regions being examined. The changes predicted for the 2080s range from decreases of 20 to 30% over most of the land gridboxes in the Low scenario, to decreases of 40 to 50% over most of the land gridboxes in the High scenario.

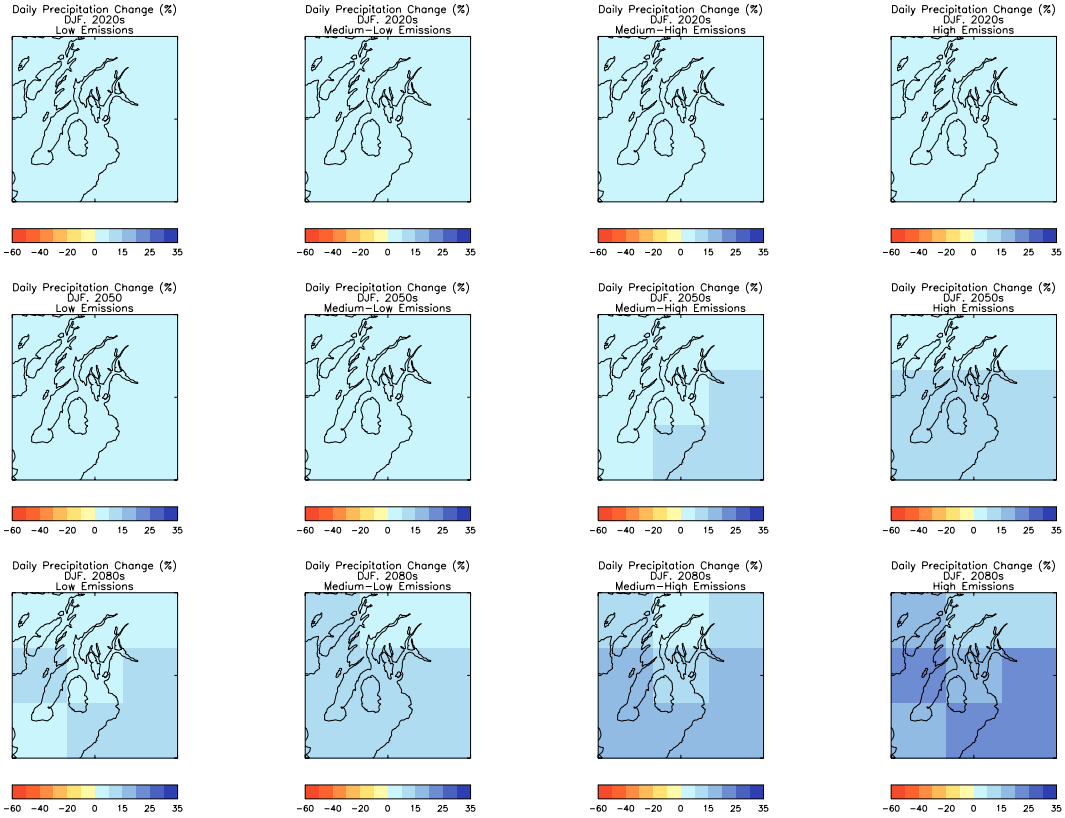

Figure 4.15 Predicted percentage change in winter (DJF) mean precipitation for the Hunterston region. Low (left hand column), Medium Low (second column), Medium High (third column) and High (right hand column) emissions scenarios, for thirty-year periods centred on the 2020s (top row), 2050s (middle row) and 2080s (bottom row).

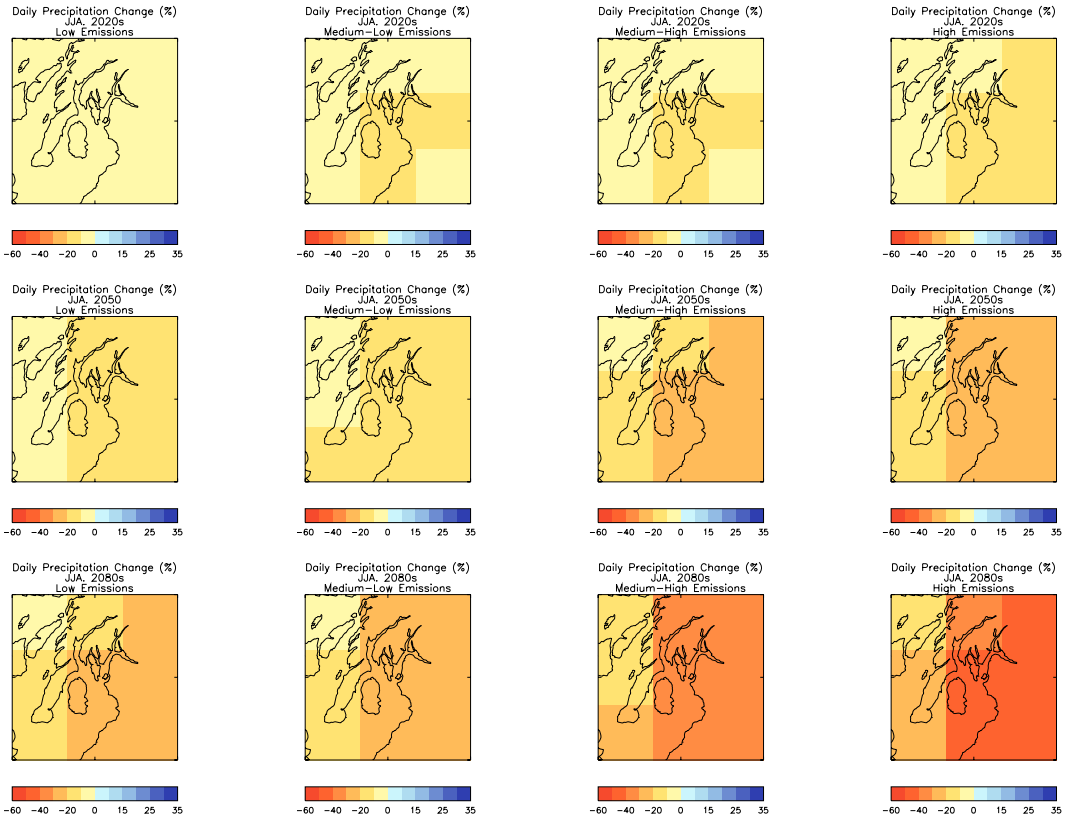

Figure 4.16 Predicted percentage change in summertime (June – August) mean precipitation for the Hunterston region. Low (left hand column), Medium Low (second column), Medium High (third column) and High (right hand column) emissions scenarios, for thirty-year periods centred on the 2020s (top row), 2050s (middle row) and 2080s (bottom row).

4.11 Figures 4.17 to 4.24 show the predicted changes in probability distributions for daily precipitation for the Medium-High scenario, for winter and summer, with the control run shown in black and the 2080s run (labelled GHG) shown in red. The probability is shown on a linear vertical axis from 0.00 to 0.50 (i.e. as a proportion not a percentage), with events of probability greater than 0.5 not shown, in order to show the changes in extreme events more clearly. The amount of daily rainfall (in mm) is shown on the horizontal axis. Since the analysis is split by season, a probability of 0.1 means that such an event will occur, on average, on approximately 9 days in a season. The analyses were done using the individual land gridboxes closest to the power stations, rather than for the groups of nine gridboxes used for the maps of changes.

4.12 Figure 4.17 shows the predicted changes in the probability distribution of daily precipitation for Heysham. The winter graph is different from those for most of the other sites (except Hinkley Point: see Figure 4.18) for winter, as both Heysham and Hinkley Point (or the regions representing them in the RCM) have a probability of approximately 0.02 of experiencing events of more than 10mm/day in winter, for both the control run and the 2080s. The other sites only have a probability of 0.01 or less for similarly-sized events. In summer the model predicts that for Heysham the probability of significant rainfall events will be lower in the future, e.g. the probability of 6mm/day decreases from about 0.03 to 0.02. In winter there appears to be a very slight increase in the probability of significant rainfall events, but the signal is approximately the same magnitude as the “noise”.

4.13 For the other sites, the predicted changes (probability reductions of up to 0.04 in the summer event range from 1 to 9 mm/day) are quite similar, as are the shapes of the probability curves for the control climate.

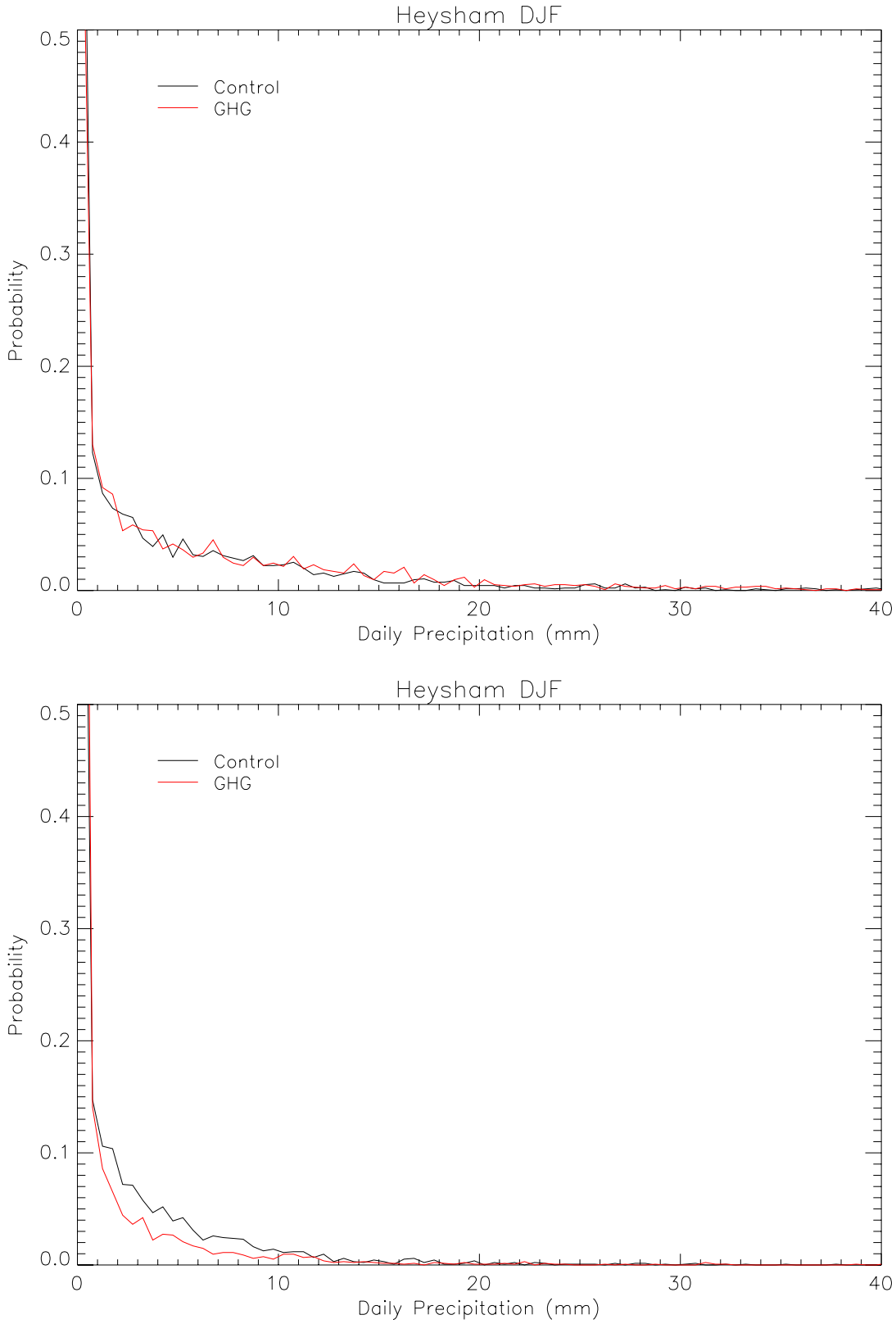

Figure 4.17 Probability of exceedence of daily precipitation totals for Heysham. Modelled current climate (black) and Medium High scenario 2080s climate (red) for winter (December – February, upper panel) and summer (June – August, lower panel)

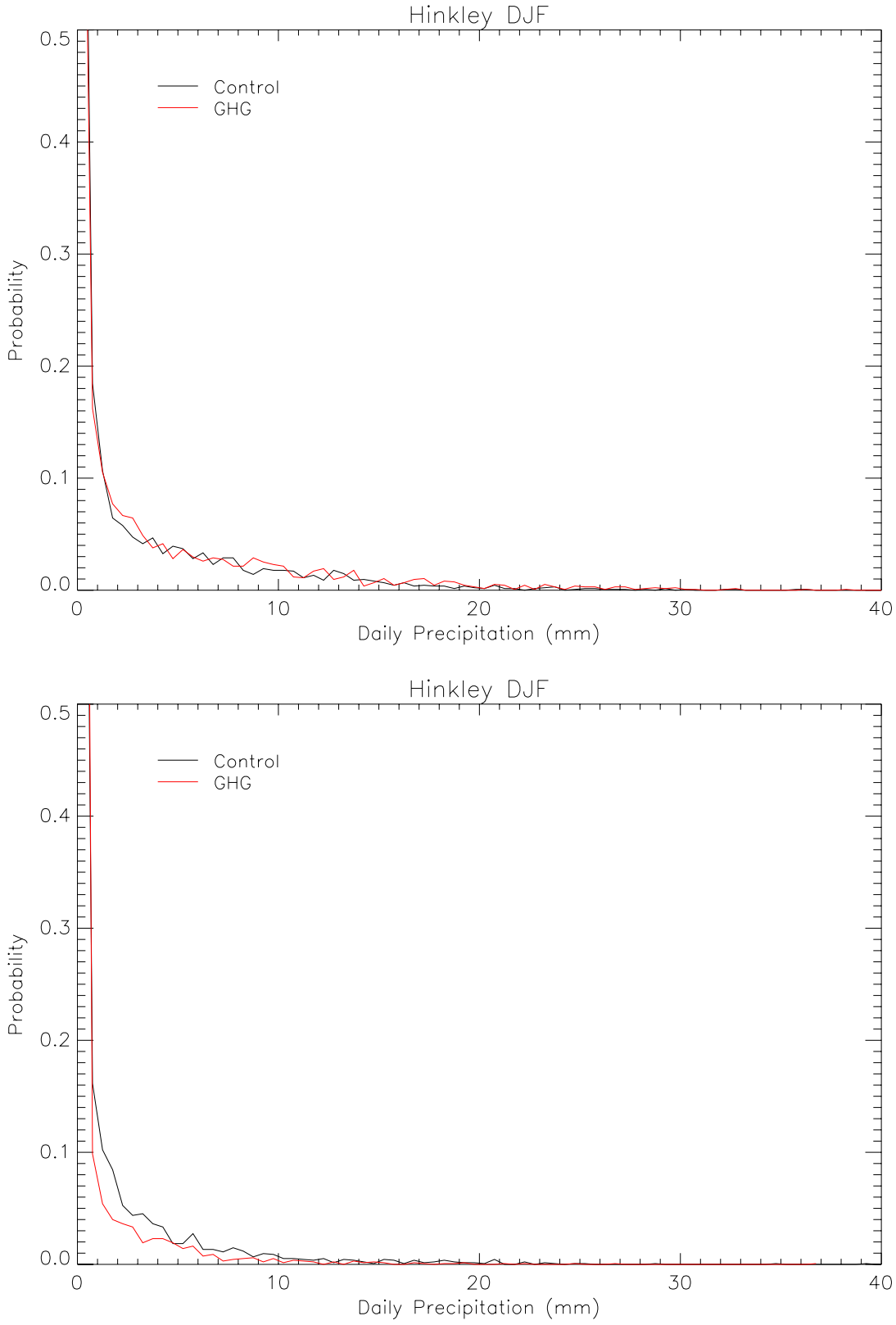

Figure 4.18 Probability of exceedence of daily precipitation totals for Hinkley Point. Modelled current climate (black) and Medium High scenario 2080s climate (red) for winter (December – February, upper panel) and summer (June – August, lower panel)

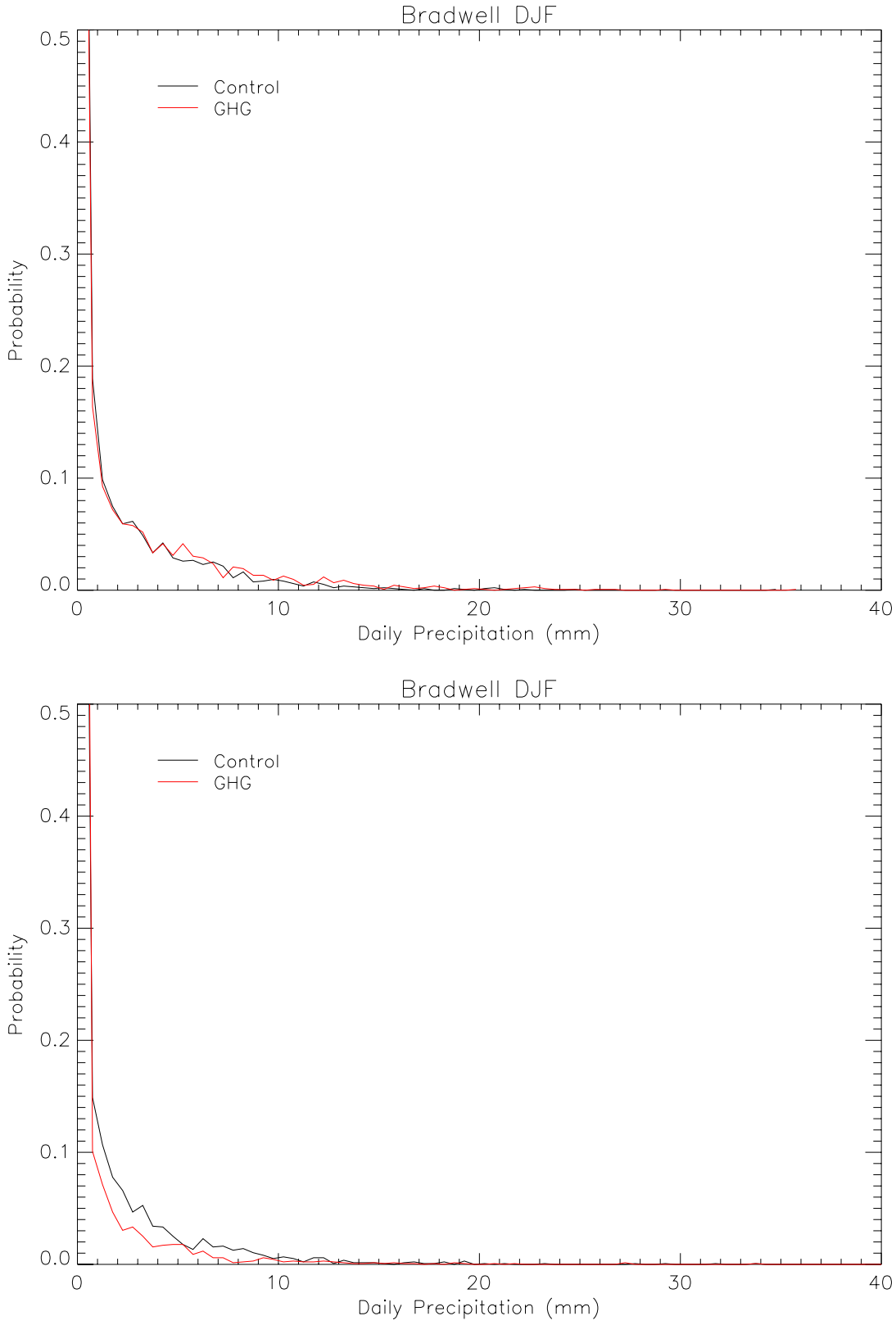

Figure 4.19 Probability of exceedence of daily precipitation totals for Bradwell. Modelled current climate (black) and Medium High scenario 2080s climate (red) for winter (December – February, upper panel) and summer (June – August, lower panel)

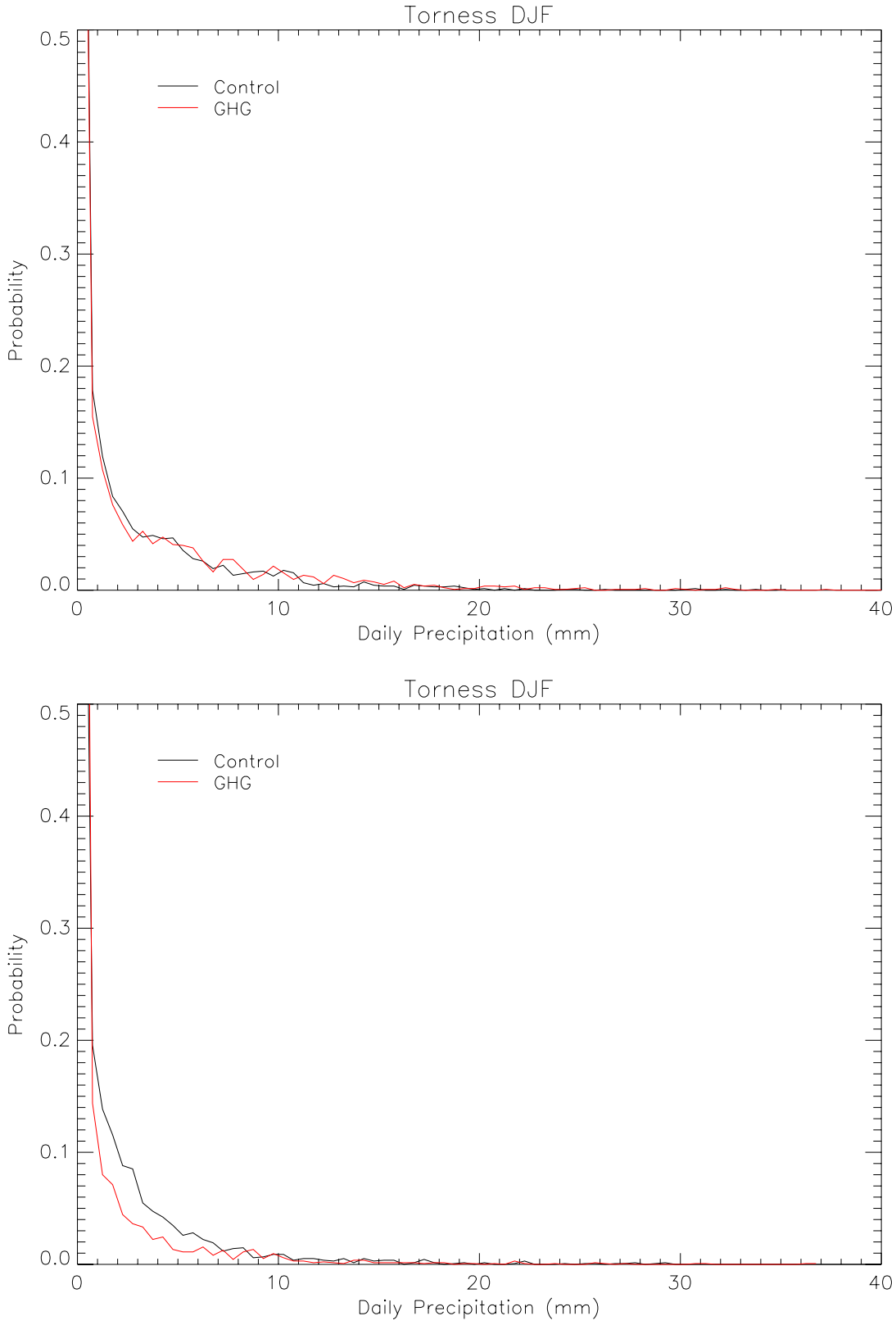

Figure 4.20 Probability of exceedence of daily precipitation totals for Torness. Modelled current climate (black) and Medium High scenario 2080s climate (red) for winter (December – February, upper panel) and summer (June – August, lower panel)

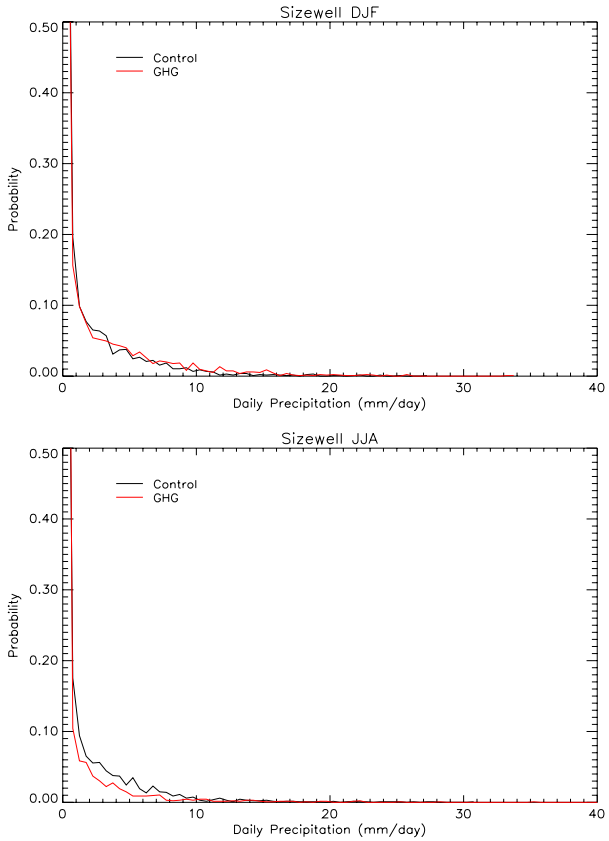

Figure 4.21 Probability of exceedence of daily precipitation totals for Sizewell. Modelled current climate (black) and Medium High scenario 2080s climate (red) for winter (December – February, upper panel) and summer (June – August, lower panel)

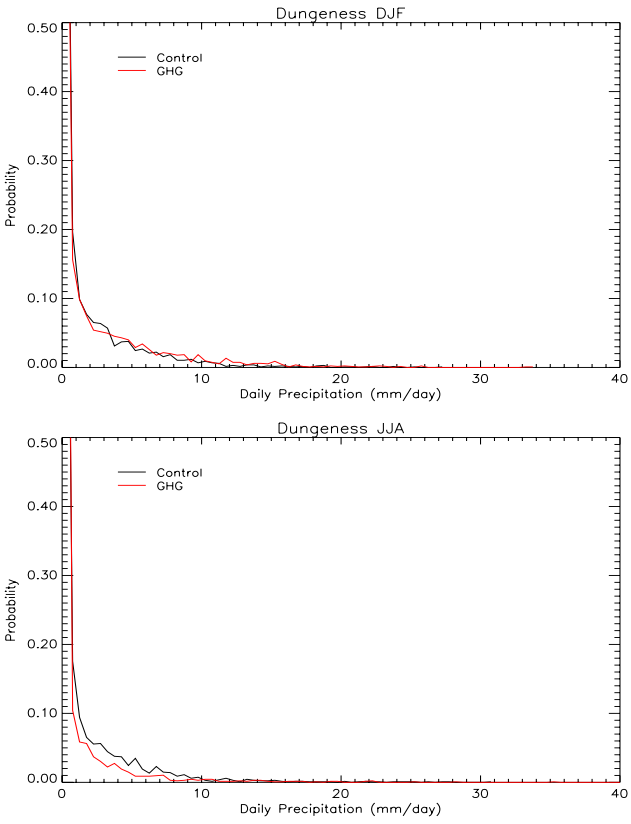

Figure 4.22 Probability of exceedence of daily precipitation totals for Dungeness. Modelled current climate (black) and Medium High scenario 2080s climate (red) for winter (December – February, upper panel) and summer (June – August, lower panel)

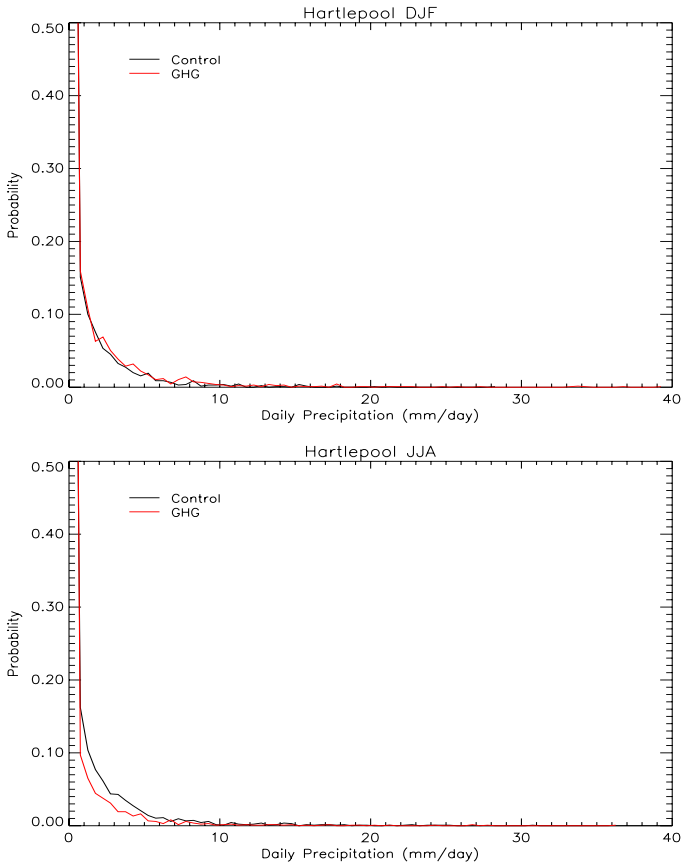

Figure 4.23 Probability of exceedence of daily precipitation totals for Hartlepool. Modelled current climate (black) and Medium High scenario 2080s climate (red) for winter (December – February, upper panel) and summer (June – August, lower panel)

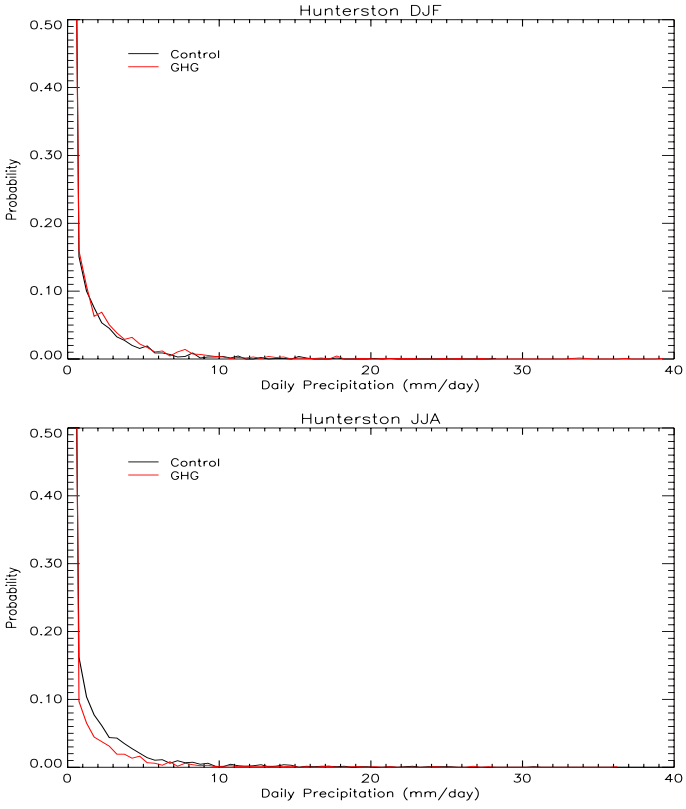

Figure 4.24 Probability of exceedence of daily precipitation totals for Hunterston. Modelled current climate (black) and Medium High scenario 2080s climate (red) for winter (December – February, upper panel) and summer (June – August, lower panel)

4.14 For all eight sites, the seasonally-split probability distributions of daily precipitation in Figures 4.17 to 4.24 show that events in the approximate range 1 to 9 mm are less likely to occur in summer by the 2080s. There is comparatively little change in the distributions of winter daily precipitation, but most of the sites seem to show a very slight increase in the probability of events in the same sort of rainfall depth range in winter by the 2080s.

4.15 Tables 4.1 to 4.8 show the predicted extreme precipitation changes, derived from the HadRM3 and previous-generation HadRM2 RCM precipitation data for the control and Medium-High 2080s runs. The future run of HadRM2 was only 20 years long, so for these extreme value analyses only 20 years of data from the HadRM3 runs was used in order to keep the methods of analysis consistent. This means that the validity of the results diminishes significantly for return periods greater than 10 to 20 years. The method used was the Peaks Over Threshold method, which involved extracting the Partial Duration Series (or PDS) of the top eighty events from the twenty years of data, fitting a statistical distribution (the Generalised Pareto) to the extracted data using the method of probability weighted moments, then using Extreme Value Analysis to derive the Return Period Amounts for various return periods. Note that because the climate model data lengths were 20 years, estimation of return period quantities for greater than 20 years is highly uncertain, so the lines for return periods of 25 years and more are italicised to show that they are indicative.

4.16 The following tables 4.1 and 4.2 are for 6-hour precipitation data from the HadRM3 regional climate model (RCM). The values are "uplifts" i.e. 2080s return period amounts (RPAs) divided by the return period amounts from the control run of the RCM. The confidence in the predictions diminishes as the Return Period (RP) increases, as the RP becomes greater than the length of the data series. Note that for Sizewell, for RP>100 years, the future 6h amounts are predicted to be slightly smaller than in the current climate. Little significance can be attached to this result, as that RP greatly exceeds the length of the data series. For Heysham there is also a predicted reduction in future return period amounts when the RP is greater than or equal to 10 years. In general the model predicts that RPAs for 6-hour precipitation events in the 2080s will be greater than the control climate, for most sites. It predicts that for an RP of 10 years, 6-hour precipitation events in the 2080s will be approximately 5 to 10% greater than the control climate for Bradwell and Dungeness, 10 to 15% greater than the control climate for Hinkley Point, Hartlepool, Hunterston and Sizewell, and 29% greater for Torness.

RP (years)	Heysham	Hinkley Point	Bradwell	Torness
1	1.10	1.15	1.03	1.11
2	1.07	1.16	1.04	1.16
5	1.02	1.17	1.05	1.22
10	0.98	1.16	1.07	1.29
20	0.93	1.16	1.09	1.37
25	*0.92*	*1.15*	*1.09*	*1.40*
50	*0.87*	*1.14*	*1.12*	*1.48*
100	*0.83*	*1.13*	*1.14*	*1.57*
1000	*0.68*	*1.09*	*1.25*	*1.90*
10000	*0.56*	*1.03*	*1.38*	*2.30*

Table 4.1 Six-hourly rainfall amount return periods, uplift for 2080s relative to present day (1961-1990). Derived from HadRM3

RP (years)	Dungeness	Hartlepool	Hunterston	Sizewell
1	1.05	1.00	1.09	1.14
2	1.05	1.02	1.08	1.13
5	1.05	1.06	1.09	1.13
10	1.05	1.11	1.11	1.11
20	1.06	1.16	1.13	1.10
25	*1.06*	*1.18*	*1.14*	*1.09*
50	*1.06*	*1.25*	*1.17*	*1.08*
100	*1.07*	*1.32*	*1.21*	*1.06*
1000	*1.09*	*1.60*	*1.36*	*0.99*
10000	*1.12*	*1.94*	*1.56*	*0.92*

Table 4.2 Six-hourly rainfall amount return periods, uplift for 2080s relative to present day (1961-1990). Derived from HadRM3

4.17 Tables 4.3 to 4.6 show the predicted extreme precipitation changes derived from the HadRM2 RCM precipitation data. Although HadRM2 is a previous generation of model, lacking some of the scientific enhancements of HadRM3, it is still a model which gives a reasonable simulation of the present climate and we have no reason to presume it does not give a reasonable simulation of the future climate. Some differences between the results of the two models arise because of the slightly different emissions scenarios used: HadRM2 used the IPCC IS92a scenario, which is closer to the medium-high (A2) UKCIP02 scenario used in HadRM3 than any of the other three UKCIP02 scenarios. The main reason for the differences in the future climates of the two models is thought to be the difference in the average atmospheric circulation in the global climate models that "drive" them, e.g. HadRM3 is driven by global model HadCM3, and HadRM2 is driven by HadCM2.

4.18 Tables 4.3 and 4.4 show the predicted extreme precipitation changes for 6-hour events, derived from the HadRM2 RCM precipitation data. It is included for comparison with the later climate model HadRM3, to illustrate some of the uncertainty in modelling climate change. It is apparent that the uplifts derived from the HadRM2 model are significantly greater than those derived from HadRM3, mostly within the range 20 to 35% greater in the 2080s than in the HadRM2 control run. However, both models show uplifts of more than 1.0 for most sites and RPs, supporting the view that future sub-daily rainfall events will become more extreme.

RP (years)	Heysham	Hinkley Point	Bradwell	Torness
1	1.27	1.19	1.30	1.26
2	1.26	1.16	1.31	1.27
5	1.27	1.12	1.34	1.28
10	1.28	1.07	1.38	1.30
20	1.30	1.02	1.42	1.31
25	*1.31*	*1.01*	*1.43*	*1.31*
50	*1.33*	*0.96*	*1.48*	*1.32*
100	*1.36*	*0.91*	*1.54*	*1.33*
1000	*1.48*	*0.77*	*1.78*	*1.36*
10000	*1.63*	*0.65*	*2.09*	*1.39*

Table 4.3 Six-hourly rainfall amount return periods, uplift for 2080s relative to present day. Derived from HadRM2.

RP (years)	Dungeness	Hartlepool	Hunterston	Sizewell
1	1.30	1.14	1.39	1.30
2	1.36	1.15	1.37	1.33
5	1.45	1.19	1.32	1.35
10	1.56	1.24	1.27	1.35
20	1.68	1.30	1.21	1.36
25	*1.72*	*1.32*	*1.19*	*1.36*
50	*1.87*	*1.38*	*1.13*	*1.35*
100	*2.03*	*1.46*	*1.08*	*1.35*
1000	*2.71*	*1.74*	*0.89*	*1.31*
10000	*3.70*	*2.08*	*0.72*	*1.26*

Table 4.4 Six-hourly rainfall amount return periods, uplift for 2080s relative to present day. Derived from HadRM2.

4.19 Tables 4.5 and 4.6 show the predicted extreme precipitation changes for 1-hour events, derived from the HadRM2 RCM six-hour and twelve-hour precipitation data using an interpolation method published in the Flood Estimation Handbook (Robson and Reed, 1999). Tables 4.7 and 4.8 show the same, but for 12-hour precipitation, derived directly from the model data. Both sets of tables show that future precipitation amounts are predicted by the HadRM2 model to be greater in the 2080s than in the current climate, for almost all return periods and locations.

RP (years)	Heysham	Hinkley Point	Bradwell	Torness
1	1.26	1.17	1.35	1.31
2	1.25	1.14	1.37	1.32
5	1.26	1.10	1.39	1.33
10	1.27	1.05	1.43	1.35
20	1.29	1.00	1.47	1.36
25	*1.30*	*0.99*	*1.49*	*1.36*
50	*1.32*	*0.94*	*1.54*	*1.37*
100	*1.35*	*0.89*	*1.60*	*1.38*
1000	*1.47*	*0.75*	*1.83*	*1.41*
10000	*1.62*	*0.62*	*2.15*	*1.44*

Table 4.5 One-hourly rainfall amount return periods, uplift for 2080s relative to present day- Derived from HadRM2.

RP (years)	Dungeness	Hartlepool	Hunterston	Sizewell
1	1.29	1.17	1.40	1.37
2	1.35	1.18	1.37	1.40
5	1.44	1.22	1.33	1.42
10	1.55	1.27	1.28	1.43
20	1.67	1.32	1.22	1.43
25	*1.71*	*1.34*	*1.20*	*1.43*
50	*1.85*	*1.41*	*1.14*	*1.43*
100	*2.01*	*1.48*	*1.08*	*1.42*
1000	*2.70*	*1.76*	*0.89*	*1.39*
10000	*3.69*	*2.10*	*0.73*	*1.34*

Table 4.6 One-hourly rainfall amount return periods, uplift for 2080s relative to present day- Derived from HadRM2.

RP (years)	Heysham	Hinkley Point	Bradwell	Torness
1	1.28	1.22	1.23	1.20
2	1.25	1.20	1.25	1.23
5	1.19	1.16	1.31	1.28
10	1.13	1.13	1.41	1.33
20	1.07	1.09	1.54	1.39
25	*1.04*	*1.08*	*1.59*	*1.41*
50	*0.97*	*1.04*	*1.76*	*1.48*
100	*0.90*	*1.00*	*1.97*	*1.55*
1000	*0.69*	*0.89*	*3.06*	*1.81*
10000	*0.51*	*0.78*	*5.07*	*2.14*

Table 4.7 Twelve-hourly rainfall amount return periods, uplift for 2080s relative to present day. Derived from HadRM2.

RP (years)	Dungeness	Hartlepool	Hunterston	Sizewell
1	1.32	1.11	1.38	1.20
2	1.37	1.16	1.40	1.22
5	1.44	1.25	1.42	1.27
10	1.51	1.35	1.44	1.36
20	1.59	1.47	1.47	1.48
25	*1.61*	*1.51*	*1.47*	*1.52*
50	*1.70*	*1.65*	*1.50*	*1.68*
100	*1.79*	*1.80*	*1.52*	*1.88*
1000	*2.14*	*2.47*	*1.59*	*2.87*
10000	*2.60*	*3.42*	*1.67*	*4.66*

Table 4.8 Twelve-hourly rainfall amount return periods, uplift for 2080s relative to present day. Derived from HadRM2.

5. Wind

5.1 The figures in this section show the winter and summer changes in the 10m (above ground) wind speed predicted by HadRM3. Changes in average wind direction predicted by the climate model are not shown because there is considerable uncertainty in climate model predictions of that aspect of the climate. The skill of climate models to predict wind speed is not as great as the skill in predicting temperature and precipitation. Changes in micro climatic effects (sea breezes) can not be modelled by a 50km resolution model, and may have an effect on coastal sites particularly in the summer. The coastlines are slightly different from those in the maps of other changes because the climate model calculates wind values on a grid which is offset by half a gridbox from the grid used for other quantities.

5.2 Figure 5.1 shows the predicted changes in average winter 10m wind speed from the 2020s to the 2080s for the Heysham region. For most timeslices and scenarios small increases (less than 4%) are predicted to occur. It is only for the two greatest emissions scenarios in the 2080s that winter increases of more than 4% are predicted.

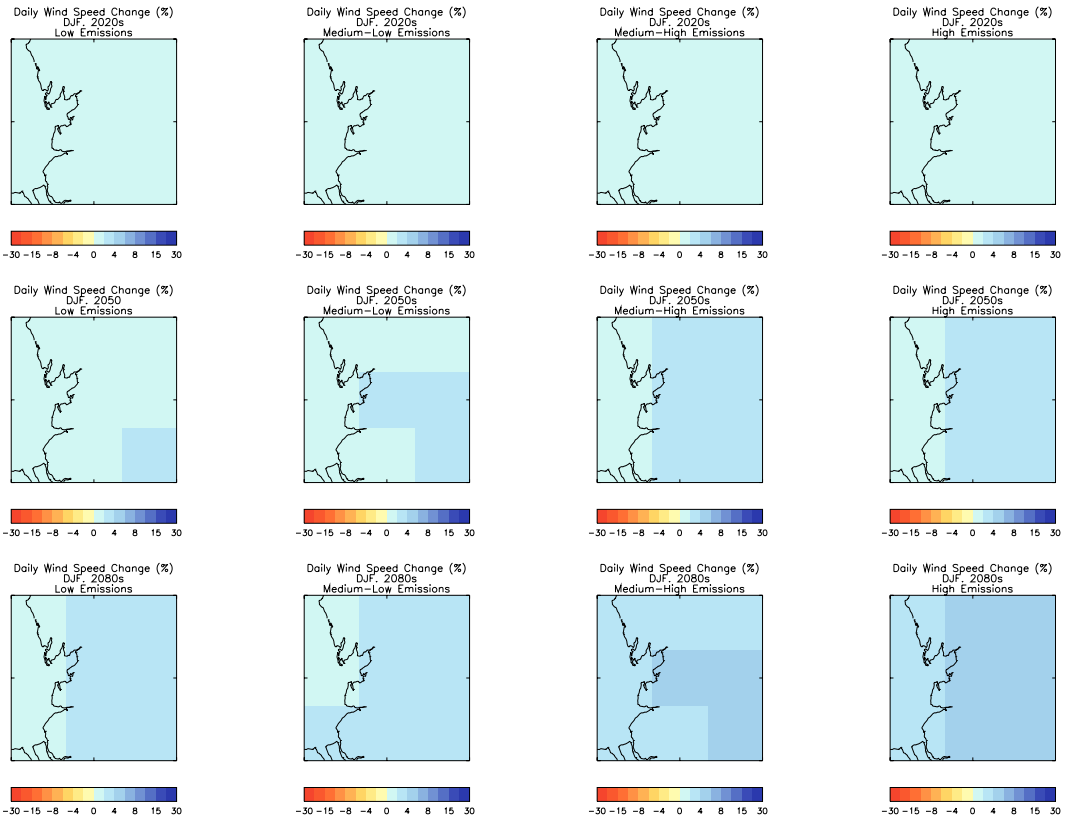

Figure 5.1 Predicted percentage change in wintertime (December – February) mean wind speed for the Heysham region. Low (left hand column), Medium Low (second column), Medium High (third column) and High (right hand column) emissions scenarios, for thirty-year periods centred on the 2020s (top row), 2050s (middle row) and 2080s (bottom row).

5.3 Figure 5.2 shows the predicted changes in average summer 10m wind speed from the 2020s to the 2080s for the Heysham region. The model predicts that there will be reductions in the summer average 10m wind speed for all timeslices and scenarios, but as with the predictions for winter in this area, the magnitude of the predicted changes is quite small (around 4%) for most gridboxes in the region. It is only in the Medium-High and High scenarios for

the 2080s that the coastal gridboxes near Heysham are predicted to experience reductions of more than 4%.

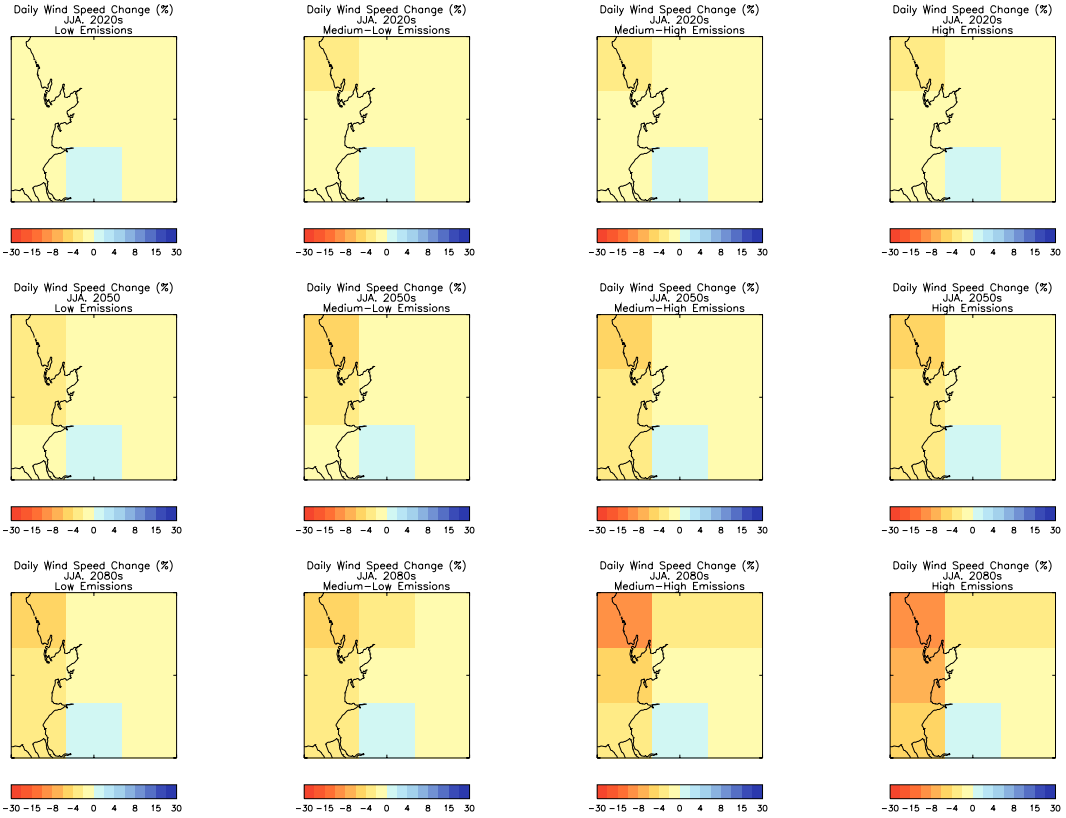

Figure 5.2 Predicted percentage change in summertime (June – August) mean wind speed for the Heysham region. Low (left hand column), Medium Low (second column), Medium High (third column) and High (right hand column) emissions scenarios, for thirty-year periods centred on the 2020s (top row), 2050s (middle row) and 2080s (bottom row).

5.4 Figure 5.3 shows the predicted changes in average winter 10m wind speed from the 2020s to the 2080s for the Hinkley Point region. Like Heysham, the winter average daily wind speed is predicted to increase (by a greater percentage than Heysham) but in contrast to Heysham, the summer average daily 10m wind speed in much of the area around Hinkley Point is predicted to increase, although in the gridbox containing the power station itself, the summer wind speed is predicted to decrease slightly, by 0 to 2%.

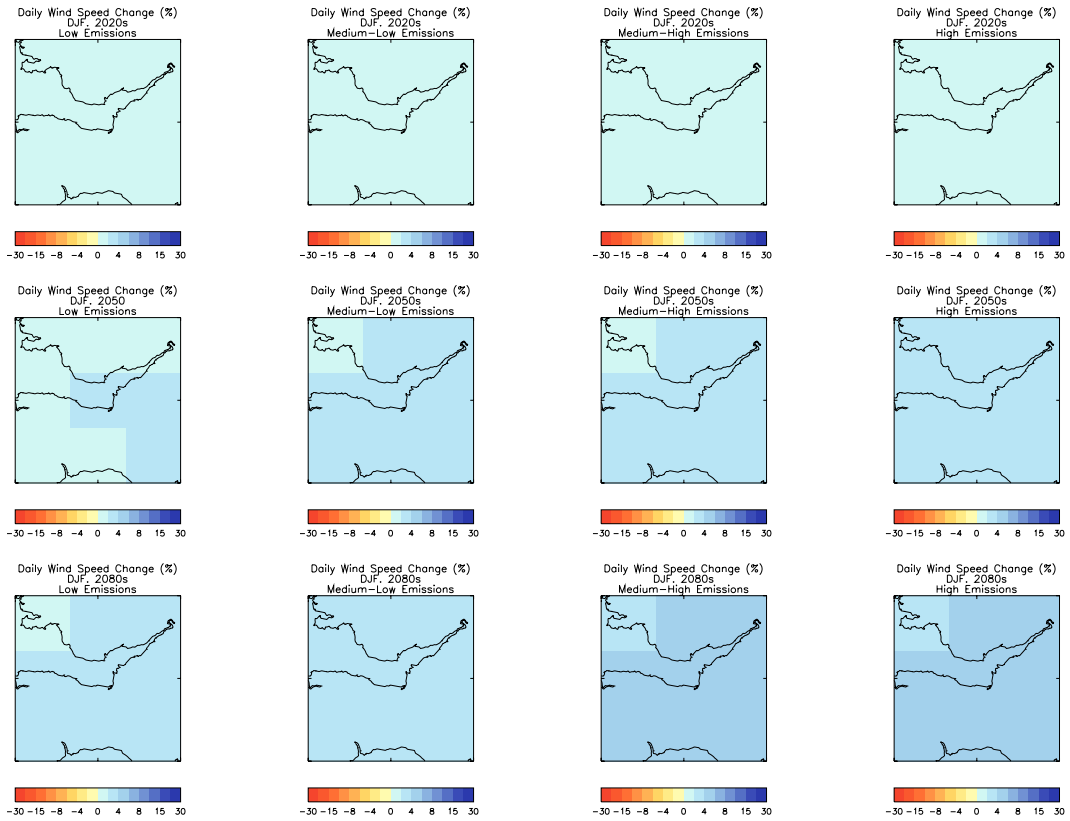

Figure 5.3 Predicted percentage change in wintertime (December – February) mean wind speed for the Hinkley Point region. Low (left hand column), Medium Low (second column), Medium High (third column) and High (right hand column) emissions scenarios, for thirty-year periods centred on the 2020s (top row), 2050s (middle row) and 2080s (bottom row).

5.5 Figure 5.4 shows the predicted changes in average summer 10m wind speed from the 2020s to the 2080s for the Hinkley Point region. The model predicts that for the Hinkley Point area both modest increases and decreases will be seen in summer, possibly not even outside the range of natural variability for the Low scenario at Hinkley Point itself (which is a land gridbox). Even for the High scenario the increases by the 2080s are predicted to be between 2 to 4% for most of the land gridboxes in the area, with reductions of less than 2% for the Hinkley Point gridbox itself, and 2 to 4% for the gridbox to the west.

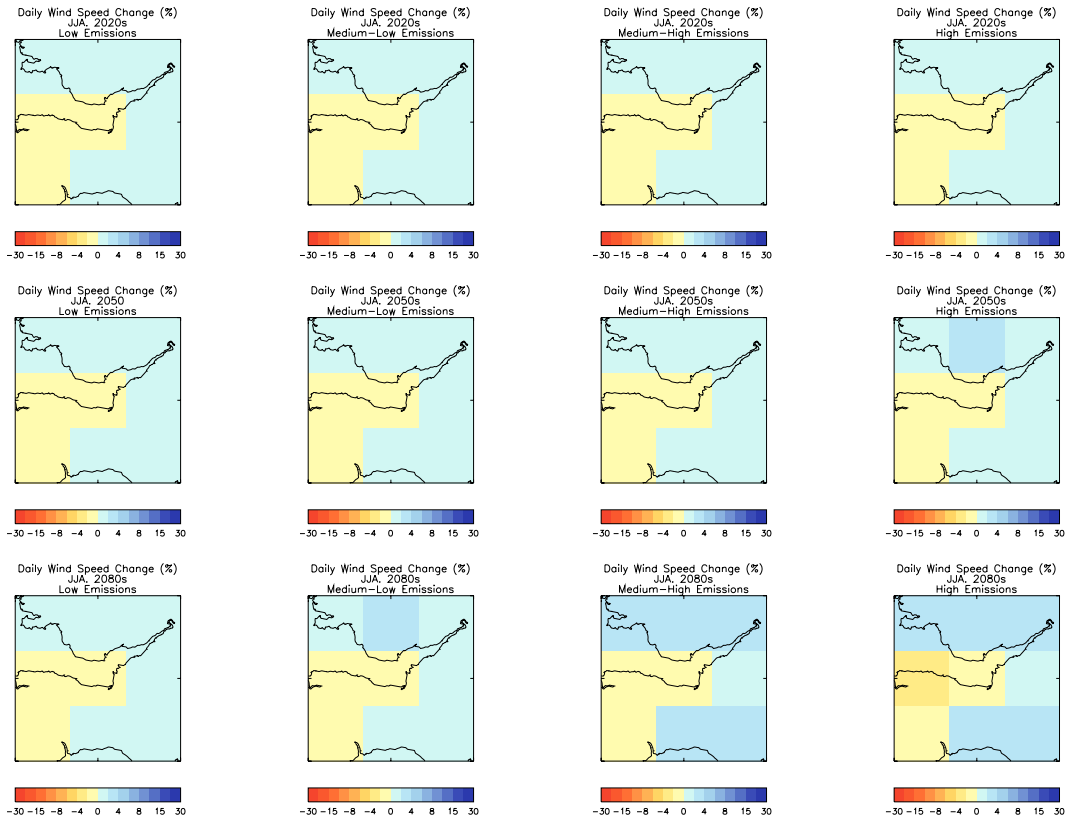

Figure 5.4 Predicted percentage change in summertime (June – August) mean wind speed for the Hinkley Point region. Low (left hand column), Medium Low (second column), Medium High (third column) and High (right hand column) emissions scenarios, for thirty-year periods centred on the 2020s (top row), 2050s (middle row) and 2080s (bottom row).

5.6 Figure 5.5 shows the predicted changes in average winter 10m wind speed from the 2020s to the 2080s for the Bradwell region. Increases are predicted for all timeslices and emissions scenarios, but the increases are less than 6% for all but the Medium-High and High scenarios in the 2080s.

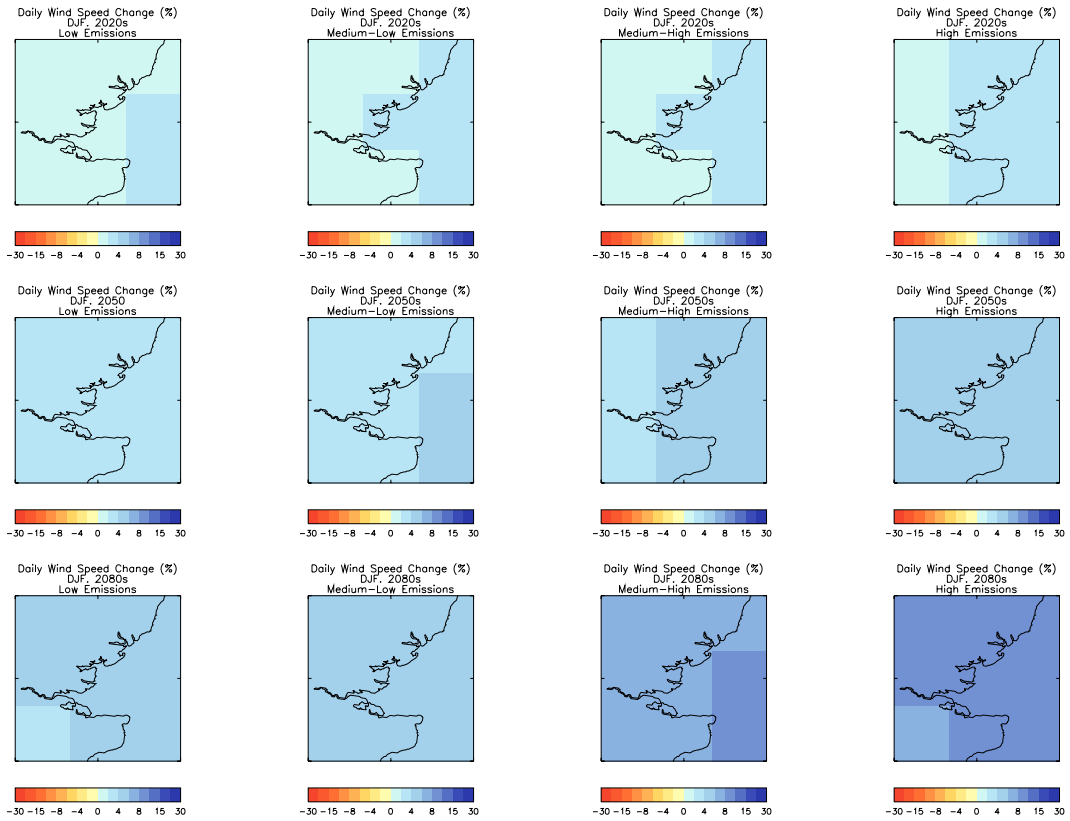

Figure 5.5 Predicted percentage change in wintertime (December – February) mean wind speed for the Bradwell region. Low (left hand column), Medium Low (second column), Medium High (third column) and High (right hand column) emissions scenarios, for thirty-year periods centred on the 2020s (top row), 2050s (middle row) and 2080s (bottom row).

5.7 Figure 5.6 shows the predicted changes in average summer 10m wind speed from the 2020s to the 2080s for the Bradwell region. It shows that the average wind speeds in the region are predicted to increase modestly for all scenarios and timeslices, for most of the land gridboxes, and that for most of the sea gridboxes and the gridbox containing Bradwell itself, small decreases of less than 2% are predicted.

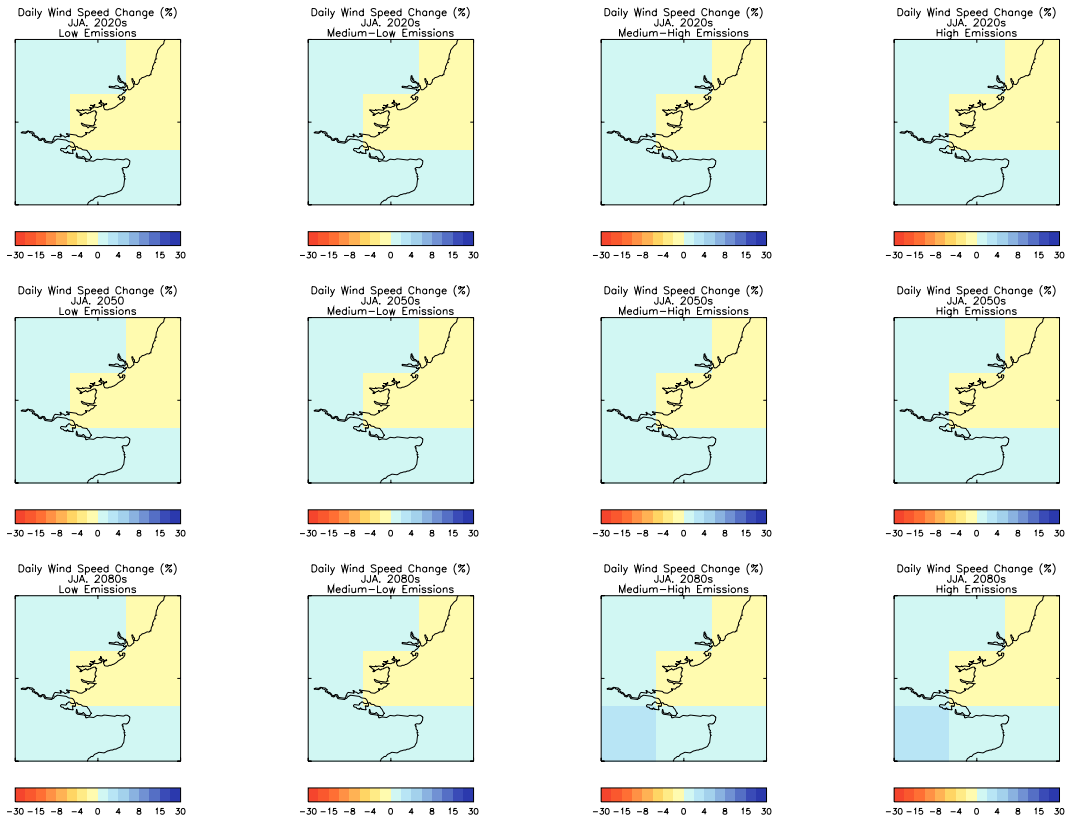

Figure 5.6 Predicted percentage change in summertime (June – August) mean wind speed for the Bradwell region. Low (left hand column), Medium Low (second column), Medium High (third column) and High (right hand column) emissions scenarios, for thirty-year periods centred on the 2020s (top row), 2050s (middle row) and 2080s (bottom row).

5.8 Figure 5.7 shows the predicted changes in average winter 10m wind speed from the 2020s to the 2080s for the Torness region. Like most other regions the predicted changes in wind speed are small, but in this area the wind speed is predicted to increase slightly over all of the gridboxes, both land and sea. Even in the High scenario by the 2080s the predicted increases are in the range 2 to 4%, which may be within the range of natural variability for the area.

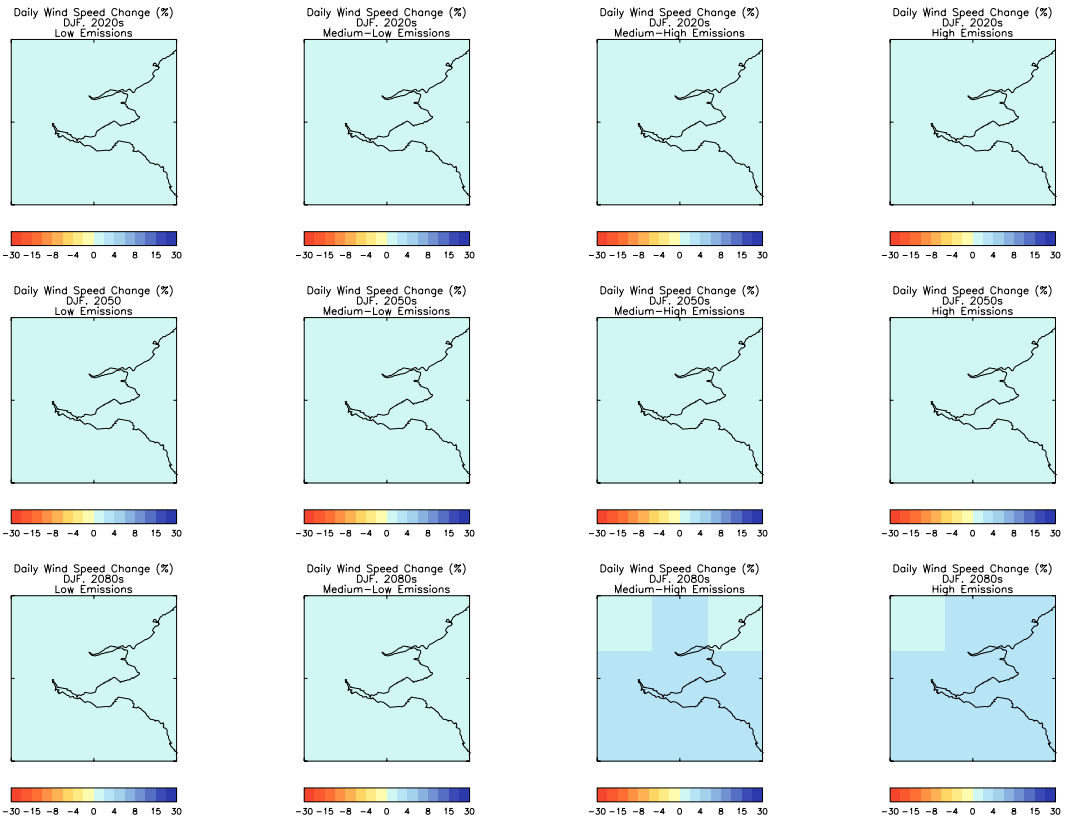

Figure 5.7 Predicted percentage change in wintertime (December – February) mean wind speed for the Torness region. Low (left hand column), Medium Low (second column), Medium High (third column) and High (right hand column) emissions scenarios, for thirty-year periods centred on the 2020s (top row), 2050s (middle row) and 2080s (bottom row).

5.9 Figure 5.8 shows the predicted changes in average summer 10m wind speed from the 2020s to the 2080s for the Torness region. Although the predicted changes (which are all reductions) are greater in magnitude than for winter in the area shown, it is in the maritime areas in the east which show the relatively large changes. For most of the land gridboxes in the west, the predicted reductions by the 2080s are of less than 2% for the Low scenario, and for the High Scenario the predicted reductions are between 2 and 4% for several of the gridboxes, with reductions of between 4 and 8% for the sea gridbox containing Torness itself.

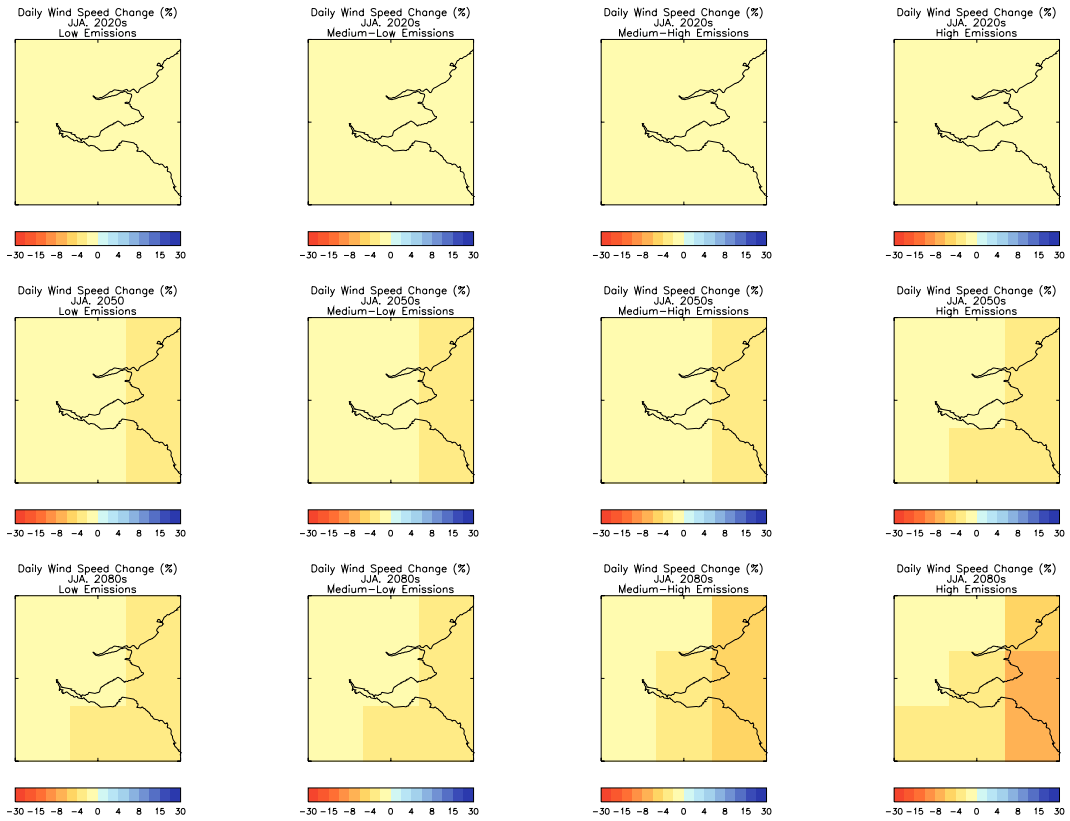

Figure 5.8 Predicted percentage change in summertime (June – August) mean wind speed for the Torness region. Low (left hand column), Medium Low (second column), Medium High (third column) and High (right hand column) emissions scenarios, for thirty-year periods centred on the 2020s (top row), 2050s (middle row) and 2080s (bottom row).

5.10 Figure 5.9 shows the predicted changes in average winter 10m wind speed from the 2020s to the 2080s for the Sizewell region. The model predicts that there will be significant increases for all scenarios by the 2080s, ranging from 4 to 6% for most land gridboxes (including the Sizewell one) in the Low scenario. For the High scenario the predicted increases range from 8 to 10% for most land gridboxes in the area shown. The predicted increases in winter wind speed for the south east of England are greater in magnitude than for any other region or season.

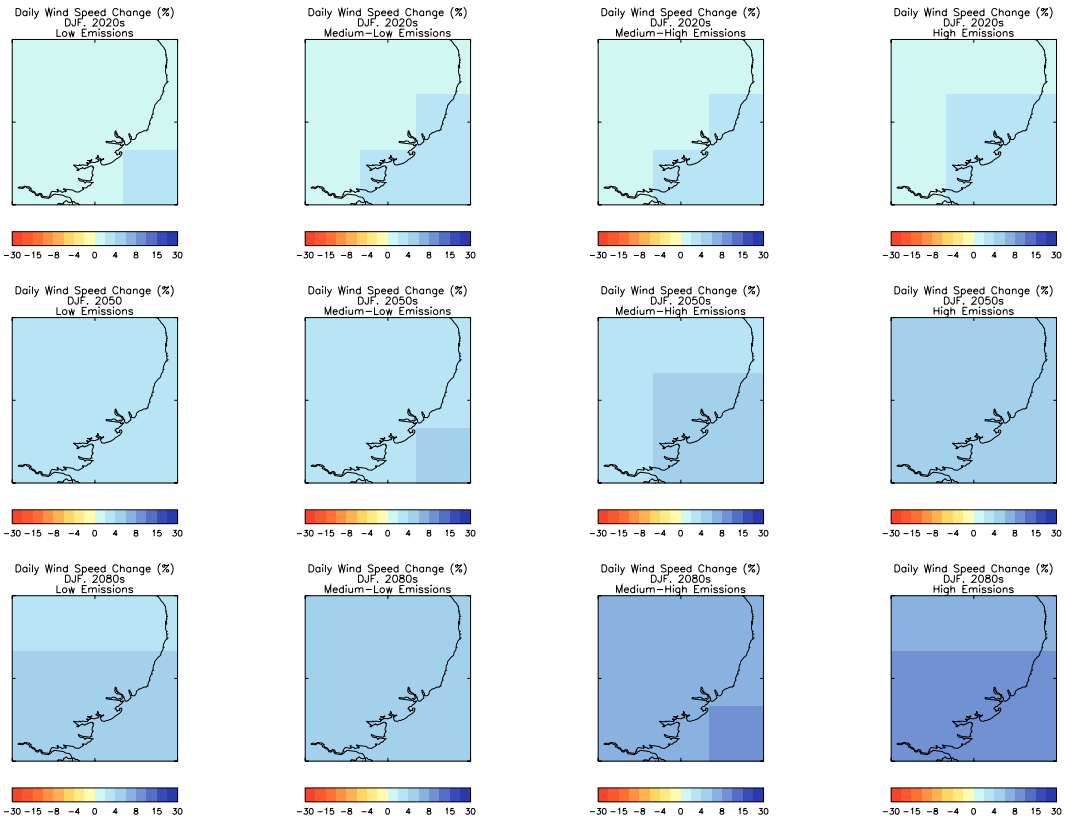

Figure 5.9 Predicted percentage change in wintertime (December – February) mean wind speed for the Sizewell region. Low (left hand column), Medium Low (second column), Medium High (third column) and High (right hand column) emissions scenarios, for thirty-year periods centred on the 2020s (top row), 2050s (middle row) and 2080s (bottom row).

5.11 Figure 5.10 shows the predicted changes in average summer 10m wind speed from the 2020s to the 2080s for the Sizewell region. The predicted changes are much smaller in magnitude than for the same region in winter, and like Torness in winter, they vary slightly around zero, with no difference between the scenarios or timeslices being apparent with the chosen contour intervals. Around the Sizewell coast the wind speed is predicted to decrease slightly, by less than 2%, even for the High scenario in the 2080s.

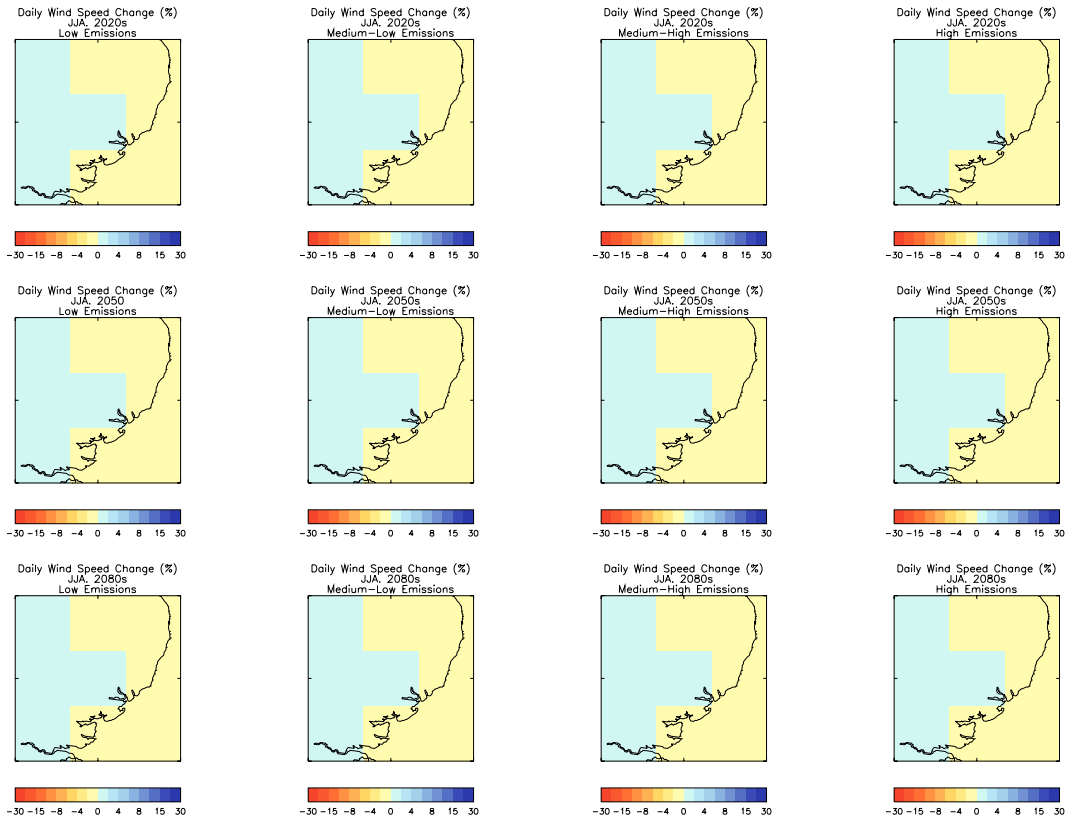

Figure 5.10 Predicted percentage change in summertime (June – August) mean wind speed for the Sizewell region. Low (left hand column), Medium Low (second column), Medium High (third column) and High (right hand column) emissions scenarios, for thirty-year periods centred on the 2020s (top row), 2050s (middle row) and 2080s (bottom row).

5.12 Figure 5.11 shows the predicted changes in average winter 10m wind speed from the 2020s to the 2080s for the Dungeness region. Like Calder Hall, the winter average daily wind speed is predicted to increase (by a greater percentage than Calder Hall) but in contrast to Calder Hall, the summer average daily 10m wind speed around Dungeness is predicted to increase. Even in the Low scenario, by the 2080s the area is predicted by the model to experience winter wind speed increases of 4 to 6%. In the High scenario the model predicts that increases of more than 6% will be seen over the whole area, with the sea gridboxes seeing greater increases (more than 8%) than the land gridboxes.

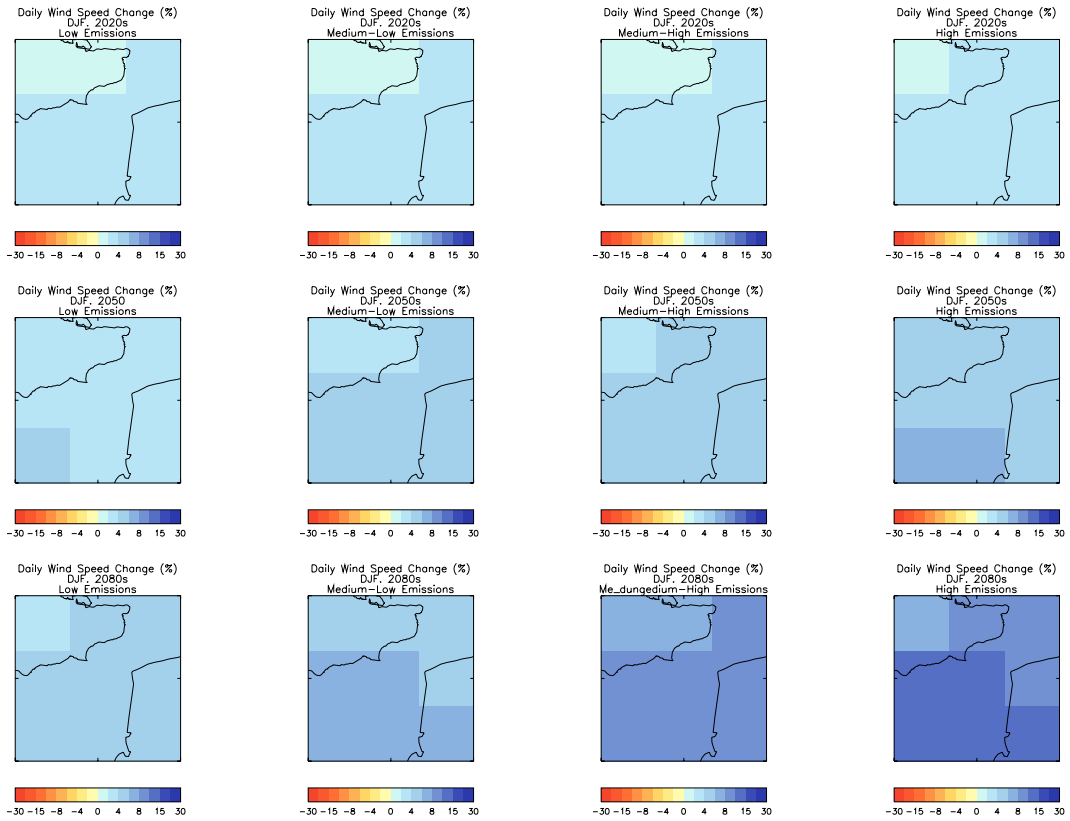

Figure 5.11 Predicted percentage change in wintertime (December – February) mean wind speed for the Dungeness region. Low (left hand column), Medium Low (second column), Medium High (third column) and High (right hand column) emissions scenarios, for thirty-year periods centred on the 2020s (top row), 2050s (middle row) and 2080s (bottom row).

5.13 Figure 5.12 shows the predicted changes in average summer 10m wind speed from the 2020s to the 2080s for the Dungeness region. The model predicts that for the Dungeness area only very modest increases will be seen in summer, not even outside the range of natural variability for the Low scenario at Dungeness itself. Even for the High scenario the increases by the 2080s are predicted to be between 2 to 4% for the land gridboxes in the area. However, this is still unique among all the sites examined, as none of the others are predicted by the model to see increases in summer wind speed over the whole region mapped.

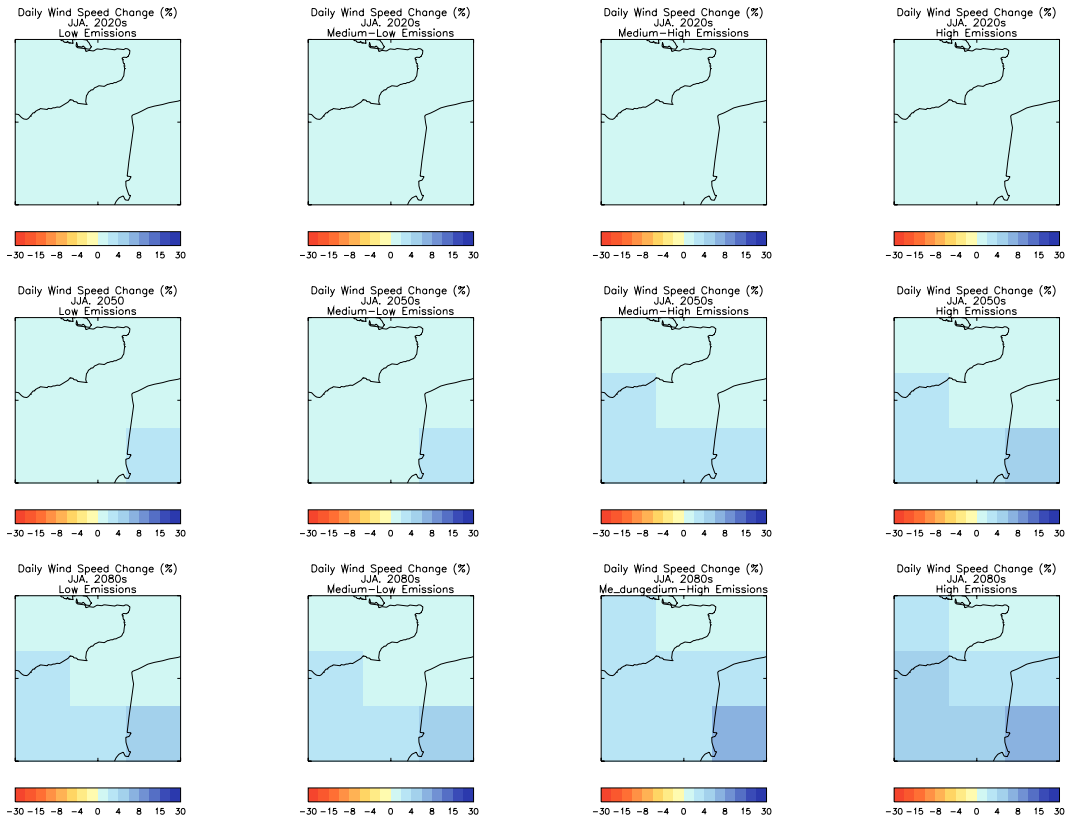

Figure 5.12 Predicted percentage change in summertime (June – August) mean wind speed for the Dungeness region. Low (left hand column), Medium Low (second column), Medium High (third column) and High (right hand column) emissions scenarios, for thirty-year periods centred on the 2020s (top row), 2050s (middle row) and 2080s (bottom row).

5.14 Figure 5.13 shows the predicted changes in average winter 10m wind speed from the 2020s to the 2080s for the Hartlepool region. Increases are predicted for all timeslices and emissions scenarios, but the increases are less than 4% for all but the Medium-High and High scenarios in the 2080s.

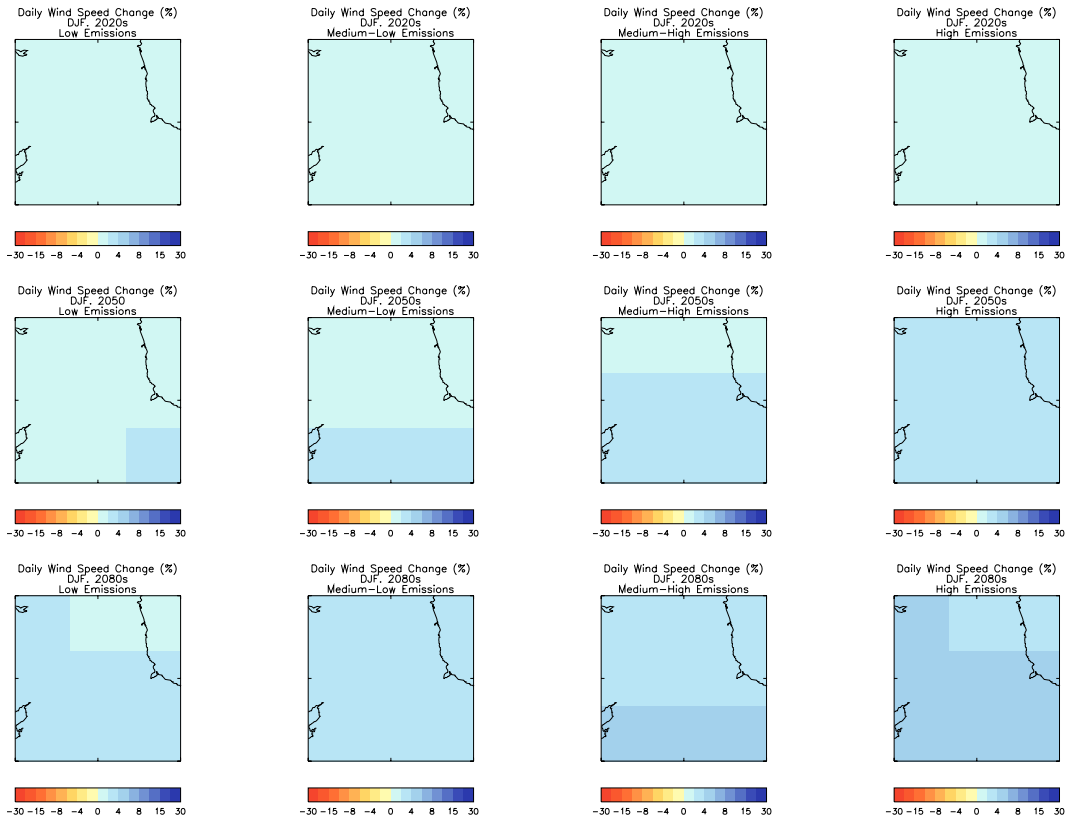

Figure 5.13 Predicted percentage change in wintertime (December – February) mean wind speed for the Hartlepool region. Low (left hand column), Medium Low (second column), Medium High (third column) and High (right hand column) emissions scenarios, for thirty-year periods centred on the 2020s (top row), 2050s (middle row) and 2080s (bottom row).

5.15 Figure 5.14 shows the predicted changes in average summer 10m wind speed from the 2020s to the 2080s for the Hartlepool region. It shows that the average wind speeds in the region are predicted to decrease for all scenarios and timeslices, but that the decreases are hardly greater than the natural variability except for the more extreme scenarios and most distant timeslices, where a decrease of around 8% is predicted for the gridboxes by the coast in the 2080s. There appears to be a trend for the magnitude of the wind decreases to become greater as one moves from the land to the coast, and this is borne out by examining the UK-scale maps in the UKCIP02 report.

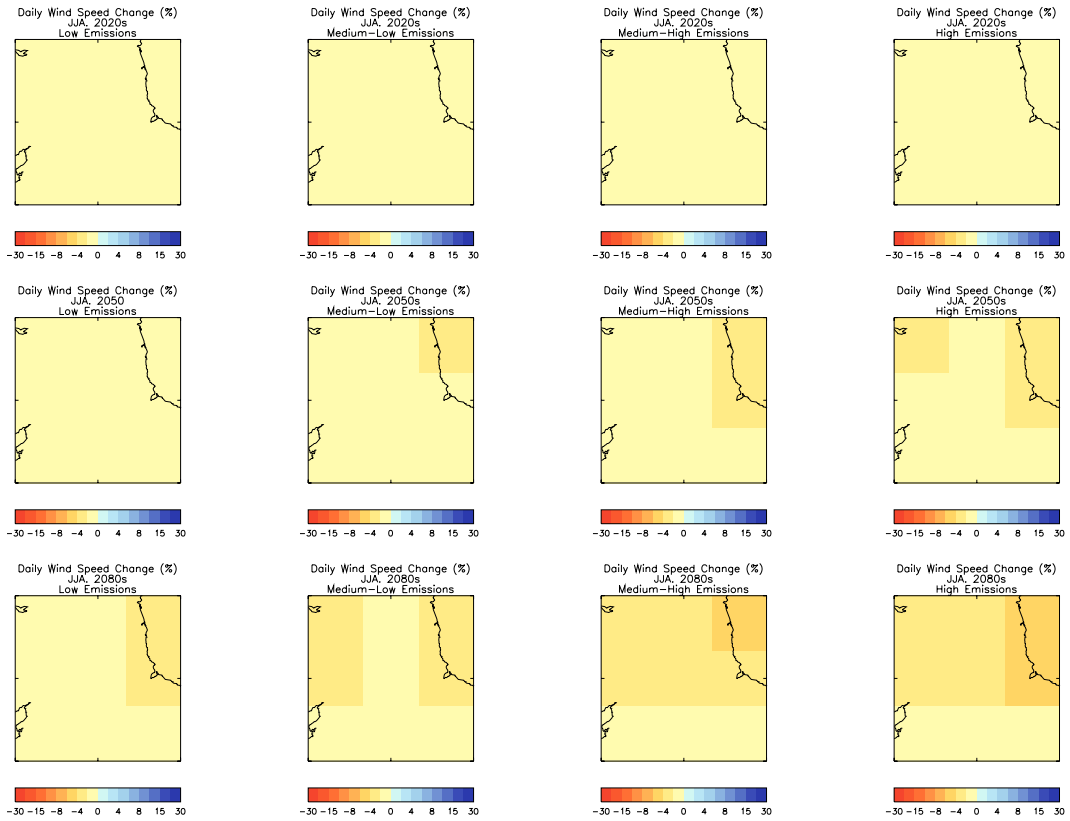

Figure 5.14 Predicted percentage change in summertime (June – August) mean wind speed for the Hartlepool region. Low (left hand column), Medium Low (second column), Medium High (third column) and High (right hand column) emissions scenarios, for thirty-year periods centred on the 2020s (top row), 2050s (middle row) and 2080s (bottom row).

5.16 Figure 5.15 shows the predicted changes in average winter 10m wind speed from the 2020s to the 2080s for the Hunterston region. Like most other regions the predicted changes in wind speed are small, but in this area the wind speed is predicted to decrease slightly over the sea gridboxes in the west of the region shown, and to increase slightly over the land gridboxes in the east of the region. Even in the High scenario by the 2080s the predicted increases are in the range 2 to 4%, which is within the range of natural variability for the area.

5.17 Figure 5.16 shows the predicted changes in average summer 10m wind speed from the 2020s to the 2080s for the Hunterston region. Although the predicted changes (which are all reductions) are greater in magnitude than for winter in the area shown, it is in the maritime gridboxes in the west which show the relatively large changes. For the land gridboxes in the east, the predicted reductions by the 2080s are of less than 2% for the Low scenario, and for the High Scenario the predicted reductions are mostly between 2 and 4%.

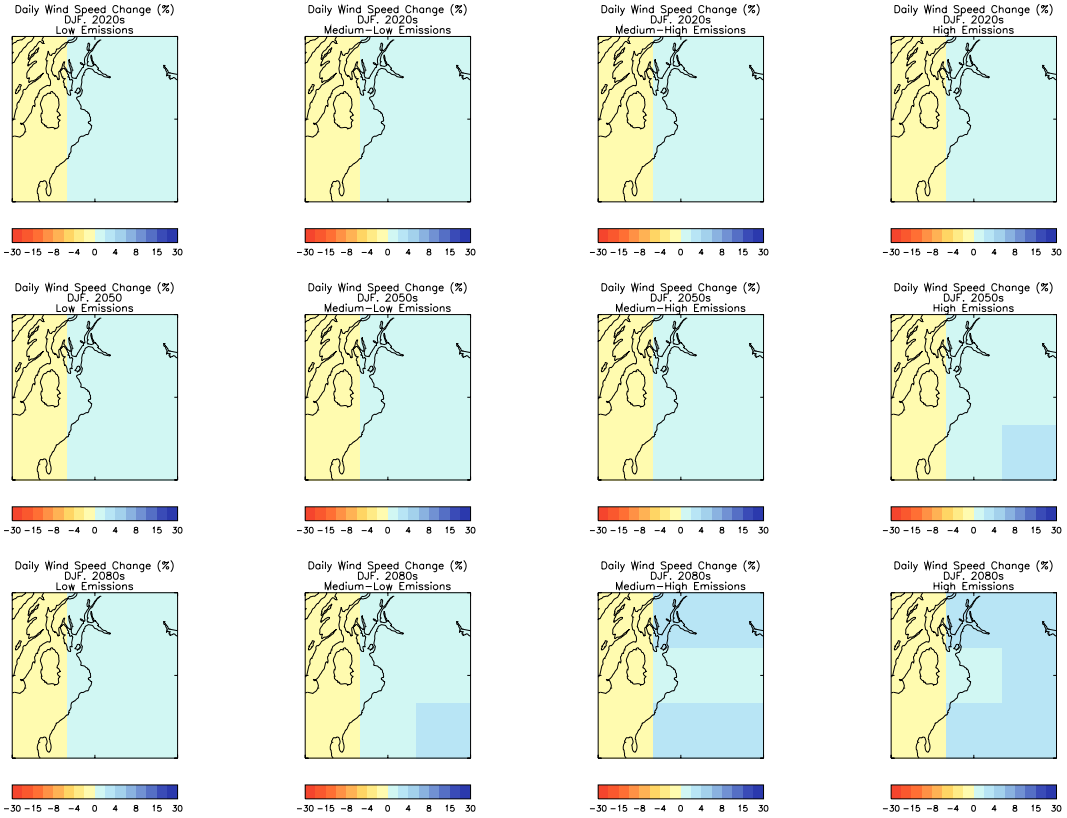

Figure 5.15 Predicted percentage change in wintertime (December – February) mean wind speed for the Hunterston region. Low (left hand column), Medium Low (second column), Medium High (third column) and High (right hand column) emissions scenarios, for thirty-year periods centred on the 2020s (top row), 2050s (middle row) and 2080s (bottom row).

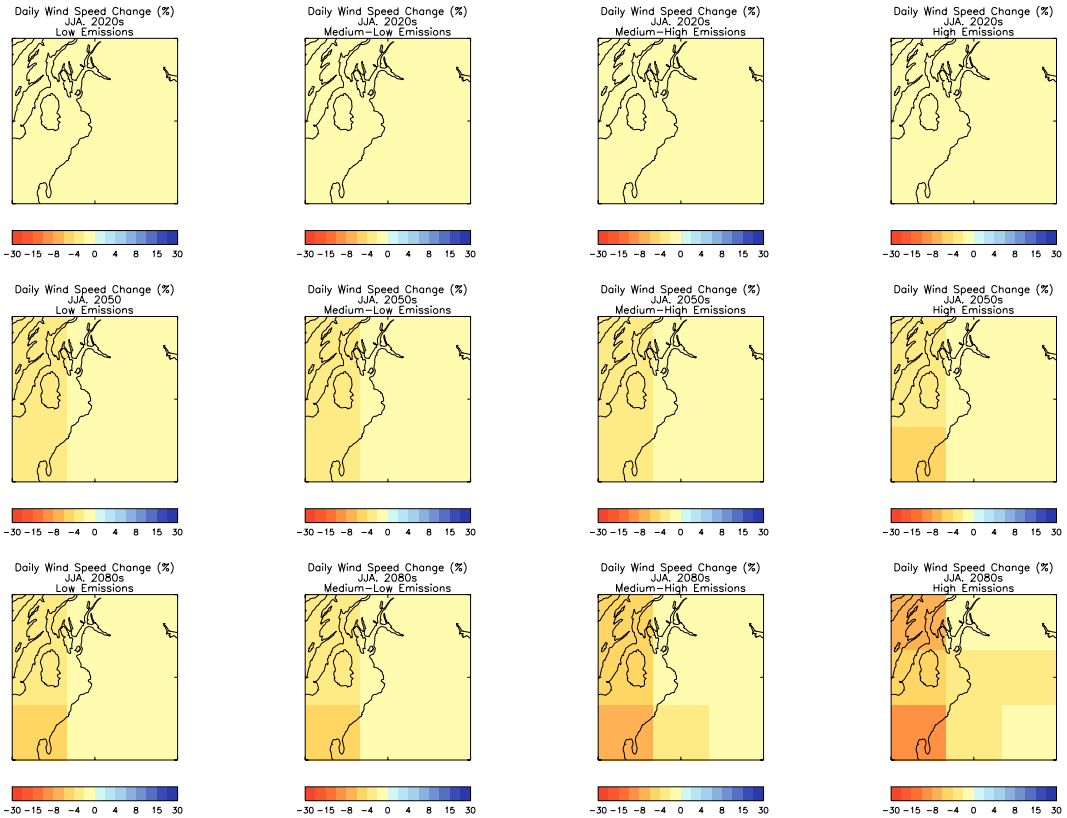

Figure 5.16 Predicted percentage change in summertime (June – August) mean wind speed for the Hunterston region. Low (left hand column), Medium Low (second column), Medium High (third column) and High (right hand column) emissions scenarios, for thirty-year periods centred on the 2020s (top row), 2050s (middle row) and 2080s (bottom row).

5.18 The changes in extreme wind shown below use the method of Tabony (1994) and published relationships between daily, hourly and gust speeds to derive the extreme wind climate (all speeds expressed in knots) for the control and 2080s runs of the RCM from thirty years of daily mean 10 metre wind speeds. The ratio between hourly mean and gust speeds (the gust ratio) calculated from Chapter 5 of Hulme, Jenkins et al., 2002, was 1.538. The ratio between daily and hourly means of 1.3 was obtained from the same source. Table 5.1 shows the data for Heysham for the control climate whilst Table 5.2 shows the predicted extreme winds for Heysham in the 2080s. For this and the other stations, the extremes in the climate model's representation of the current climate tend to be less than those based on real observations. The most likely reason for this is the 50km resolution of the model compared to the point location of real observations. It follows that it is just the change in speed between the RCM control and anomaly runs which is important to look at rather than the absolute speeds predicted by the model. Note that because the climate model simulations were 30 years in length, estimation of return period quantities for greater than 30 years is highly uncertain, so in this chapter the lines in the tables for return periods of 50 years and more are italicised to show that they are indicative.

Return Period (Years)	Mean Hourly Wind	Standard error Mean Wind	Gust	Standard Error Gust
2	29.7	1.1	45.7	1.7
5	33.0	1.1	50.8	1.8
10	35.0	1.2	53.9	1.9
20	36.8	1.3	56.7	2.0
50	*39.0*	*1.4*	*60.1*	*2.2*
100	*40.6*	*1.5*	*62.4*	*2.3*
200	*42.0*	*1.6*	*64.7*	*2.5*
500	*43.8*	*1.8*	*67.5*	*2.9*
1000	*45.1*	*2.0*	*69.4*	*3.1*
10000	*48.9*	*2.7*	*75.2*	*4.2*
100000	*52.0*	*3.5*	*80.1*	*5.3*
1000000	*54.6*	*4.2*	*84.1*	*6.5*

Table 5.1 Heysham control climate

Return Period (Years)	Mean Hourly Wind	Standard error Mean Wind	Gust	Standard Error Gust
2	30.9	1.1	47.6	1.8
5	34.3	1.2	52.9	1.9
10	36.4	1.2	56.1	1.9
20	38.3	1.3	59.0	2.0
50	*40.6*	*1.4*	*62.5*	*2.2*
100	*42.2*	*1.5*	*65.0*	*2.4*
200	*43.7*	*1.7*	*67.4*	*2.6*
500	*45.6*	*1.9*	*70.3*	*2.9*
1000	*46.9*	*2.1*	*72.3*	*3.2*
10000	*50.9*	*2.8*	*78.4*	*4.3*
100000	*54.1*	*3.6*	*83.4*	*5.5*
1000000	*56.9*	*4.4*	*87.6*	*6.8*

Table 5.2 Heysham 2080s climate

5.19 Tables 5.1 and 5.2 show that the HadRM3 model predicts that for Heysham in the Medium High scenario, the 2 year gust speed will increase by about 4%,

and the 10,000 year gust speed (and the gust speeds for the rest of the range of return periods shown) will also increase by just over 4%.

5.20 Tables 5.3 and 5.4 show the modelled control and 2080s extreme winds for Hinkley Point. They show that the climate model predicts that gust speeds will increase by approximately 6% for the whole range of return periods.

Return Period (Years)	Mean Hourly Wind	Standard error Mean Wind	Gust	Standard Error Gust
2	29.4	1.1	45.2	1.7
5	32.6	1.1	50.2	1.8
10	34.6	1.2	53.3	1.8
20	36.4	1.2	56.0	1.9
50	*38.6*	*1.4*	*59.4*	*2.1*
100	*40.2*	*1.5*	*61.8*	*2.3*
200	*41.6*	*1.6*	*64.0*	*2.5*
500	*43.4*	*1.8*	*66.7*	*2.8*
1000	*44.7*	*2.0*	*68.7*	*3.1*
10000	*48.4*	*2.6*	*74.4*	*4.1*
100000	*51.5*	*3.4*	*79.2*	*5.2*
1000000	*54.1*	*4.2*	*83.2*	*6.4*

Table 5.3 Hinkley Point control climate

Return Period (Years)	Mean Hourly Wind	Standard error Mean Wind	Gust	Standard Error Gust
2	31.3	1.2	48.1	1.8
5	34.8	1.2	53.4	1.9
10	36.9	1.2	56.7	1.9
20	38.8	1.3	59.6	2.0
50	*41.1*	*1.4*	*63.2*	*2.2*
100	*42.8*	*1.5*	*65.7*	*2.4*
200	*44.3*	*1.7*	*68.1*	*2.6*
500	*46.2*	*1.9*	*71.0*	*2.9*
1000	*47.6*	*2.1*	*73.1*	*3.2*
10000	*51.5*	*2.8*	*79.2*	*4.3*
100000	*54.8*	*3.6*	*84.3*	*5.5*
1000000	*57.6*	*4.4*	*88.5*	*6.8*

Table 5.4 Hinkley Point 2080s climate

5.21 Tables 5.5 and 5.6 show the modelled control and 2080s extreme winds for Bradwell. They show that the climate model predicts that extreme mean hourly wind speeds and gust speeds will not increase by the 2080s. However, during the analysis of the 30 years of data that is used in the extreme value analysis, it was noted that the average of the series, as well as the absolute maximum, were both higher in the 2080s data than in the control climate data, by 2% for the average and 5% for the maximum.

Return Period (Years)	Mean Hourly Wind	Standard error Mean Wind	Gust	Standard Error Gust
2	37.6	1.4	57.8	2.2
5	41.8	1.4	64.2	2.2
10	44.3	1.5	68.1	2.3
20	46.6	1.5	71.7	2.4
50	*49.4*	*1.6*	*76.0*	*2.6*
100	*51.4*	*1.8*	*79.0*	*2.8*
200	*53.2*	*1.9*	*81.8*	*3.0*
500	*55.5*	*2.2*	*85.3*	*3.4*
1000	*57.1*	*2.4*	*87.8*	*3.7*
10000	*61.9*	*3.2*	*95.2*	*4.9*
100000	*65.9*	*4.2*	*101.3*	*6.4*
1000000	*69.2*	*5.2*	*106.4*	*7.9*

Table 5.5 Bradwell control climate

Return Period (Years)	Mean Hourly Wind	Standard error Mean Wind	Gust	Standard Error Gust
2	37.6	1.4	57.8	2.2
5	41.8	1.4	64.2	2.2
10	44.3	1.5	68.1	2.3
20	46.6	1.5	71.7	2.4
50	*49.4*	*1.6*	*76.0*	*2.6*
100	*51.4*	*1.8*	*79.0*	*2.8*
200	*53.2*	*1.9*	*81.8*	*3.0*
500	*55.5*	*2.2*	*85.3*	*3.4*
1000	*57.1*	*2.4*	*87.8*	*3.7*
10000	*61.9*	*3.2*	*95.2*	*4.9*
100000	*65.9*	*4.2*	*101.3*	*6.4*
1000000	*69.2*	*5.2*	*106.4*	*7.9*

Table 5.6 Bradwell 2080s climate

5.22 Tables 5.7 and 5.8 show the modelled control and 2080s extreme winds for Torness. They show that the climate model predicts that gust speeds will decrease by approximately 1.8% for the whole range of return periods, which is less than the standard error.

Return Period (Years)	Mean Hourly Wind	Standard error Mean Wind	Gust	Standard Error Gust
2	32.5	1.2	50.0	1.9
5	36.1	1.2	55.5	1.9
10	38.3	1.3	58.9	2.0
20	40.3	1.4	62.0	2.1
50	*42.7*	*1.5*	*65.7*	*2.3*
100	*44.4*	*1.6*	*68.3*	*2.5*
200	*46.0*	*1.8*	*70.8*	*2.7*
500	*48.0*	*2.0*	*73.8*	*3.1*
1000	*49.4*	*2.2*	*76.0*	*3.4*
10000	*53.5*	*2.9*	*82.3*	*4.5*
100000	*56.9*	*3.7*	*87.6*	*5.7*
1000000	*59.8*	*4.6*	*92.0*	*7.1*

Table 5.7 Torness control climate

Return Period (Years)	Mean Hourly Wind	Standard error Mean Wind	Gust	Standard Error Gust
2	31.9	1.2	49.1	1.9
5	35.4	1.2	54.5	1.9
10	37.6	1.3	57.9	2.0
20	39.5	1.3	60.9	2.1
50	*41.9*	*1.5*	*64.5*	*2.3*
100	*43.6*	*1.6*	*67.1*	*2.5*
200	*45.2*	*1.7*	*69.5*	*2.7*
500	*47.1*	*2.0*	*72.5*	*3.0*
1000	*48.5*	*2.1*	*74.6*	*3.3*
10000	*52.5*	*2.9*	*80.8*	*4.4*
100000	*55.9*	*3.7*	*86.0*	*5.7*
1000000	*58.7*	*4.5*	*90.3*	*7.0*

Table 5.8 Torness 2080s climate

5.23 Tables 5.9 and 5.10 show the modelled control and 2080s extreme winds for Sizewell. They show that the climate model predicts that gust speeds will increase by approximately 3.5% for the whole range of return periods.

Return Period (Years)	Mean Hourly Wind	Standard error Mean Wind	Gust	Standard Error Gust
2	36.9	1.4	56.8	2.1
5	41.0	1.4	63.1	2.2
10	43.5	1.4	66.9	2.3
20	45.7	1.5	70.4	2.3
50	*48.5*	*1.6*	*74.6*	*2.5*
100	*50.4*	*1.7*	*77.6*	*2.7*
200	*52.2*	*1.9*	*80.4*	*2.9*
500	*54.5*	*2.1*	*83.8*	*3.3*
1000	*56.1*	*2.3*	*86.3*	*3.6*
10000	*60.8*	*3.2*	*93.5*	*4.9*
100000	*64.7*	*4.1*	*99.5*	*6.3*
1000000	*67.9*	*5.1*	*104.5*	*7.8*

Table 5.9 Sizewell control climate

Return Period (Years)	Mean Hourly Wind	Standard error Mean Wind	Gust	Standard Error Gust
2	38.2	1.4	58.8	2.2
5	42.4	1.4	65.3	2.3
10	45.0	1.5	69.3	2.3
20	47.4	1.5	72.9	2.4
50	*50.2*	*1.7*	*77.3*	*2.6*
100	*52.2*	*1.8*	*80.3*	*2.8*
200	*54.1*	*1.9*	*83.2*	*3.0*
500	*56.4*	*2.2*	*86.8*	*3.4*
1000	*58.0*	*2.4*	*89.3*	*3.7*
10000	*62.9*	*3.2*	*96.8*	*5.0*
100000	*66.9*	*4.2*	*103.0*	*6.5*
1000000	*70.3*	*5.2*	*108.2*	*8.1*

Table 5.10 Sizewell 2080s climate

5.24 Tables 5.11 and 5.12 show the modelled control and 2080s extreme winds for Dungeness. They show that the climate model predicts that gust speeds will increase by approximately 2% (actually close to 2.5%) for the whole range of return periods.

Return Period (Years)	Mean Hourly Wind	Standard error Mean Wind	Gust	Standard Error Gust
2	40.7	1.5	62.6	2.4
5	45.2	1.5	69.5	2.4
10	48.0	1.6	73.8	2.5
20	50.5	1.6	77.6	2.6
50	*53.5*	*1.8*	*82.3*	*2.7*
100	*55.6*	*1.9*	*85.5*	*2.9*
200	*57.6*	*2.0*	*88.6*	*3.2*
500	*60.1*	*2.3*	*92.4*	*3.6*
1000	*61.8*	*2.5*	*95.1*	*3.9*
10000	*67.0*	*3.4*	*103.1*	*5.3*
100000	*71.3*	*4.5*	*109.7*	*6.9*
1000000	*74.9*	*5.5*	*115.2*	*8.5*

Table 5.11 Dungeness control climate

Return Period (Years)	Mean Hourly Wind	Standard error Mean Wind	Gust	Standard Error Gust
2	41.7	1.5	64.1	2.4
5	46.3	1.6	71.2	2.5
10	49.1	1.6	75.5	2.5
20	51.7	1.7	79.5	2.6
50	*54.8*	*1.8*	*84.2*	*2.8*
100	*57.0*	*1.9*	*87.6*	*3.0*
200	*59.0*	*2.1*	*90.7*	*3.3*
500	*61.6*	*2.4*	*94.6*	*3.7*
1000	*63.4*	*2.6*	*97.4*	*4.0*
10000	*68.7*	*3.5*	*105.5*	*5.4*
100000	*73.1*	*4.6*	*112.3*	*7.0*
1000000	*76.7*	*5.7*	*117.9*	*8.7*

Table 5.12 Dungeness 2080s climate

5.25 Tables 5.13 and 5.14 show the modelled control and 2080s extreme winds for Hartlepool. They show that the climate model predicts that gust speeds will increase by approximately 2.5% for the whole range of return periods.

Return Period (Years)	Mean Hourly Wind	Standard error Mean Wind	Gust	Standard Error Gust
2	36.0	1.3	55.4	2.1
5	40.0	1.4	61.5	2.1
10	42.4	1.4	65.3	2.2
20	44.6	1.5	68.7	2.3
50	*47.3*	*1.6*	*72.8*	*2.5*
100	*49.2*	*1.7*	*75.7*	*2.7*
200	*51.0*	*1.9*	*78.4*	*2.9*
500	*53.1*	*2.1*	*81.8*	*3.3*
1000	*54.7*	*2.3*	*84.2*	*3.6*
10000	*59.3*	*3.1*	*91.2*	*4.8*
100000	*63.1*	*4.0*	*97.1*	*6.2*
1000000	*66.2*	*5.0*	*101.9*	*7.7*

Table 5.13 Hartlepool control climate

Return Period (Years)	Mean Hourly Wind	Standard error Mean Wind	Gust	Standard Error Gust
2	36.9	1.4	56.8	2.2
5	41.0	1.4	63.1	2.2
10	43.5	1.4	66.9	2.3
20	45.7	1.5	70.4	2.4
50	*48.5*	*1.6*	*74.6*	*2.6*
100	*50.4*	*1.8*	*77.6*	*2.8*
200	*52.2*	*1.9*	*80.4*	*3.0*
500	*54.5*	*2.2*	*83.8*	*3.4*
1000	*56.1*	*2.4*	*86.3*	*3.7*
10000	*60.8*	*3.2*	*93.5*	*4.9*
100000	*64.7*	*4.1*	*99.5*	*6.4*
1000000	*67.9*	*5.1*	*104.5*	*7.9*

Table 5.14 Hartlepool 2080s climate

5.26 Tables 5.15 and 5.16 show the modelled control and 2080s extreme winds for Hunterston. They show that the climate model predicts that gust speeds will increase by approximately 4.5% for the whole range of return periods.

Return Period (Years)	Mean Hourly Wind	Standard error Mean Wind	Gust	Standard Error Gust
2	27.1	1.0	41.8	1.6
5	30.1	1.1	46.4	1.7
10	31.9	1.1	49.3	1.7
20	33.6	1.2	51.8	1.9
50	*35.6*	*1.3*	*54.9*	*2.0*
100	*37.0*	*1.4*	*57.1*	*2.2*
200	*38.4*	*1.6*	*59.2*	*2.4*
500	*40.0*	*1.8*	*61.7*	*2.7*
1000	*41.2*	*1.9*	*63.5*	*3.0*
10000	*44.6*	*2.6*	*68.8*	*4.0*
100000	*47.5*	*3.2*	*73.2*	*5.0*
1000000	*49.9*	*4.0*	*76.9*	*6.1*

Table 5.15 Hunterston control climate

Return Period (Years)	Mean Hourly Wind	Standard error Mean Wind	Gust	Standard Error Gust
2	28.4	1.1	43.7	1.7
5	31.5	1.1	48.5	1.7
10	33.5	1.2	51.5	1.8
20	35.2	1.2	54.2	1.9
50	*37.3*	*1.4*	*57.4*	*2.1*
100	*38.8*	*1.5*	*59.7*	*2.3*
200	*40.2*	*1.6*	*61.9*	*2.5*
500	*41.9*	*1.8*	*64.5*	*2.8*
1000	*43.1*	*2.0*	*66.4*	*3.1*
10000	*46.8*	*2.6*	*71.9*	*4.1*
100000	*49.8*	*3.4*	*76.6*	*5.2*
1000000	*52.3*	*4.1*	*80.4*	*6.4*

Table 5.16 Hunterston 2080s climate

5.27 Tables 5.17 to 5.24 show the extreme gusts and hourly winds for the current climate based on observations using the method of Tabony (1994). The winds are not necessarily based on wind data from the power station sites themselves. A computer program written by R. Tabony was used which, given a location in National Grid coordinates and an altitude (shown below each table) accesses a database of extreme wind data from actual observations gathered from around the UK, interpolates to the specified location, and computes the mean hourly wind and the gust speeds for various return periods.

Return Period (Years)	Mean Hourly Wind	Standard error Mean Wind	Gust	Standard Error Gust
2	41.3	3.7	63.6	5.7
5	45.9	3.7	70.7	5.7
10	48.7	3.8	75.0	5.8
20	51.2	3.8	78.9	5.8
50	54.3	3.8	83.6	5.9
100	56.5	3.9	87.0	6.0
200	58.5	4.0	90.1	6.1
500	61.0	4.1	94.0	6.4
1000	62.8	4.3	96.7	6.6
10000	68.0	4.9	104.8	7.5
100000	72.4	5.7	111.5	8.7
1000000	76.0	6.6	117.1	10.2

Table 5.17 Heysham Actual, 3401E, 4596N, 5M + Extremes of wind (knots)

Return Period (Years)	Mean Hourly Wind	Standard error Mean Wind	Gust	Standard Error Gust
2	39.8	3.6	61.2	5.5
5	44.1	3.6	68.0	5.5
10	46.8	3.6	72.1	5.6
20	49.3	3.6	75.9	5.6
50	52.2	3.7	80.4	5.7
100	54.3	3.8	83.6	5.8
200	56.3	3.8	86.6	5.9
500	58.7	4.0	90.4	6.1
1000	60.4	4.1	93.0	6.3
10000	65.4	4.7	100.8	7.2
100000	69.6	5.5	107.3	8.4
1000000	73.1	6.3	112.6	9.8

Table 5.18 Hinkley Point Actual, 3211E, 1460N, 8M + Extremes of wind (knots)

Return Period (Years)	Mean Hourly Wind	Standard error Mean Wind	Gust	Standard Error Gust
2	37.8	3.4	58.2	5.2
5	42.0	3.4	64.6	5.3
10	44.5	3.4	68.6	5.3
20	46.9	3.5	72.2	5.3
50	49.7	3.5	76.5	5.4
100	51.6	3.6	79.5	5.5
200	53.5	3.7	82.4	5.6
500	55.8	3.8	85.9	5.8
1000	57.4	3.9	88.4	6.0
10000	62.2	4.5	95.8	6.9
100000	66.2	5.2	102.0	8.0
1000000	69.5	6.0	107.1	9.3

Table 5.19 Bradwell Actual, 6002E, 2088N, 6M + Extremes of wind (knots)

Return Period (Years)	Mean Hourly Wind	Standard error Mean Wind	Gust	Standard Error Gust
2	42.4	3.8	65.3	5.9
5	47.1	3.8	72.5	5.9
10	49.9	3.8	76.9	5.9
20	52.5	3.9	80.9	6.0
50	55.7	3.9	85.8	6.1
100	57.9	4.0	89.2	6.2
200	60.0	4.1	92.4	6.3
500	62.6	4.2	96.3	6.5
1000	64.4	4.4	99.1	6.8
10000	69.8	5.0	107.4	7.7
100000	74.2	5.8	114.3	9.0
1000000	78.0	6.8	120.1	10.4

Table 5.20 Torness Actual, 3745E, 6751N, 20M + Extremes of wind (knots)

Return Period (Years)	Mean Hourly Wind	Standard error Mean Wind	Gust	Standard Error Gust
2	37.7	3.4	58.1	5.2
5	41.9	3.4	64.6	5.2
10	44.5	3.4	68.5	5.3
20	46.8	3.5	72.1	5.3
50	49.6	3.5	76.4	5.4
100	51.6	3.6	79.4	5.5
200	53.4	3.6	82.3	5.6
500	55.7	3.8	85.8	5.8
1000	57.4	3.9	88.3	6.0
10000	62.1	4.5	95.7	6.9
100000	66.1	5.2	101.9	8.0
1000000	69.5	6.0	107.0	9.3

Table 5.21 Sizewell Actual, 6473E, 2635N, 10M + Extremes of wind (knots)

Return Period (Years)	Mean Hourly Wind	Standard error Mean Wind	Gust	Standard Error Gust
2	37.2	3.3	57.3	5.2
5	41.3	3.4	63.6	5.2
10	43.8	3.4	67.5	5.2
20	46.1	3.4	71.0	5.2
50	48.9	3.5	75.2	5.3
100	50.8	3.5	78.2	5.4
200	52.6	3.6	81.0	5.5
500	54.9	3.7	84.5	5.7
1000	56.5	3.8	87.0	5.9
10000	61.2	4.4	94.3	6.8
100000	65.1	5.1	100.3	7.9
1000000	68.4	5.9	105.4	9.1

Table 5.22 Dungeness Actual, 6082E, 1167N, 2M + Extremes of wind (knots)

Return Period (Years)	Mean Hourly Wind	Standard error Mean Wind	Gust	Standard Error Gust
2	40.8	3.7	62.8	5.7
5	45.3	3.7	69.7	5.7
10	48.1	3.7	74.0	5.7
20	50.6	3.7	77.9	5.7
50	53.6	3.8	82.5	5.8
100	55.7	3.9	85.8	5.9
200	57.7	3.9	88.9	6.1
500	60.2	4.1	92.7	6.3
1000	62.0	4.2	95.4	6.5
10000	67.1	4.8	103.4	7.4
100000	71.4	5.6	110.0	8.6
1000000	75.0	6.5	115.5	10.0

Table 5.23 Hartlepool Actual, 4529E, 5269N, 5M + Extremes of wind (knots)

Return Period (Years)	Mean Hourly Wind	Standard error Mean Wind	Gust	Standard Error Gust
2	43.4	3.9	66.9	6.0
5	48.2	3.9	74.3	6.0
10	51.2	3.9	78.8	6.1
20	53.8	4.0	82.9	6.1
50	57.1	4.0	87.9	6.2
100	59.3	4.1	91.4	6.3
200	61.5	4.2	94.7	6.5
500	64.1	4.3	98.7	6.7
1000	66.0	4.5	101.6	6.9
10000	71.5	5.1	110.1	7.9
100000	76.1	6.0	117.2	9.2
1000000	79.9	6.9	123.1	10.7

Table 5.24 Hunterston Actual, 2184E, 6513N, 8M + Extremes of wind (knots)

5.28 To summarise the changes in extreme winds predicted by the climate model, the HadRM3 RCM predicts that extreme hourly winds and extreme gusts will be slightly higher in future for all the sites studied, but the increases only range from just over 2% for Heysham to 4.5% for Torness.

6. Coastal and other Factors

6.1 Throughout the next century, and beyond, global mean sea-level will rise, mainly due to thermal expansion of the oceans due to global warming. Land ice, such as glaciers, will continue to melt as the planet warms adding further water to the oceans, thus contributing to sea level rise. It is thought that although the Greenland Ice sheet will continue to melt, the increase in sea level this would cause may be offset by increased precipitation over the Earth's other major ice sheet, Antarctica. However, the exact contribution to global sea-level by each of these factors is very uncertain. Individual climate models estimate each of the components differently even for the same emissions scenario. The range of predictions of global average sea level rise (relative to the 1961-90 average) by the climate models included in the IPCC Third Assessment Report (TAR) under each of the emissions scenarios is presented in Table 6.1. It can be seen that by the 2020s the choice of emission scenario has no impact on the level of sea level rise predicted, it is only by the 2050s that differences begin to become apparent. This is because of the large thermal inertia of the oceans which causes sea level to respond very slowly to changes in emissions. The Summary for Policy Makers of the IPCC Fourth Assessment Report (2007) does not give directly comparable figures, but gives sea level rises from 1980-1999 to 2090-2099 of 0.18m as a minimum for the B1 (Low) scenario to 0.59m as a maximum for the A1FI (High) scenario.

Emissions scenario	2020s	2050s	2080s
Low	4-14 cm	7-30 cm	9-48 cm
Medium-Low	4-14 cm	7-32 cm	11-54 cm
Medium-High	4-14 cm	8-32 cm	13-59 cm
High	4-14 cm	9-36 cm	16-69 cm

Table 6.1 Ranges of global-mean sea-level rise (relative to present day, i.e. 1961-90 average) given by the IPCC Third Assessment Report, for the four emissions scenarios and three 30-year time periods used in UKCIP02.

6.2 While sea level is predicted to rise almost everywhere, the changes in sea level are not expected to occur uniformly over the whole ocean. The Met Office climate model and those of other modelling centres predict that some regions may experience almost no increase in sea level while others may experience rises much greater than the global mean. The regional pattern of sea level rise predicted by a climate model is determined by a number of factors, including ocean circulation and local air pressure patterns above the oceans (the inverse barometer effect) as well as differing rates of heat uptake by different parts of the oceans. The lack of consensus between models is partly a reflection of the differences in ocean model formulation that are also responsible for the spread in the global average heat uptake and thermal expansion (as noted above). In addition, the models predict different changes in surface wind patterns, with consequences for changes in ocean circulation. Thus, it should be noted that the regional details of sea level rise predictions are model dependent and confidence in predicted patterns of sea level rise are much lower than our confidence in temperature change patterns (Gregory et al, 2001).

6.3 Figure 6.1 shows the recent estimated changes in the height of land around the UK relative to sea level (excluding sea level rise) due to "rebound" after the ice sheets covering most of the UK retreated at the end of the last ice age thousands of years ago. These vertical land movements, known as isostatic changes, are shown in mm/year, and derived from Shennan (1989). These rates of isostatic change are expected to continue into the foreseeable future, at least over the timescale of climate model predictions. For more details about this figure, see the UKCIP02 report. UKCIP later created an updated map of

isostatic change (see Figures 6.2 and 6.3) based on Shennan and Horton (2002) and these later data are also used in this report. Both are used in order to show the differences that can arise from changes in one parameter.

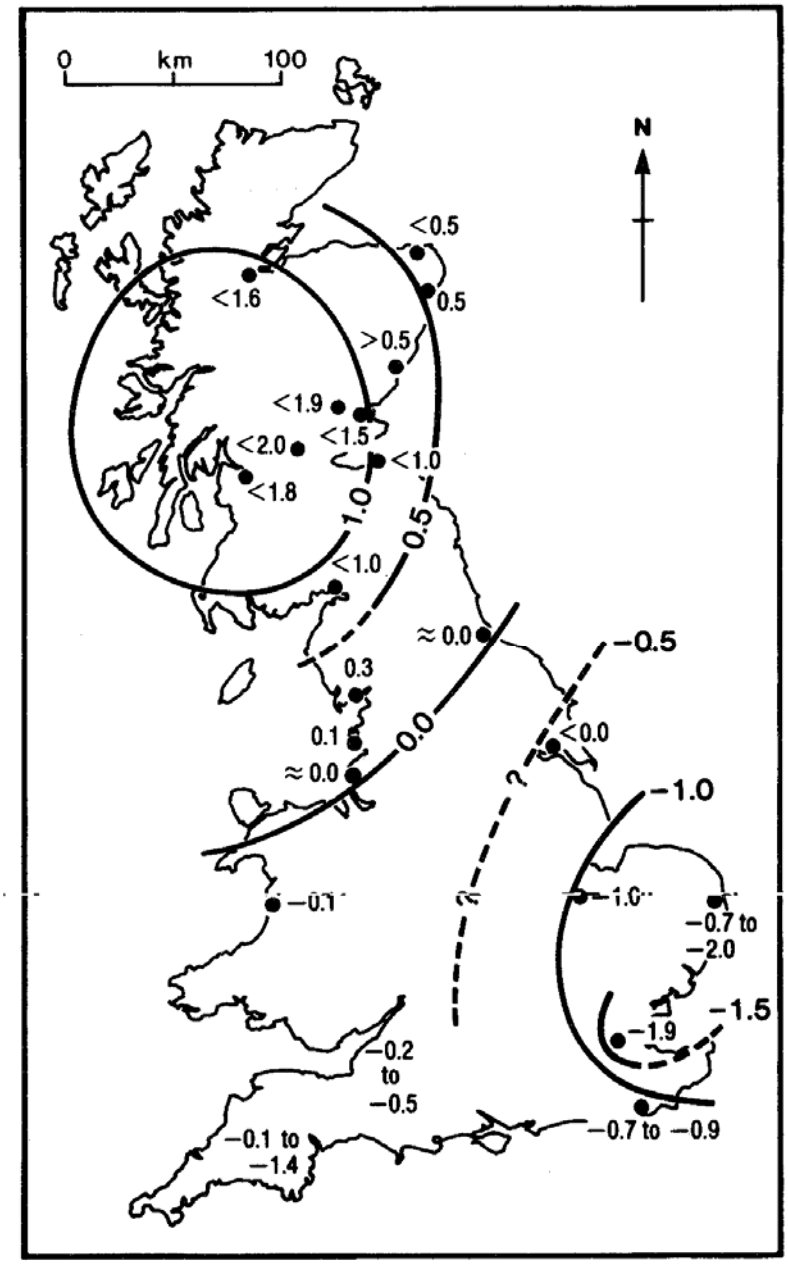

Figure 6.1 Map of estimated current rates (mm/year) of crustal movement in Great Britain. Negative values indicate land subsidence. Point estimates are shown for guidance. Effects of sediment consolidation are not included. From UKCIP02, derived from Shennan (1989).

6.4 As highlighted previously, little confidence can be placed in predictions of regional variations in sea level, excluding those that will occur as a result of predictable land movements such as isostatic rebound. Unfortunately, given this uncertainty it is not possible to give predicted local sea level rises at each of the locations which are a focus of this report. It is however reasonable to provide an estimate of effective local sea level rises for guidance. The approach taken in the UKCIP02 report was to note that predicted regional differences in climate induced sea level rise can be fifty percent more or less than the globally averaged predicted rise, and states that for sensitivity studies it is advisable to consider changes in sea level which are +/- fifty percent of the full IPCC range of predicted global mean changes. It is thus reasonable, for the purposes of this

study, to make an estimate of local effective mean sea level rise by combining the isostatic changes with the estimates of global mean sea level and then adding a further error margin due to possible regional effects. This is presented in table 6.2 for the eight locations being focused upon in this report, as well as Calder Hall (co-sited with Sellafield: see figure 2.1 for location). Although Calder Hall is not a BE site, figures for this site are included in the tables in this chapter to give a greater sense of the regional variation around the coast. It is likely that the actual change in sea level experienced at each location by the 2080s will lie somewhere within the range below. The very large range of values for each location is an indication of the uncertainty in prediction of regional sea level rise and these figures are given as guidance only.

Location	Isostatic change (cm) 2080s – present day (1961-90)	2080s global sea-level rise (cm) – lower/upper	Net 2080s local sea-level rise (cm) – lower /upper estimate	
			Global mean plus local land movement	Regional sea level variation plus land movement
Calder Hall	+5.5	9 – 69	3.5 – 63.5	(-1) – 98
Dungeness	-11.0	9 – 69	20 – 80	16 – 115
Hartlepool	0.0	9 – 69	9 – 69	5 - 104
Hunterston	+19.8	9 – 69	(-10.8) – 49.2	(-15) – 84
Sizewell	-22.0	9 – 69	31 - 91	27 - 126
Heysham	+2.2	9 – 69	6.8 – 66.8	2 – 101
Hinkley Point	-5.5	9 – 69	14.5 – 74.5	10 – 109
Bradwell	-17.6	9 – 69	26.6 – 86.6	22 – 121
Torness	+9.9	9 – 69	(-0.9) – 59.1	(-5) – 94

Table 6.2 Upper and lower estimates of effective sea-level rise (i.e. sea-level rise plus land movement) based upon figures from **Shennan 1989** and the IPCC TAR with an additional estimate due to regional variations (+/-fifty percent of the global mean), following UKCIP02. "Present day" is the modelled thirty year period 1961-90 hence estimates of isostatic change by the 2080s are based upon 110 years of expected land movement.

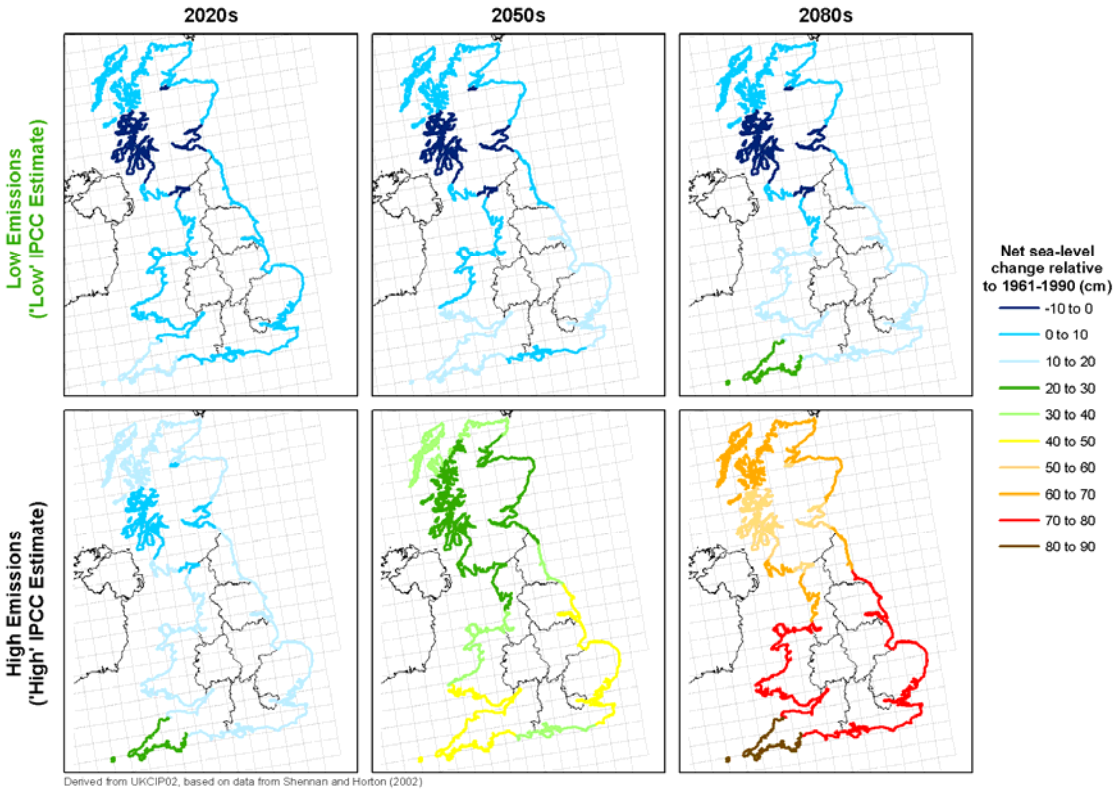

Figure 6.2 Map of net sea-level change relative to 1961-90 (present day), for the 2020s, 2050s and 2080s, for low and high emissions scenarios. From UKCIP02, incorporating data from Shennan and Horton (2002).

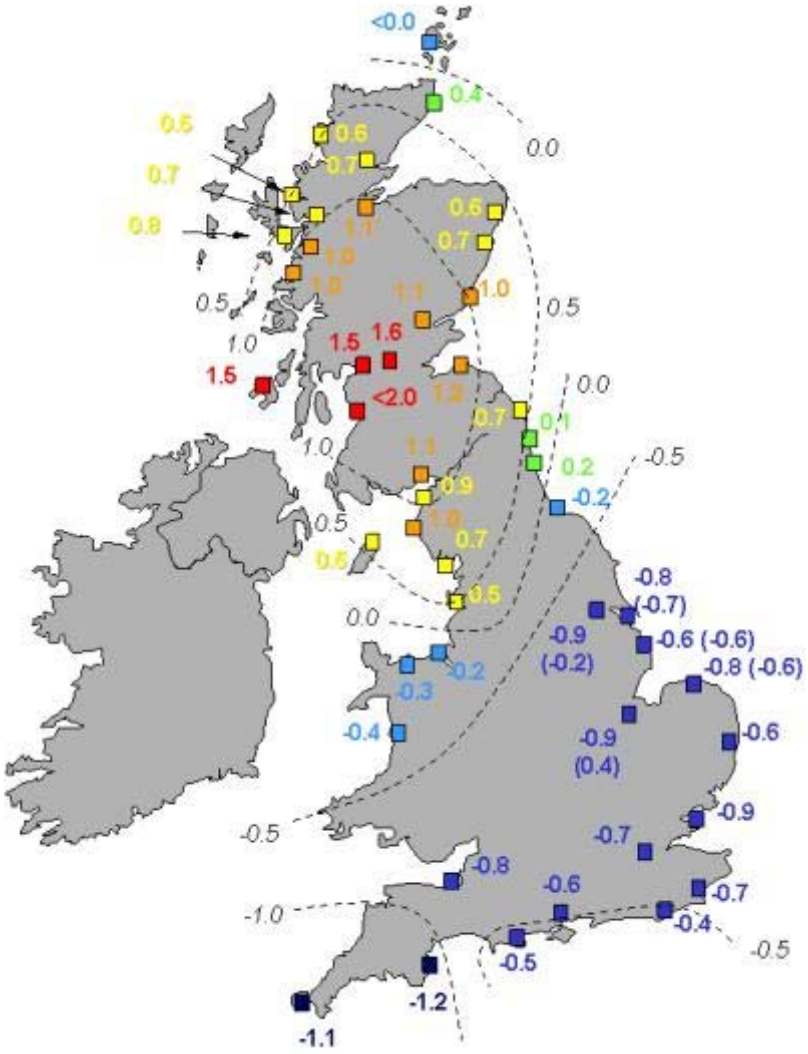

Figure 6.3 Map of estimated current rates (mm/year) of crustal movement in Great Britain. Negative values indicate land subsidence. Point estimates are shown for guidance. Effects of sediment consolidation are not included. From UKCIP02, incorporating data from Shennan and Horton (2002).

Location	**Isostatic change (cm) 2080s – present day (1961-90)**	**2080s global sea-level rise (cm) – lower/upper**	**Net 2080s local sea-level rise (cm) – lower /upper estimate**	
			Global mean plus local land movement	**Regional sea level variation plus land movement**
Calder Hall	+11.0	9 – 69	(-2.0) –58.0	(-7) – 93
Dungeness	-7.7	9 – 69	16.7 – 76.7	12 – 111
Hartlepool	-2.2	9 – 69	11.2 – 71.2	7 - 106
Hunterston	+16.5	9 – 69	(-7.5) – 52.5	(-12) – 87
Sizewell	-6.6	9 – 69	15.6 – 75.6	11 – 110
Heysham	+7.7	9 – 69	1.3 – 61.3	(-3) – 96
Hinkley Point	-8.8	9 – 69	17.8 – 77.8	13 – 112
Bradwell	-9.9	9 – 69	18.9 – 78.9	14 – 113
Torness	+11.0	9 – 69	(-2.0) – 58.0	(-7) – 93

Table 6.2b Upper and lower estimates of effective sea-level rise (i.e. sea-level rise plus land movement) based upon figures from **Shennan & Horton 2002** and the IPCC TAR with an additional estimate due to regional variations (+/-fifty percent of the global mean), following UKCIP02. “Present day” is the modelled thirty year period 1961-90 hence estimates of isostatic change by the 2080s are based upon 110 years of expected land movement

6.5 Using Shennan and Horton's 2002 isostatic change data, the site with the greatest decrease in land height by the 2080s is expected to be Bradwell, and the greatest increase in land height by the 2080s is Hunterston. Although Bradwell is the site with the greatest net local sea level rise, Dungeness, Sizewell and Hinkley Point have very similar expected net rises.

6.6 Using Shennan 1989 (table 6.2), Dungeness is in a region where land is subsiding following deglaciation, with a net decrease in elevation of 11 centimetres by the 2080s. This will act to enhance the impact of local sea rise, contributing as much to the net change as the lower estimates of climate change induced sea level rise. The resulting local effective sea level rise in this region will be in the between 20 and 80 cm by the 2080s. Including the guidance estimate of regional effects this range increases to a net rise in sea level of between 16 and 115 cm.

6.7 Using Shennan 1989, as Hartlepool is located in a region where isostatic changes are expected to be zero the global mean sea level rise of between 9 and 69 cm rise by the 2080s holds. Adding the estimated impact of regional impacts this range extends to a net local sea level rise of between 5 and 104 cm.

6.8 Using Shennan 1989, of all the sites in this report Hunterston is located in the region of greatest uplift, with the area predicted to rise by 20 cm by the 2080s. This will moderate the impacts of any sea level rise and hence estimated net sea level rises are lower in this location than elsewhere. In fact the lowest estimates would result in a net decrease in local sea level, with the range of net sea level predictions being a possible fall of 11 cm to a rise of 49 cm. Inclusion of the additional regional effect extends the range to a potential fall in local sea level of 15 cm up to a local rise in sea level of 84 cm.

6.9 Using Shennan's 1989 data, continuing isostatic rebound in south eastern Britain means that by the 2080s it is estimated that the area around Sizewell will have fallen by approximately 22 cm, the greatest reduction in land elevation for the five locations under consideration. This will act to increase the local sea level rises with a predicted range of between 31 and 91 centimetres. As before, inclusion of an estimate of possible regional impacts increases this range to a prediction of between 27 and 126 cm, the largest predicted net sea level rise within this report.

6.10 Using Shennan and Horton's 2002 data (table 6.2b), the site with the largest predicted net sea level rise is Bradwell with between 14 and 113 cm, although Dungeness, Sizewell and Hinkley Point have maximum predicted net sea level rises of only a few centimetres less.

6.11 Although climate induced sea level rise may put some unprotected low-lying coastal regions at risk, it is assumed (given the lack of detailed site level information) that all of the cores of all eight sites in this report are situated at elevations above even the most extreme estimates of local net sea level rise. For example, taking the height above mean sea level of the Hinkley Point A power station as 2.5m ASL (as given in Fullwood, 2003), that exceeds the maximum local sea level rise for Hinkley Point of 1.15m by the 2080s given in Table 6.2. A potential risk of inundation does exist however in the form of storm surges. Storm surges are the temporary extremes of sea level, caused by low atmospheric pressure and strong winds. They occur in regions of shallow water such as on the continental shelf around the UK, including the North Sea, and the height of a surge may be increased by the shape of the coastline, particularly in estuaries and river mouths where a funnelling effect can occur.

Storm surges reach their most extreme levels when they coincide with high tides, but can occur at any time of day.

Port Name	Observed	Current climate (modelled)	
	50 year surge height (m)	5 year surge height (m)	50 year surge height (m)
Aberdeen	1.11	0.63	0.82
North Shields	1.66	0.74	0.96
Whitby	1.98	0.81	1.09
Lowestoft	2.36	1.29	1.85
Felixstowe	2.50	1.42	2.05
Southend	2.91	1.63	2.36
Dover	1.77	1.06	1.44
Ilfracombe	1.49	0.66	0.88
Swansea	2.27	0.87	1.19
Heysham	3.16	1.16	1.60
Millport	1.72	1.01	1.34

Table 6.3 Observed and modelled extreme storm surge heights relative to mean sea level for UK sites that roughly bracket the nuclear sites of interest to this report (following Lowe et al, 2001).

6.12 For illustration an earlier comparison of modelled and observed storm surges (taken from Lowe et al, 2001) is shown in Table 6.3. The heights are relative to mean sea level rather than relative to any chart datum. These results were derived using an earlier version of the Hadley Centre regional model (HadRM2) and focussed upon UK ports, a subset of which is shown above. While it is apparent that the model underestimates surge heights at all locations it should also be noted that the model does capture many features of the observed surge climatology. The replication of climatological features enables some confidence to be placed in the results from the model however the systematic underestimation of surge heights demonstrates the difficulties in modelling the phenomena and the uncertainties in these predictions. This must be borne in mind when considering predicted changes in future surge heights.

6.13 The values presented in Table 6.4 are based upon results using data from the latest Hadley Centre regional model HadRM3. All predicted changes in mean sea level, vertical land movement and changing meteorological forcing are included. It can be seen that the fifty year return period surge heights are predicted to either stay the same or increase at all locations under all scenarios. This is the same as saying that high water levels which are rarely attained in present day climate will be reached more frequently in the future.

6.14 The only sites which were already sinking according to Shennan (1989) that suffer greater surge heights (in table 6.4b), due to sinking more than the 1989 rates, are Hinkley Point and Hartlepool. The only site which was reckoned to be rising according to Shennan (1989) and which is reckoned to be rising at a slower rate in the 2002 analysis is Hunterston. The only sites where the surge height change by the 2080s is altered (due to new isostatic rates) by an amount equal to or more than 8cm are Sizewell and Bradwell.

6.15 The 2080s storm surge heights in Table 6.4b are based on storminess changes and local vertical land movements from Shennan (2002) and the predicted global average sea level rise, but they do not take into account local sea level rise due to changes in, for example, atmospheric pressure (the inverse barometer effect), local ocean warming/expansion and local changes in ocean circulation.

6.16 Therefore to get the absolute maximum rise, one would add the regional variation of sea level rise to the "High" surge change amounts in Table 6.4b (which only uses the global average sea level rise). Note that the right-hand column in table 6.2b of effective sea-level rise (see above) already includes local land movement and a proportion of the global average sea level rise (since the IPCC advises allowing for local sea level rises to be +/-fifty percent of the global mean). The global average sea level rise by the 2080s for the High scenario is 69cm. Therefore, the upper estimate of the change in the 1:50y surge height for Sizewell would be 1.35 + (0.5*0.69) m = 1.695m (the 1.35m comes from the High scenario column of table 6.4b of 2080s 1:50 year surge height changes). Hinkley Point could be up to 0.875m [0.53 + (0.5*0.69)]. Given the uncertainty in the sea level and surge changes, quoting the changes to .005 m is spurious, but it makes it easier to see where the numbers have come from, given that there are several components to the calculations. These "worst case scenarios" are given in the "High plus local sea level rise" column in Table 6.4b.

6.17 The implications, and effective heights, of increased surges for each location (excluding Heysham, Hinkley Point, Bradwell and Torness) are discussed in the supplementary report by Arup which appears as Appendix 6 of the 2004 report, however it is noted that without site levels and a knowledge of the flood defences, interpretation of possible impacts on the nuclear sites is not possible (the authors understand that a consideration of the site specific flood defence and coastal geohazard implications is to be dealt with by a subsequent study, to which this current effort will provide the necessary inputs on climate change).

Location	**2080s 1:50 year surge height change by 2080s (m)**	
	Low	**High**
Dungeness	0.3	0.9
Hartlepool	0.1	0.7
Hunterston	0.0	0.6
Calder Hall	0.1	0.7
Sizewell	0.9	1.5
Heysham	0.0	0.6
Hinkley Pt	-0.1	0.5
Bradwell	0.8	1.4
Torness	0.0	0.6

Table 6.4: Changes in 50-year return period surge height (metres) for the 2080s. The combined effect of global average sea level rise, storminess changes and vertical land movements (from Shennan, 1989) are considered. (The Low estimate is based upon an assumed global mean sea level rise of 9 cm while the High estimate assumes a mean sea level rise of 69 cm)

Location	2080s 1:50 year surge height change by 2080s (m)		
	Low	High	High plus local sea level rise
Dungeness	0.27	0.87	1.22
Hartlepool	0.12	0.72	1.07
Hunterston	0.04	0.64	0.99
Calder Hall	0.05	0.65	1.00
Sizewell	0.75	1.35	1.70
Heysham	-0.06	0.55	0.90
Hinkley Pt	-0.07	0.53	0.88
Bradwell	0.72	1.32	1.67
Torness	-0.01	0.59	0.94

Table 6.4b: Changes in 50-year return period surge height (metres) for the 2080s. The combined effect of global average sea level rise, storminess changes and vertical land movements (from Shennan and Horton, 2002) are considered. (The Low estimate is based upon an assumed global mean sea level rise of 9 cm while the High estimate assumes a mean sea level rise of 69 cm). The rightmost column includes potential local sea level rise effects.

6.18 Predicted increases in near-sea surface temperatures are shown in Table 6.5. The range of values predicted is greater than expected for the actual sea surface temperatures (as is to be expected due to the greater thermal inertia of the sea), but the HadRM3 model does not include an ocean: it is an atmosphere-only model. As the changes in sea surface temperature are not judged as significant for the decommissioned structures at each location (see Appendix 6 of the 2004 report) these figures are included for completeness only and are not discussed further.

Location	Sea surface temperature change (°C) – lower summer estimate	Sea surface temperature change (°C) – upper summer estimate	Sea surface temperature change (°C) – lower winter estimate	Sea surface temperature change (°C) – upper winter estimate
Dungeness	2.0 to 2.5	4.0 to 4.5	1.5 to 2.0	3.5 to 4.0
Hartlepool	1.5 to 2.0	3.0 to 3.5	1.0 to 1.5	2.5 to 3.0
Hunterston	0.5 to 2.0	1.5 to 2.0	0.5 to 2.0	1.5 to 2.0
Calder Hall	1.0 to 1.5	2.0 to 2.5	1.0 to 1.5	2.0 to 2.5
Sizewell	2.0 to 2.5	4.0 to 4.5	1.5 to 2.0	3.0 to 3.5
Heysham	1.0 to 1.5	2.0 to 2.5	1.0 to 1.5	2.0 to 2.5
Hinkley Pt	1.5 to 2.0	3.5 to 4.0	1.0 to 1.5	2.5 to 3.0
Bradwell	2.0 to 2.5	4.0 to 4.5	1.5 to 2.0	3.0 to 3.5
Torness	1.5 to 2.0	2.5 to 3.0	1.0 to 1.5	2.0 to 2.5

Table 6.5 Predicted changes in near-surface temperature over the sea by the 2080s

6.19 For comments on the effect of river flows on the sites (excluding Heysham, Hinkley Point, Bradwell and Torness), see Arup's appendix to the 2004 report.

7. Conclusions

7.1 This report is designed to give an overview of climate change for the sites and covers the magnitude of predicted change in the climate of those sites for several variables for the next 100 years. Predictions are made for a variety of greenhouse gas emission scenarios, where possible, as the future path of emissions is one of the biggest uncertainties in predicting the future climate.

7.2 The Met Office Regional Climate Model (RCM) predicts that seasonal average temperatures will increase significantly for all the sites, with the greatest increases seen in the summer and for sites in the south. The RCM also suggests that both daily maximum and minimum temperatures will increase in all seasons. Maximum daily temperatures will increase most during summer with increases being slightly less during winter. Extremely warm days will occur more frequently in summer although, as noted in the supplementary report by Arup (Appendix 6) of the 2004 report, temperatures will not approach the operating temperature of the cores of the decommissioned stations. Minimum, or night time, temperatures also increase at all locations resulting in fewer nights with freezing conditions and less severe temperatures for each of the decommissioned power station sites.

7.3 Significant changes are also expected in rainfall, especially in summer, with large reductions in the average amount of summer rainfall. Seasonal average precipitation amounts are predicted to increase in winter and to decrease in summer for all the sites examined. In general, extreme precipitation amounts are predicted to increase for events of duration from one hour up to twelve hours, and for return periods from two years up to very rare events with return periods of one hundred years and more.

7.4 In general the seasonal average wind speeds are predicted to increase during winter and decrease during summer, but with some exceptions, e.g. Hinkley Point where wind speeds are predicted to increase in both winter and summer. The HadRM3 RCM predicts that extreme hourly winds and extreme gusts will be slightly higher in future for all the sites studied, but the increases only range from just under 2% for Torness to 6% for Hinkley Point.

7.5 Although mean sea level increases in themselves are not thought to be a major future hazard, the increases in future surge heights of potentially more than a metre in places could, when combined with wind speed increases, threaten some sites unless the existing defences are enhanced.

7.6 It is recommended that a similar study should be carried out after the UKCIP08 report is published in 2008, for risk-based planning calculations, and that similar studies should be carried out periodically after subsequent improvements in regional climate model predictions.

8. References

Fullwood, J., The climate of Hinkley Point 'A', Met Office/BNFL, 2003

Fullwood, J., The climate of Dungeness 'A', Met Office/BNFL, 2003

Fullwood, J., The climate of Heysham, Met Office/BNFL, 2002

Fullwood, J., Climatology of Torness, Met Office/BNFL, 2000

Fullwood, J., Climatology of Sizewell, Met Office/BNFL, 2000

Fullwood, J., Climatology of Hunterston, Met Office/BNFL, 2000

Fullwood, J., Climatology of Bradwell, Met Office/BNFL, July 2000

Hulme, M., Jenkins, G.J., Lu, X., Turnpenny, J.R., Mitchell, T.D., Jones, R.G., Lowe, J., Murphy, J.M., Hassell, D., Boorman, P., McDonald, R., Hill, S., Climate Change Scenarios for the United Kingdom: The UKCIP02 Scientific Report, Tyndall Centre for Climate Change Research, School of Environmental Sciences, University of East Anglia, Norwich, UK. 120 pp, 2002.

IPCC, Emissions Scenarios. 2000. Special Report of the Intergovernmental Panel on Climate Change. Nebojsa Nakicenovic and Rob Swart (Eds.) Cambridge University Press, UK. 570 pp. Available from Cambridge University Press, The Edinburgh Building Shaftesbury Road, Cambridge CB2 2RU

IPCC, Emissions Scenarios. 2000. Special Report of the Intergovernmental Panel on Climate Change. Summary for Policymakers. IPCC, Geneva, Switzerland. 20 pp

IPCC, Climate Change 2001: The Scientific Basis. Contribution of Working Group I to the Third Assessment Report of the Intergovernmental Panel on Climate Change (IPCC). J. T. Houghton, Y. Ding, D.J. Griggs, M. Noguer, P. J. van der Linden and D. Xiaosu (Eds.) Cambridge University Press, UK. 944 pp. Available from Cambridge University Press, The Edinburgh Building Shaftesbury Road, Cambridge CB2 2RU

IPCC, Climate Change 2001: The Scientific Basis. Summary for Policymakers (SPM) and Technical Summary (TS). IPCC, Geneva, Switzerland. 98 pp

IPCC, Climate Change 2007: The Scientific Basis. Summary for Policymakers (SPM) and Technical Summary (TS). IPCC, Geneva, Switzerland

Leggett, J., W. Pepper, R.J. Swart, J. Edmonds, L.G. Meira Filho, I. Mintzer, M.X. Wang, J. Watson (1992) Emissions Scenarios for the IPCC: An Update pp.75-92 in Climate Change 1992: The Supplementary Report to the IPCC Scientific Assessment, Cambridge University Press, Cambridge, UK

Lowe, J. A., Gregory J. M. and Flather R. A., Changes in the occurrence of storm surges around the United Kingdom under a future climate scenario using a dynamic storm surge model driven by the Hadley Centre climate models, Climate Dynamics v. 18 n.3/4 pp.179-188; 2001 Dec

Robson A., Reed D., Flood Estimation Handbook, Vol. 3, Statistical procedures for flood frequency estimation. Wallingford, Institute of Hydrology, 1999

Shennan, I., Holocene crustal movements and sea level changes in Great Britain. Journal of Quaternary Science, v.4 n.1 pp.77-89, 1989

Shennan, I., Horton, B. (2002) Holocene land- and sea-level changes in Great Britain . Journal of Quaternary Science 17: 511-526

Tabony, R.C., Historical data for extreme wind. Final report. Nuclear Electric/Met Office, 1994

Tabony, R.C., Extreme ambient temperatures. Final report, Nuclear Electric/Met Office, 1996

Acknowledgements

Thanks to my colleagues Mark Beswick and John Fullwood for valuable input, and to Rob Harrison and Mo Mylne for reviewing and making helpful suggestions.

Appendix 1: summaries of 1961-90 climate (selected sites)

CLIMATE ESTIMATES (1961 - 1990): Heysham

EASTING: 340100 NORTHING: 459600 [NGR]
LATITUDE: 54.029 LONGITUDE: -02.915

Altitude 3 metres above msl

Variable		Jan	Feb	Mar	Apr	May	Jun	Jul	Aug	Sep	Oct	Nov	Dec	Year
Max Temp	deg C	6.5	6.6	8.4	10.9	14.5	17.1	18.4	18.3	16.3	13.5	9.4	7.3	12.3
Min Temp	deg C	2.2	2.1	3.2	4.9	7.8	10.8	12.6	12.7	10.9	8.5	4.8	3.0	7.0
Mean Temp	deg C	4.4	4.3	5.8	7.9	11.1	13.8	15.4	15.5	13.6	11.0	7.1	5.2	9.6
Temp Range	deg C	4.3	4.5	5.2	6.1	6.7	6.3	5.9	5.8	5.6	5.1	4.6	4.4	5.4
Highest Max	deg C	14	14	23	22	27	30	32	33	26	24	17	14	33
Lowest Min	deg C	-10	-10	-7	-5	-1	2	4	4	1	-3	-6	-11	-11
Lowest Max	deg C	-4	-2	1	4	7	11	14	13	10	6	2	-2	-4
Highest Min	deg C	9	10	11	12	15	18	19	19	17	16	12	11	19
Grass Min	deg C	0.1	0.0	1.0	2.3	5.1	7.9	10.1	10.2	8.6	6.3	2.6	0.9	4.6
30cm Soil Temp	deg C	4.3	4.2	5.5	8.1	11.5	14.5	16.0	15.9	14.0	11.3	7.8	5.5	9.9
Sunshine	hours	50	73	110	159	206	203	188	172	131	99	64	46	1501
Rainfall	mm	98	54	65	62	60	66	62	83	107	110	87	97	949
Wind at 10 m	knots	12.2	11.6	11.9	10.1	10.1	9.8	10.2	10.0	11.1	11.8	12.2	12.1	11.1
Minimum hourly RH	%	83	79	75	71	67	70	71	72	74	77	80	83	75
Maximum hourly RH	%	88	88	88	88	89	90	90	91	91	90	89	89	89
Air Frost	days	7.3	7.1	3.6	1.2	0.1	0.0	0.0	0.0	0.0	0.2	2.9	5.9	28.3
Grass Frost	days	13.3	12.8	10.7	7.3	2.5	0.4	0.0	0.0	0.6	2.2	7.9	12.0	69.7
>= 10mm rain	days	2.7	1.7	2.3	1.6	1.6	2.1	2.2	3.2	3.7	3.6	3.3	3.0	31.0
>= 1mm rain	days	15.0	10.2	12.3	10.1	11.2	10.7	10.2	12.3	13.0	14.3	14.7	14.1	148.2
>= 0.2mm rain	days	19.0	13.8	16.0	13.7	14.3	13.6	13.4	15.4	16.0	17.5	17.9	17.9	188.5
Sleet/Snow fall	days	5.2	4.5	3.7	2.0	0.4	0.0	0.0	0.0	0.0	0.1	1.7	2.2	19.7
Snow lying	days	2.4	1.6	0.7	0.2	0.0	0.0	0.0	0.0	0.0	0.0	0.3	1.2	6.4
Hail	days	1.1	0.9	0.7	0.6	0.4	0.2	0.1	0.1	0.1	0.5	1.2	1.0	7.0
Thunder heard	days	0.1	0.1	0.2	0.4	1.5	1.4	1.2	1.2	0.7	0.4	0.2	0.1	7.4

notes:

These estimates are interpolated from values on a regular grid derived from station observations.

Where relevant and possible the effects of altitude, urban areas and proximity to the coast are taken into account.

Local, effects are not taken into account in producing these estimates. As a general rule this makes them less accurate in mountainous areas. In particular, Days of thunder, Hail, Snow falling and Snow lying may be unreliable in sparse data areas such as central and northern Scotland.

CLIMATE ESTIMATES (1961 - 1990): Torness

EASTING: 374500 NORTHING: 675100 [NGR]
LATITUDE: 55.968 LONGITUDE: -02.409

Altitude 14 metres above msl

Variable		Jan	Feb	Mar	Apr	May	Jun	Jul	Aug	Sep	Oct	Nov	Dec	Year
Max Temp	deg C	6.4	6.4	8.2	10.1	12.9	16.1	17.7	17.7	15.8	13.0	9.0	7.3	11.7
Min Temp	deg C	1.6	1.4	2.6	4.0	6.4	9.3	11.0	11.1	9.6	7.3	3.8	2.4	5.9
Mean Temp	deg C	4.0	3.9	5.4	7.1	9.6	12.7	14.4	14.4	12.7	10.2	6.5	4.9	8.8
Temp Range	deg C	4.9	5.0	5.7	6.2	6.6	6.9	6.9	6.7	6.4	5.7	5.2	4.9	5.9
Highest Max	deg C	13	14	19	21	23	28	28	31	24	21	17	14	31
Lowest Min	deg C	-14	-10	-8	-6	-2	0	3	4	0	-3	-6	-10	-14
Lowest Max	deg C	-6	-3	0	2	5	7	10	11	8	5	0	-4	-6
Highest Min	deg C	10	10	10	11	14	15	17	19	16	15	12	10	19
Grass Min	deg C	-0.4	-0.6	0.5	1.9	4.5	7.7	9.4	9.3	7.7	5.1	1.6	0.2	3.9
30cm Soil Temp	deg C	3.3	3.4	4.8	7.4	10.9	14.1	15.7	15.5	13.1	10.2	6.6	4.5	9.1
Sunshine	hours	54	76	114	152	187	190	183	169	130	100	68	45	1469
Rainfall	mm	52	32	43	35	49	47	51	63	53	55	56	46	584
Wind at 10 m	knots	13.7	12.9	13.5	11.1	10.2	9.6	9.2	9.8	11.3	11.8	13.5	13.8	11.7
Minimum hourly RH	%	82	80	75	73	72	71	71	73	75	78	80	82	76
Maximum hourly RH	%	88	87	87	88	90	90	91	91	91	90	88	88	89
Air Frost	days	8.9	8.4	5.3	2.8	0.5	0.0	0.0	0.0	0.1	0.8	4.7	7.5	39.2
Grass Frost	days	15.6	14.7	12.4	8.0	3.1	0.5	0.1	0.2	0.9	3.2	9.8	14.0	82.6
>= 10mm rain	days	0.4	0.2	0.4	0.5	0.9	1.1	1.2	1.2	0.9	0.8	0.8	0.5	8.9
>= 1mm rain	days	11.1	8.3	9.6	8.5	9.8	8.1	8.4	9.7	9.5	10.1	10.2	10.1	113.4
>= 0.2mm rain	days	16.3	12.9	14.7	13.5	13.9	11.7	12.2	14.0	13.9	14.9	15.2	15.2	168.3
Sleet/Snow fall	days	5.7	6.1	4.6	2.4	0.3	0.0	0.0	0.0	0.0	0.1	1.7	3.7	24.8
Snow lying	days	2.8	2.5	0.9	0.3	0.0	0.0	0.0	0.0	0.0	0.0	0.4	1.1	8.0
Hail	days	1.0	0.9	0.9	1.0	0.6	0.1	0.0	0.0	0.1	0.2	1.0	1.2	7.1
Thunder heard	days	0.1	0.1	0.1	0.2	1.1	1.1	0.9	1.0	0.4	0.2	0.1	0.1	5.4

notes:

These estimates are interpolated from values on a regular grid derived from station observations.

Where relevant and possible the effects of altitude, urban areas and proximity to the coast are taken into account.

Local, effects are not taken into account in producing these estimates. As a general rule this makes them less accurate in mountainous areas. In particular, Days of thunder, Hail, Snow falling and Snow lying may be unreliable in sparse data areas such as central and northern Scotland.

CLIMATE ESTIMATES (1961 - 1990): Hartlepool

EASTING: 453000 NORTHING: 527000 [NGR]
LATITUDE: 54.635 LONGITUDE: -01.179

Altitude 1.5 metres above msl

Variable		Jan	Feb	Mar	Apr	May	Jun	Jul	Aug	Sep	Oct	Nov	Dec	Year
Max Temp	deg C	6.8	7.0	9.1	11.0	14.1	17.4	19.3	19.2	17.2	14.0	9.5	7.5	12.7
Min Temp	deg C	1.4	1.6	2.7	4.4	7.0	9.9	11.9	11.8	10.0	7.5	3.9	2.2	6.2
Mean Temp	deg C	4.1	4.3	5.9	7.7	10.6	13.7	15.6	15.5	13.6	10.7	6.7	4.9	9.4
Temp Range	deg C	5.2	5.2	6.3	6.6	7.1	7.4	7.3	7.2	7.2	6.3	5.5	5.2	6.4
Highest Max	deg C	15	15	22	22	25	29	30	33	26	25	17	16	33
Lowest Min	deg C	-13	-12	-10	-6	-2	0	3	3	0	-2	-7	-12	-13
Lowest Max	deg C	-4	-2	0	3	6	9	12	12	9	4	0	-3	-4
Highest Min	deg C	10	11	11	11	13	17	18	18	17	16	12	12	18
Grass Min	deg C	-0.4	-0.3	0.6	1.9	5.0	8.2	9.9	10.1	8.0	5.5	1.9	0.1	4.2
30cm Soil Temp	deg C	3.8	3.8	5.2	7.8	11.2	14.5	16.1	15.9	13.9	11.0	7.3	5.0	9.6
Sunshine	hours	49	64	102	134	176	177	168	160	129	96	63	42	1357
Rainfall	mm	39	31	40	38	44	49	50	59	43	42	56	46	537
Wind at 10 m	knots	13.4	12.9	12.8	9.7	10.5	10.3	9.4	9.7	11.7	11.3	12.7	14.2	11.6
Minimum hourly RH	%	78	76	70	69	67	66	67	68	69	74	76	79	72
Maximum hourly RH	%	88	87	87	88	89	90	91	92	91	91	89	89	89
Air Frost	days	8.8	8.0	4.6	1.7	0.1	0.0	0.0	0.0	0.0	0.4	4.1	7.6	35.3
Grass Frost	days	16.0	14.5	12.5	7.8	2.8	0.3	0.0	0.0	0.7	3.2	9.9	14.4	82.2
>= 10mm rain	days	0.5	0.4	0.6	0.7	0.9	1.3	1.2	1.6	1.0	0.7	1.1	0.7	10.7
>= 1mm rain	days	11.4	8.7	10.2	9.3	9.5	9.0	8.2	9.5	8.8	9.5	11.3	11.0	116.5
>= 0.2mm rain	days	16.6	13.1	15.2	13.9	13.5	12.5	12.0	13.2	12.9	14.0	15.9	15.9	168.8
Sleet/Snow fall	days	7.4	7.2	5.4	2.6	0.3	0.0	0.0	0.0	0.0	0.1	2.1	4.7	29.8
Snow lying	days	3.1	3.1	1.3	0.2	0.0	0.0	0.0	0.0	0.0	0.0	0.8	1.9	10.3
Hail	days	0.7	0.7	0.7	0.9	0.5	0.2	0.1	0.1	0.1	0.2	0.5	0.8	5.5
Thunder heard	days	0.1	0.1	0.2	0.5	1.8	1.7	1.5	1.5	0.8	0.3	0.1	0.1	8.6

notes:

These estimates are interpolated from values on a regular grid derived from station observations.

Where relevant and possible the effects of altitude, urban areas and proximity to the coast are taken into account.

Local, effects are not taken into account in producing these estimates. As a general rule this makes them less accurate in mountainous areas. In particular, Days of thunder, Hail, Snow falling and Snow lying may be unreliable in sparse data areas such as central and northern Scotland.

Appendix 2: Probabilities of daily maximum temperature exceeding given thresholds.

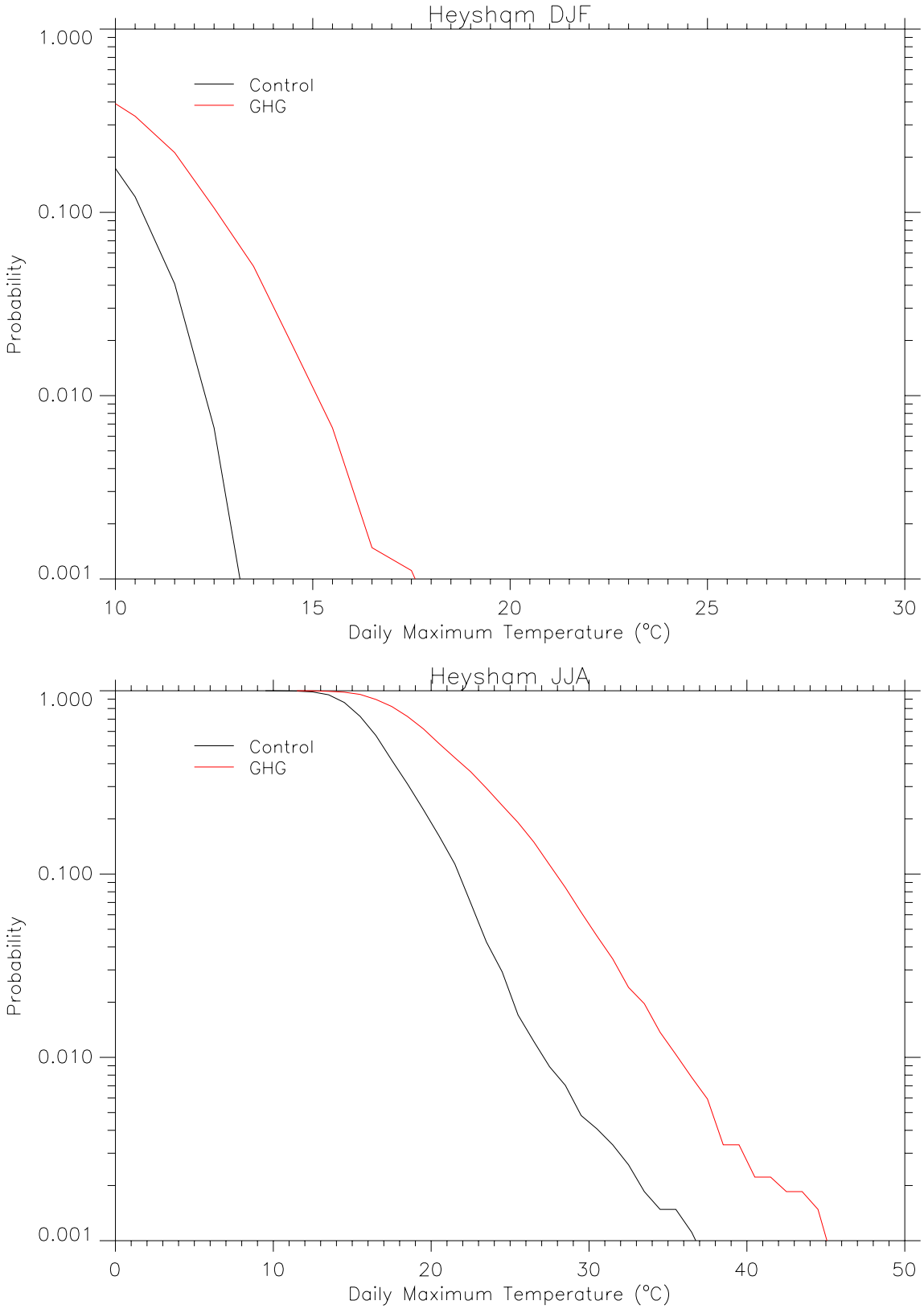

Figure A2.1 Probability of exceedence of daily maximum temperature thresholds for Heysham. Modelled current climate (black) and Medium High scenario 2080s climate (red) for winter (December – February, upper panel) and summer (June – August, lower panel)

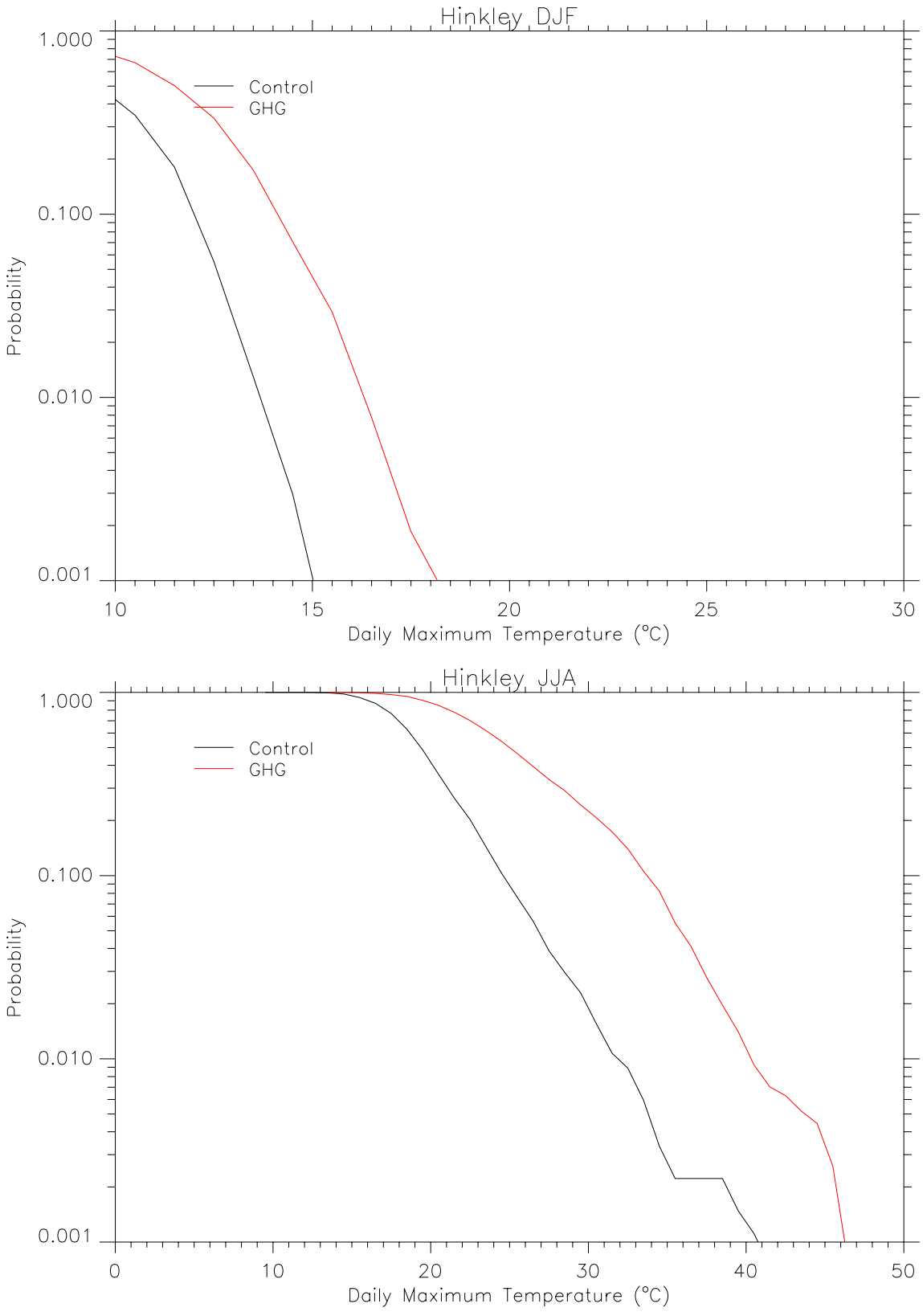

Figure A2.2 Probability of exceedence of daily maximum temperature thresholds for Hinkley Point. Modelled current climate (black) and Medium High scenario 2080s climate (red) for winter (December – February, upper panel) and summer (June – August, lower panel)

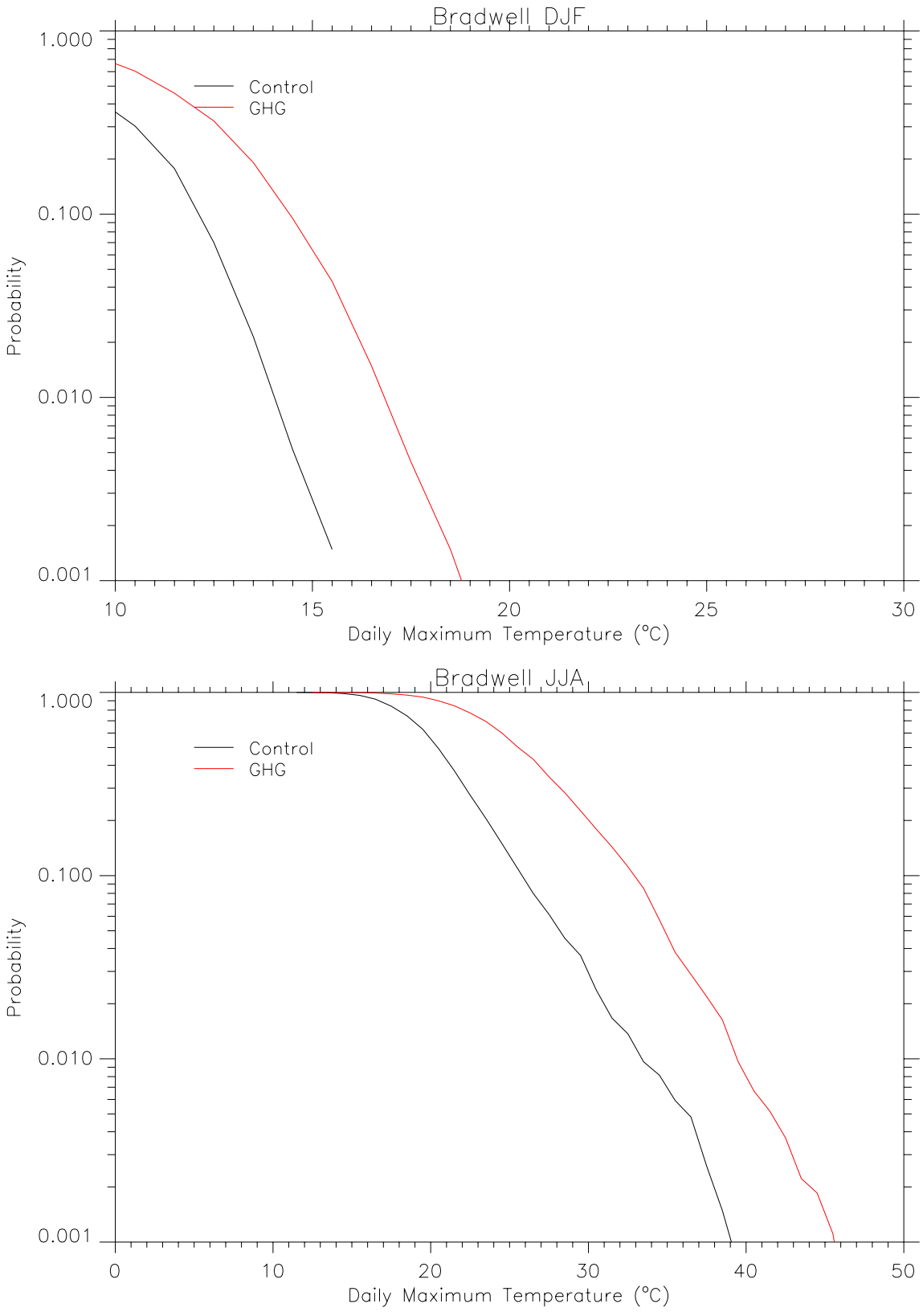

Figure A2.3 Probability of exceedence of daily maximum temperature thresholds for Bradwell. Modelled current climate (black) and Medium High scenario 2080s climate (red) for winter (December – February, upper panel) and summer (June – August, lower panel)

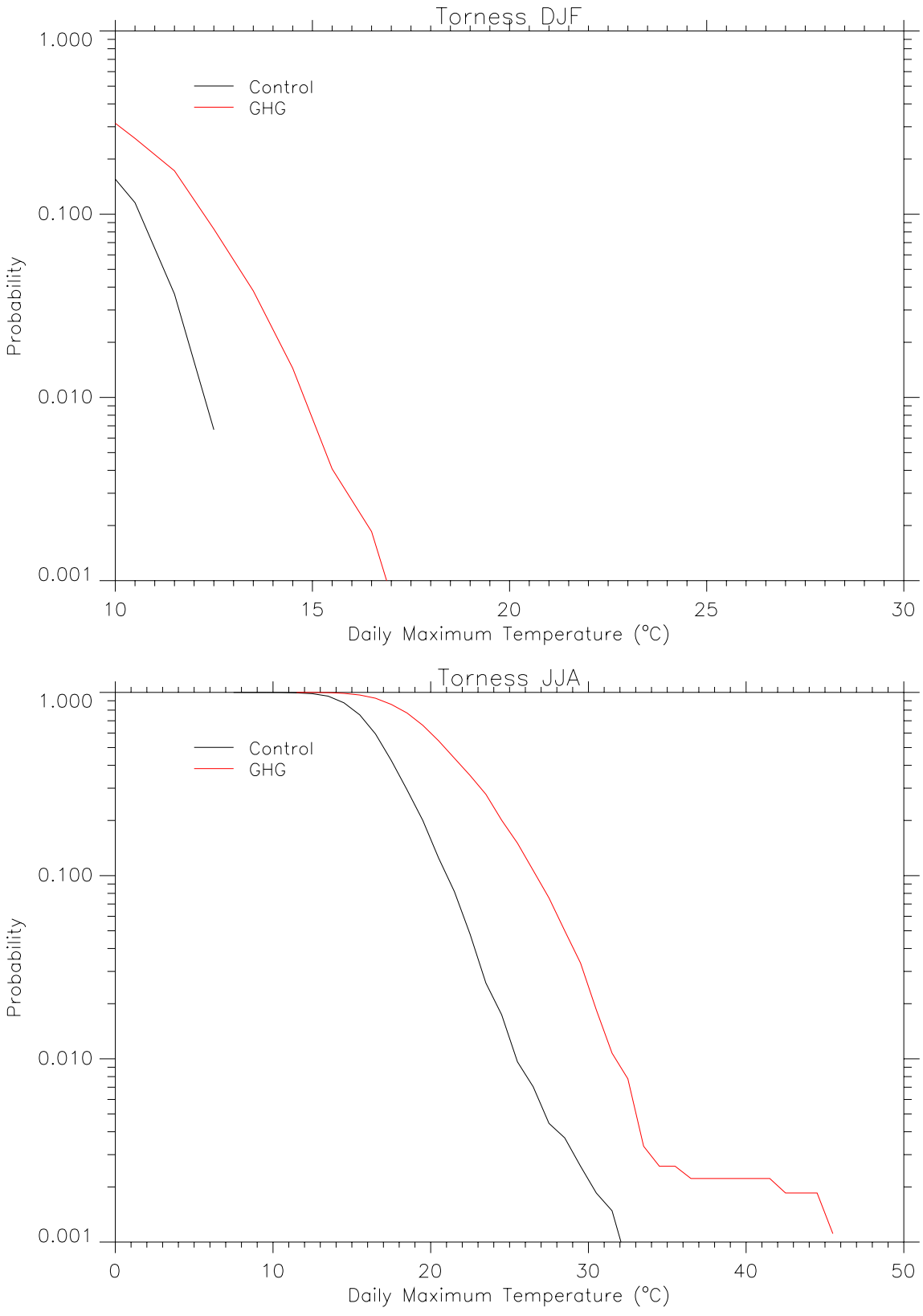

Figure A2.4 Probability of exceedence of daily maximum temperature thresholds for Torness. Modelled current climate (black) and Medium High scenario 2080s climate (red) for winter (December – February, upper panel) and summer (June – August, lower panel)

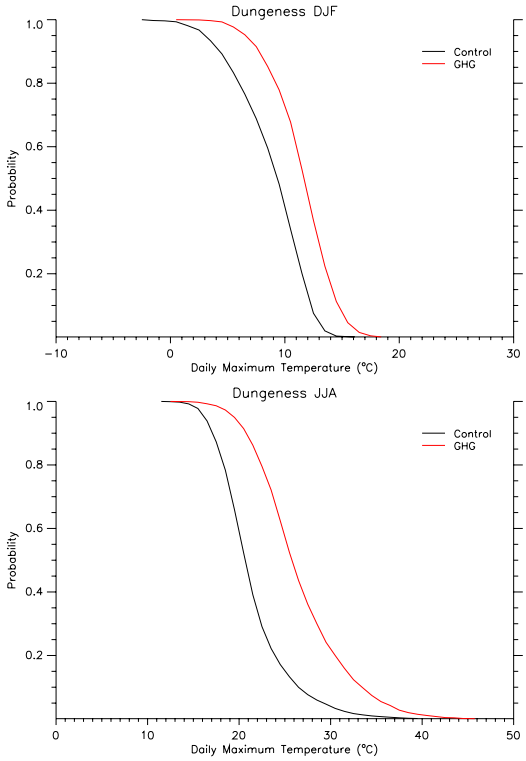

Figure A2.2 Probability of exceedence of daily maximum temperature thresholds for Dungeness. Modelled current climate (black) and Medium High scenario 2080s climate (red) for winter (December – February, upper panel) and summer (June – August, lower panel)

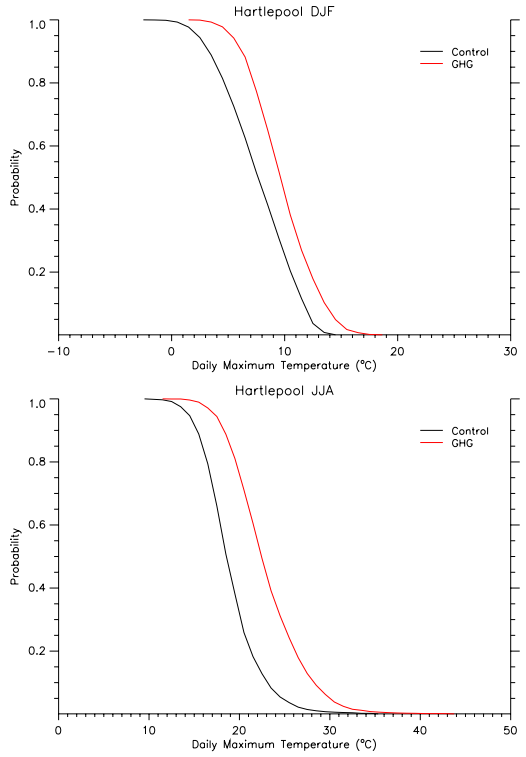

Figure A2.3 Probability of exceedence of daily maximum temperature thresholds for Hartlepool. Modelled current climate (black) and Medium High scenario 2080s climate (red) for winter (December – February, upper panel) and summer (June – August, lower panel)

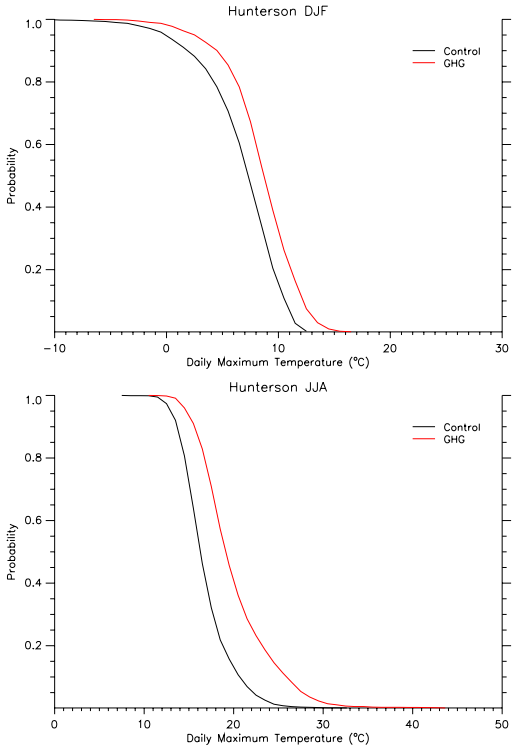

Figure A2.4 Probability of exceedence of daily maximum temperature thresholds for Hunterston. Modelled current climate (black) and Medium High scenario 2080s climate (red) for winter (December – February, upper panel) and summer (June – August, lower panel)

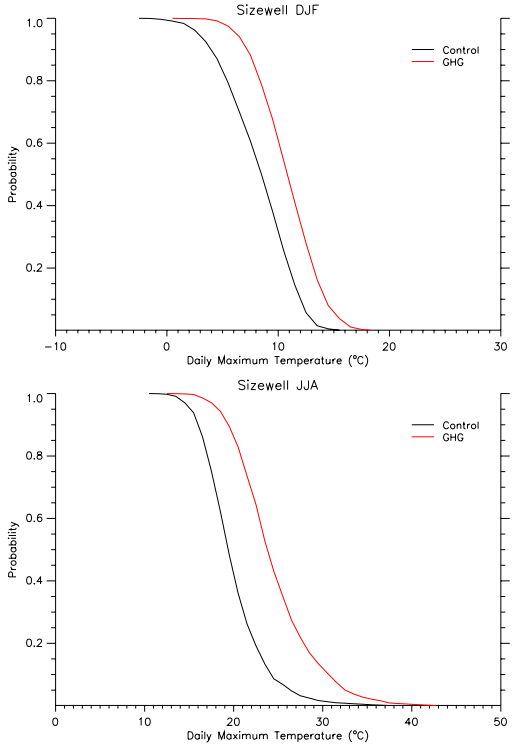

Figure A2.5 Probability of exceedence of daily maximum temperature thresholds for Sizewell. Modelled current climate (black) and Medium High scenario 2080s climate (red) for winter (December – February, upper panel) and summer (June – August, lower panel)

Appendix 3: Winter average daily maximum temperatures

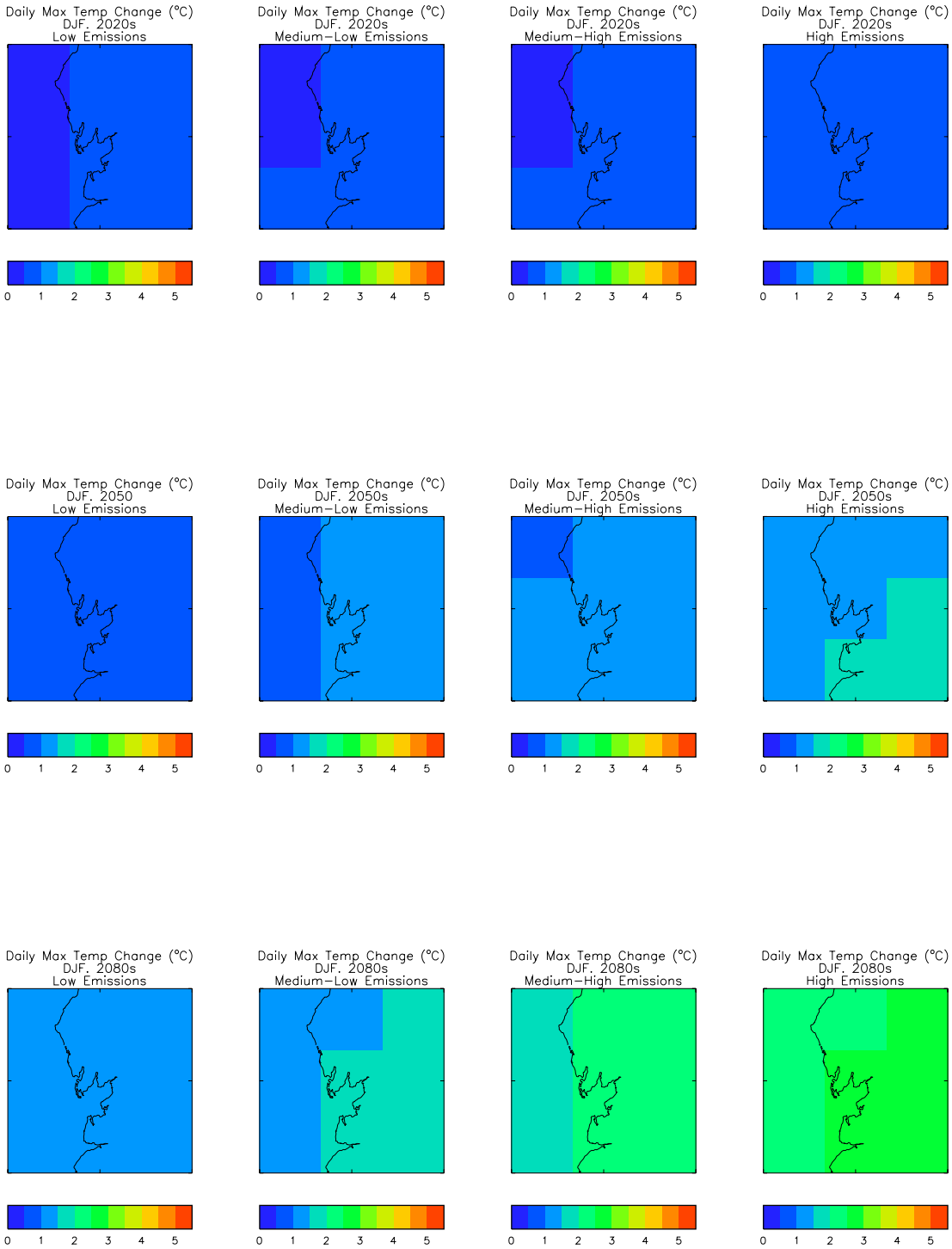

Figure A3.1. Predicted changes (˚C), in Heysham winter (December - February) average maximum temperatures (relative to the simulated 1961-90 climate) for four emissions scenarios (Low - left column, High – right column), for thirty-year periods centred on the 2020s, 2050s and 2080s (rows, top to bottom).

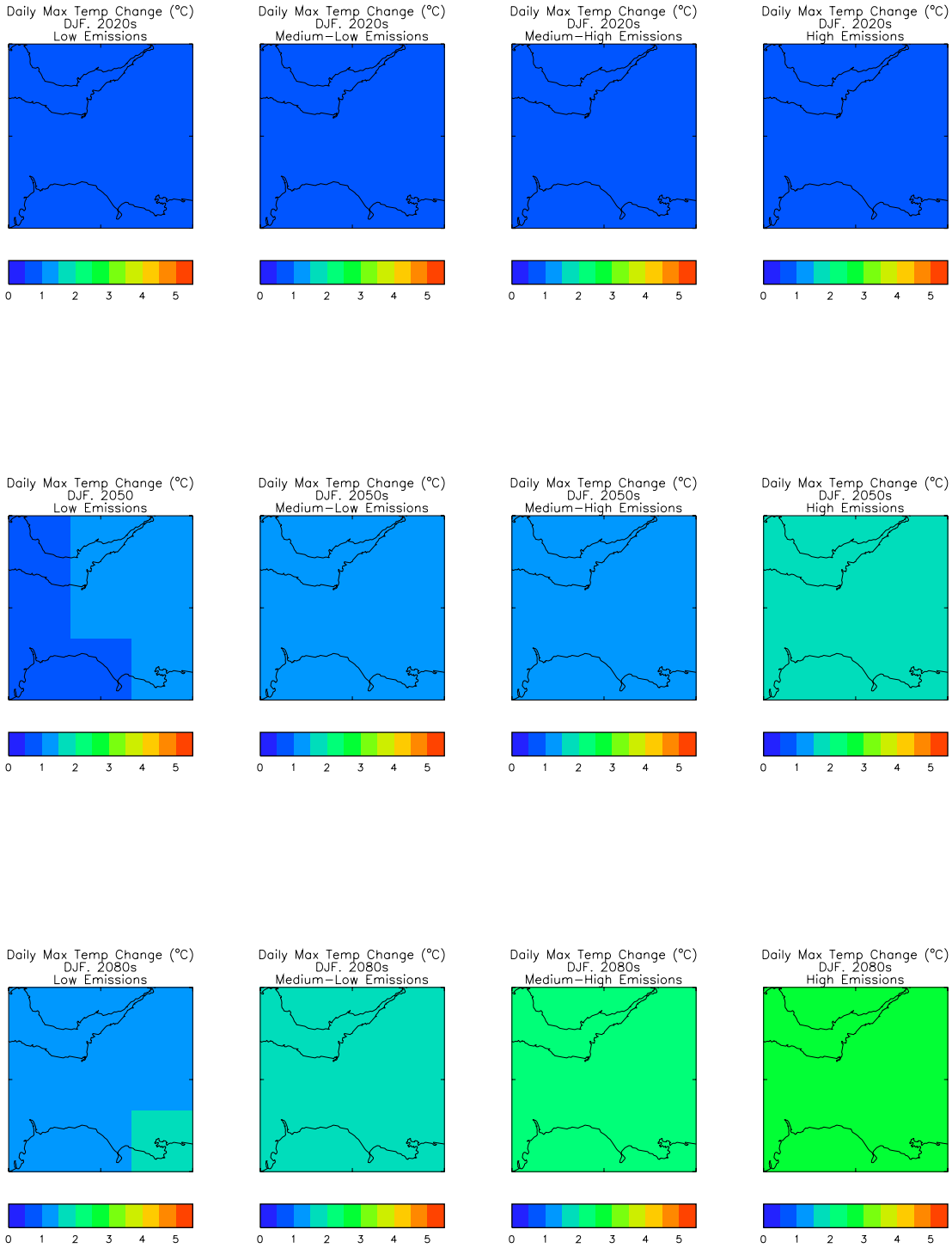

Figure A3.2. Predicted changes (˚C), in Hinkley Point winter (December - February) average maximum temperatures (relative to the simulated 1961-90 climate) for four emissions scenarios (Low - left column, High – right column), for thirty-year periods centred on the 2020s, 2050s and 2080s (rows, top to bottom).

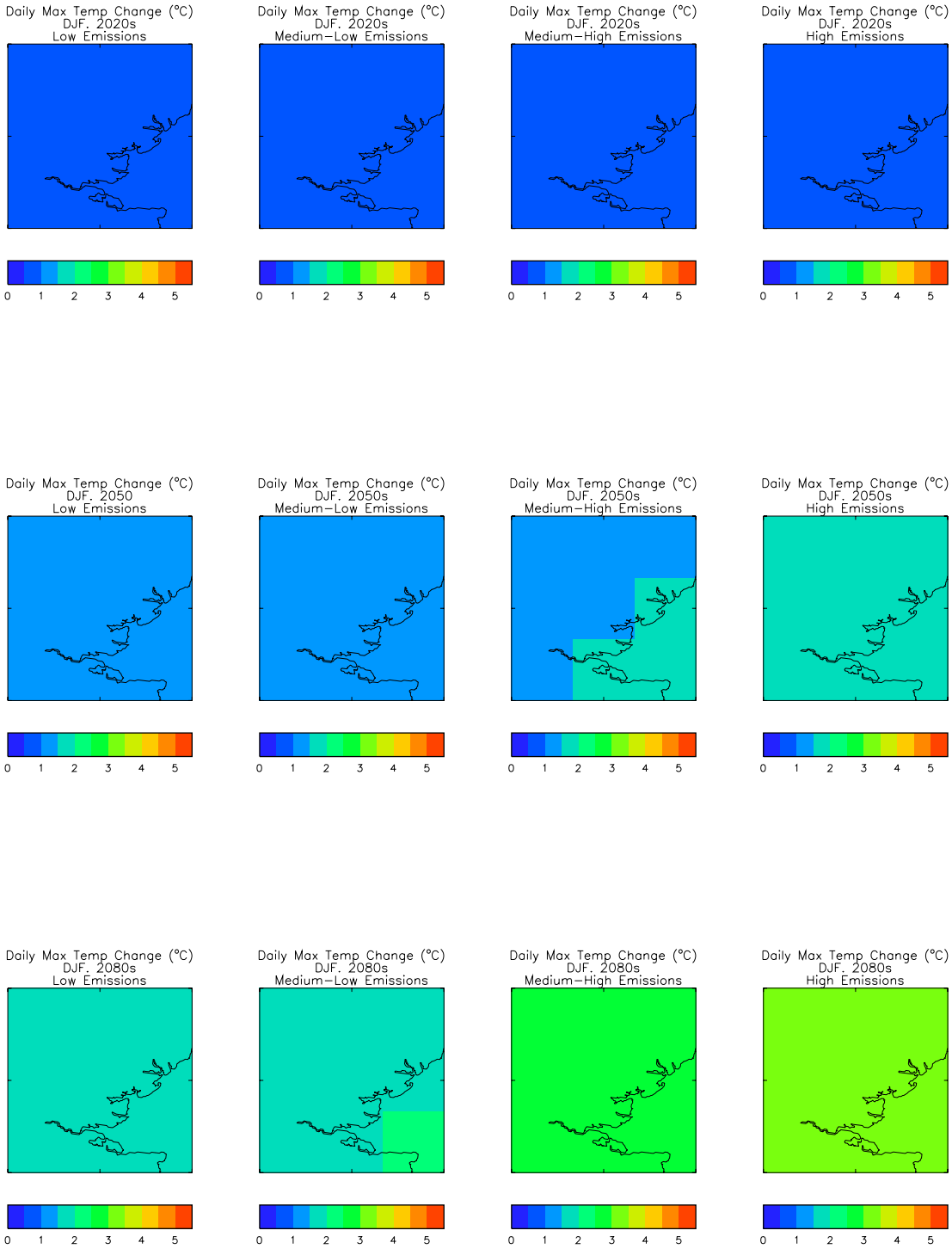

Figure A3.3. Predicted changes (˚C), in Bradwell winter (December - February) average maximum temperatures (relative to the simulated 1961-90 climate) for four emissions scenarios (Low - left column, High – right column), for thirty-year periods centred on the 2020s, 2050s and 2080s (rows, top to bottom).

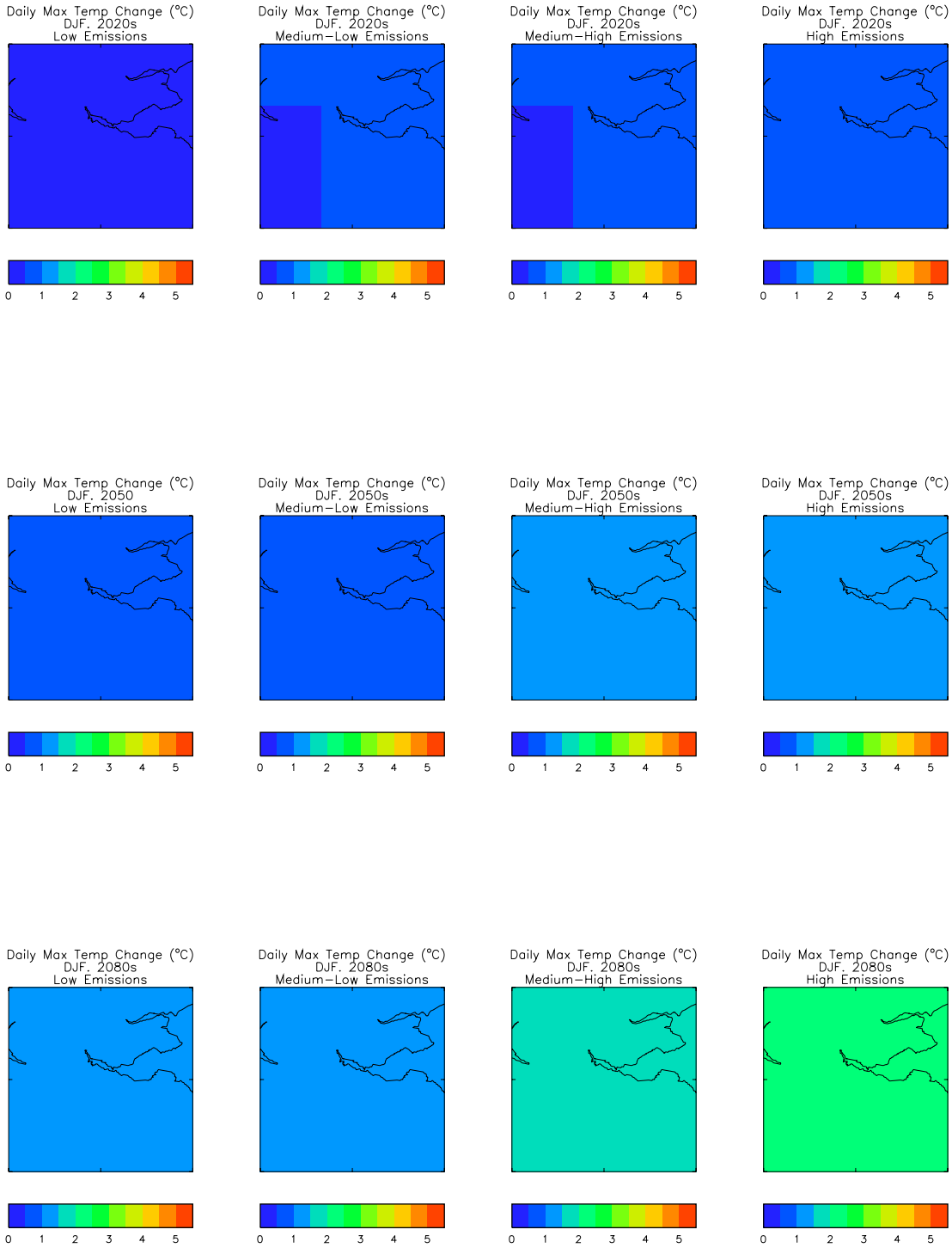

Figure A3.4. Predicted changes (˚C), in Torness winter (December - February) average maximum temperatures (relative to the simulated 1961-90 climate) for four emissions scenarios (Low - left column, High – right column), for thirty-year periods centred on the 2020s, 2050s and 2080s (rows, top to bottom).

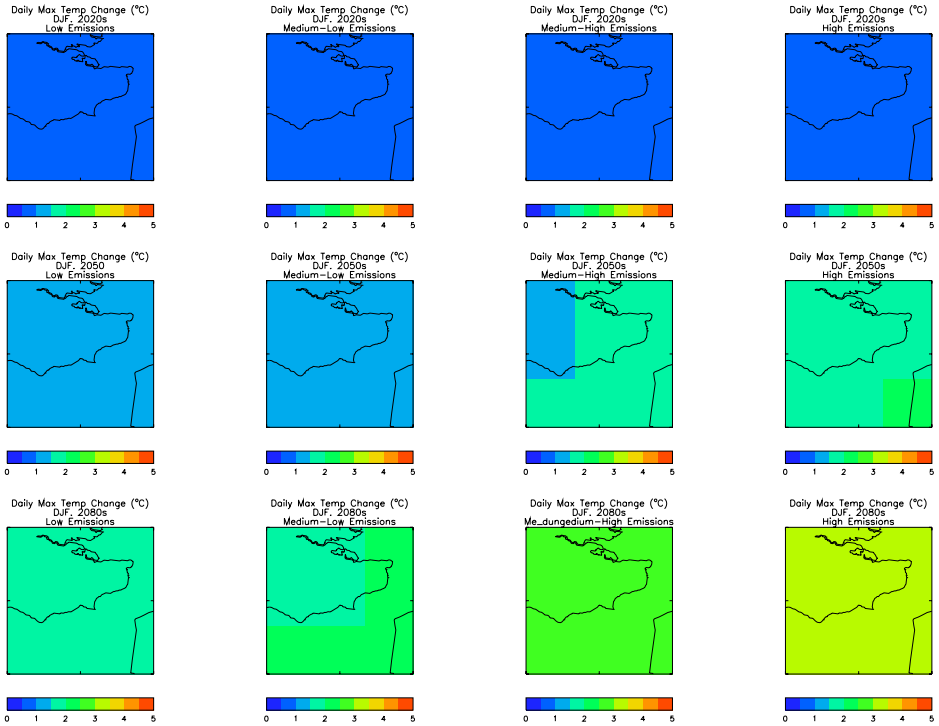

Figure A3.5. Predicted changes (°C), in Dungeness winter (December - February) average maximum temperatures (relative to the simulated 1961-90 climate) for four emissions scenarios (Low - left column, High – right column), for thirty-year periods centred on the 2020s, 2050s and 2080s (rows, top to bottom).

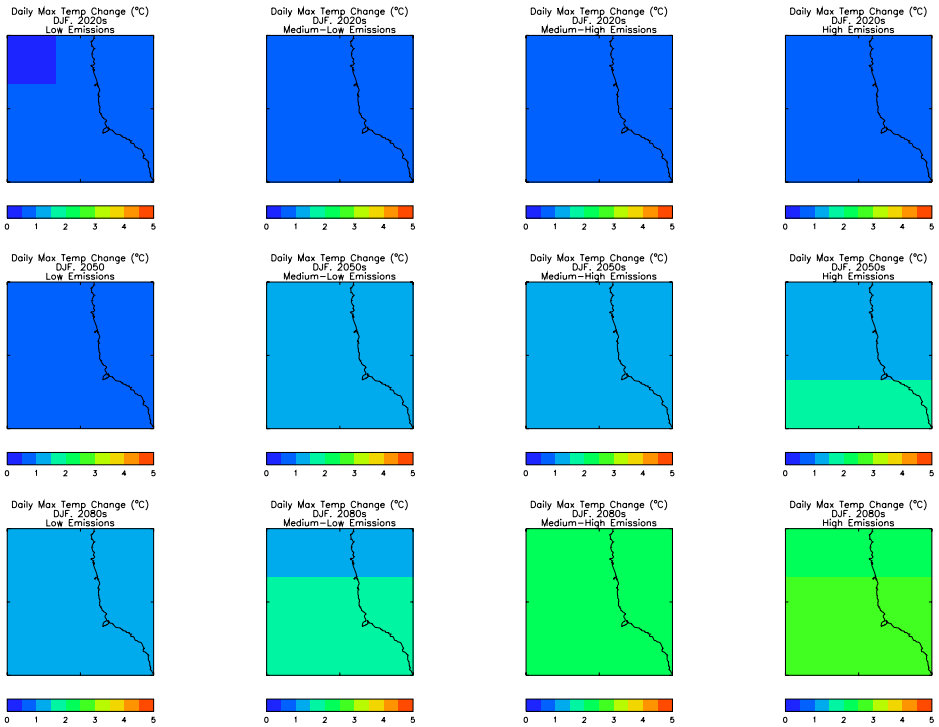

Figure A3.6. Predicted changes (°C), in Hartlepool winter (December - February) average maximum temperatures (relative to the simulated 1961-90 climate) for four emissions scenarios (Low - left column, High – right column), for thirty-year periods centred on the 2020s, 2050s and 2080s (rows, top to bottom).

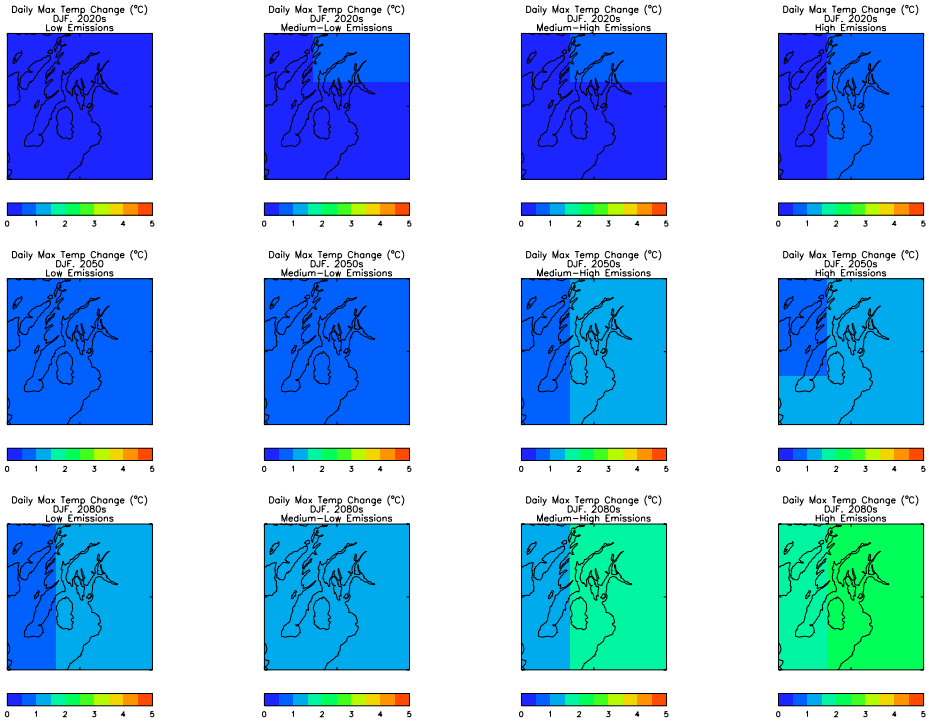

Figure A3.7. Predicted changes (˚C), in Hunterston winter (December - February) average maximum temperatures (relative to the simulated 1961-90 climate) for four emissions scenarios (Low - left column, High – right column), for thirty-year periods centred on the 2020s, 2050s and 2080s (rows, top to bottom).

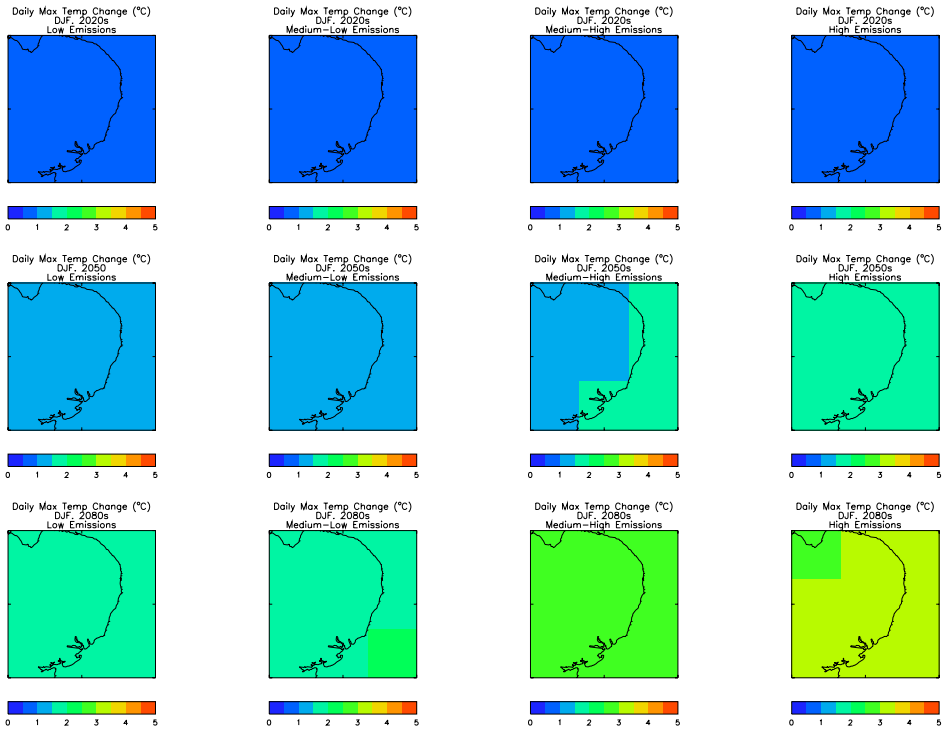

Figure A3.8. Predicted changes (˚C), in Sizewell winter (December - February) average maximum temperatures (relative to the simulated 1961-90 climate) for four emissions scenarios (Low - left column, High – right column), for thirty-year periods centred on the 2020s, 2050s and 2080s (rows, top to bottom).

Appendix 4: Probabilities of winter and summer daily minimum temperatures falling below given thresholds.

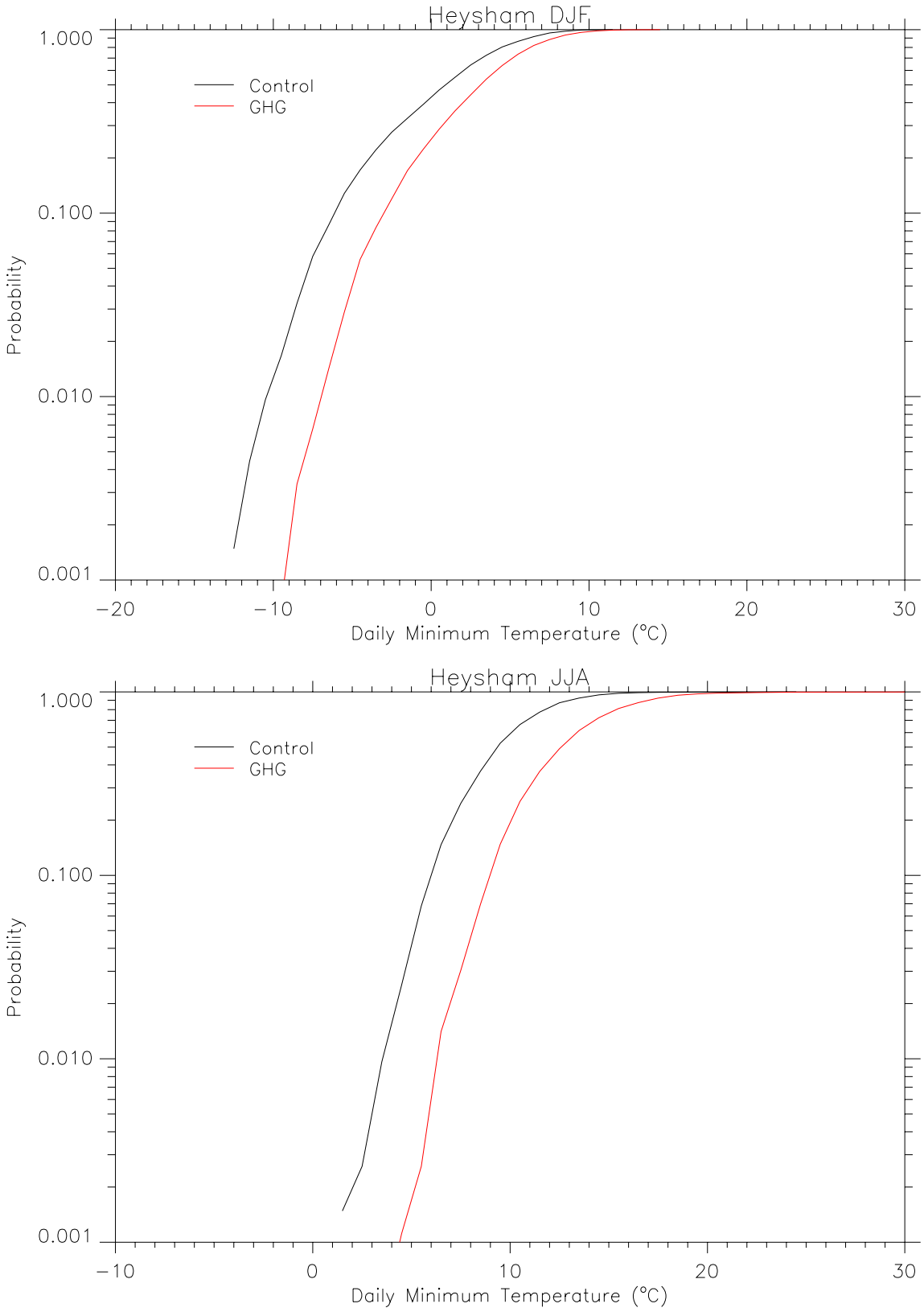

Figure A4.1 Probability of daily minimum temperature falling below given thresholds for Heysham. Modelled current climate (black) and Medium High scenario 2080s climate (red) for winter (December – February, upper panel) and summer (June – August, lower panel)

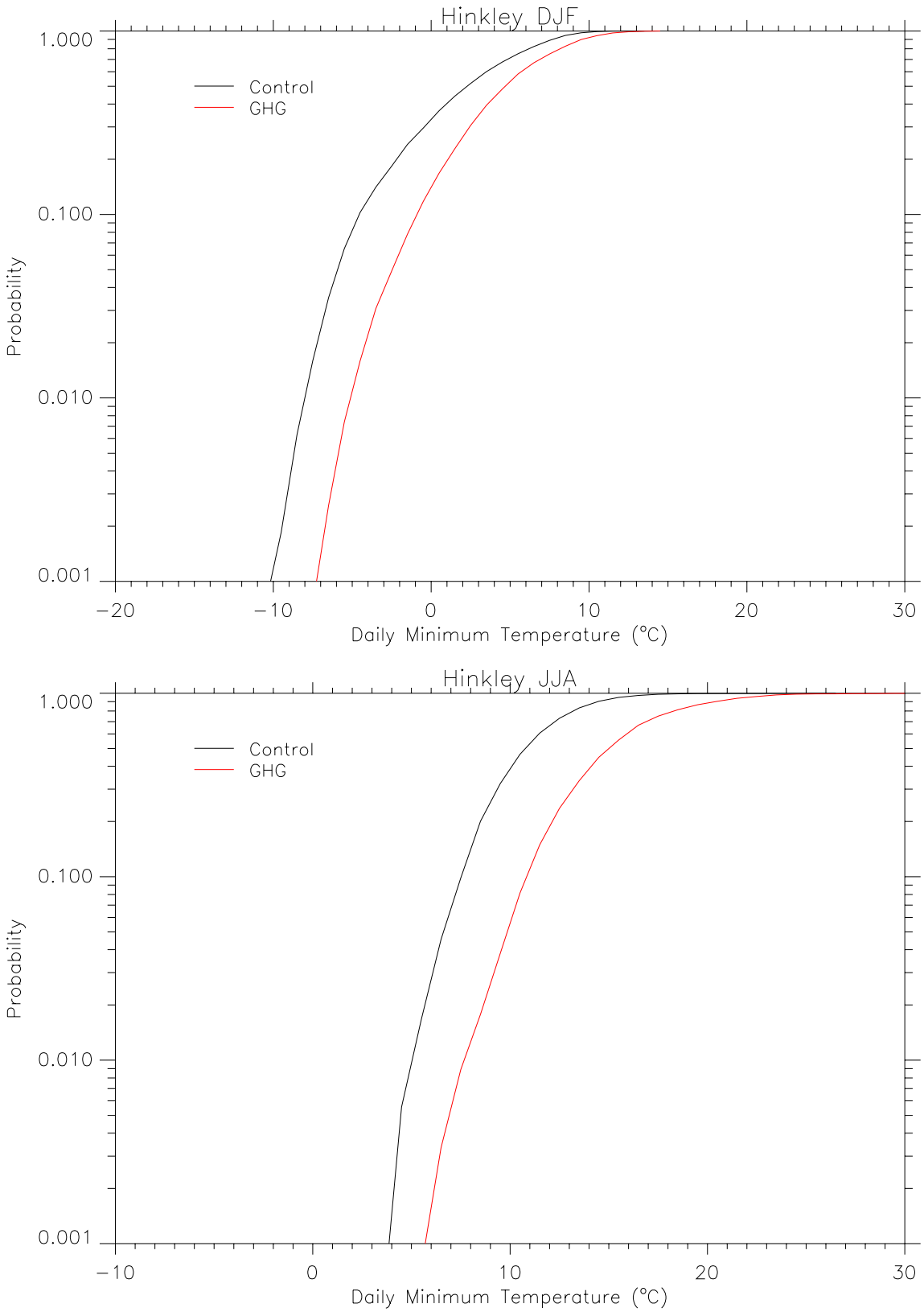

Figure A4.2 Probability of daily minimum temperature falling below given thresholds for Hinkley Point. Modelled current climate (black) and Medium High scenario 2080s climate (red) for winter (December – February, upper panel) and summer (June – August, lower panel)

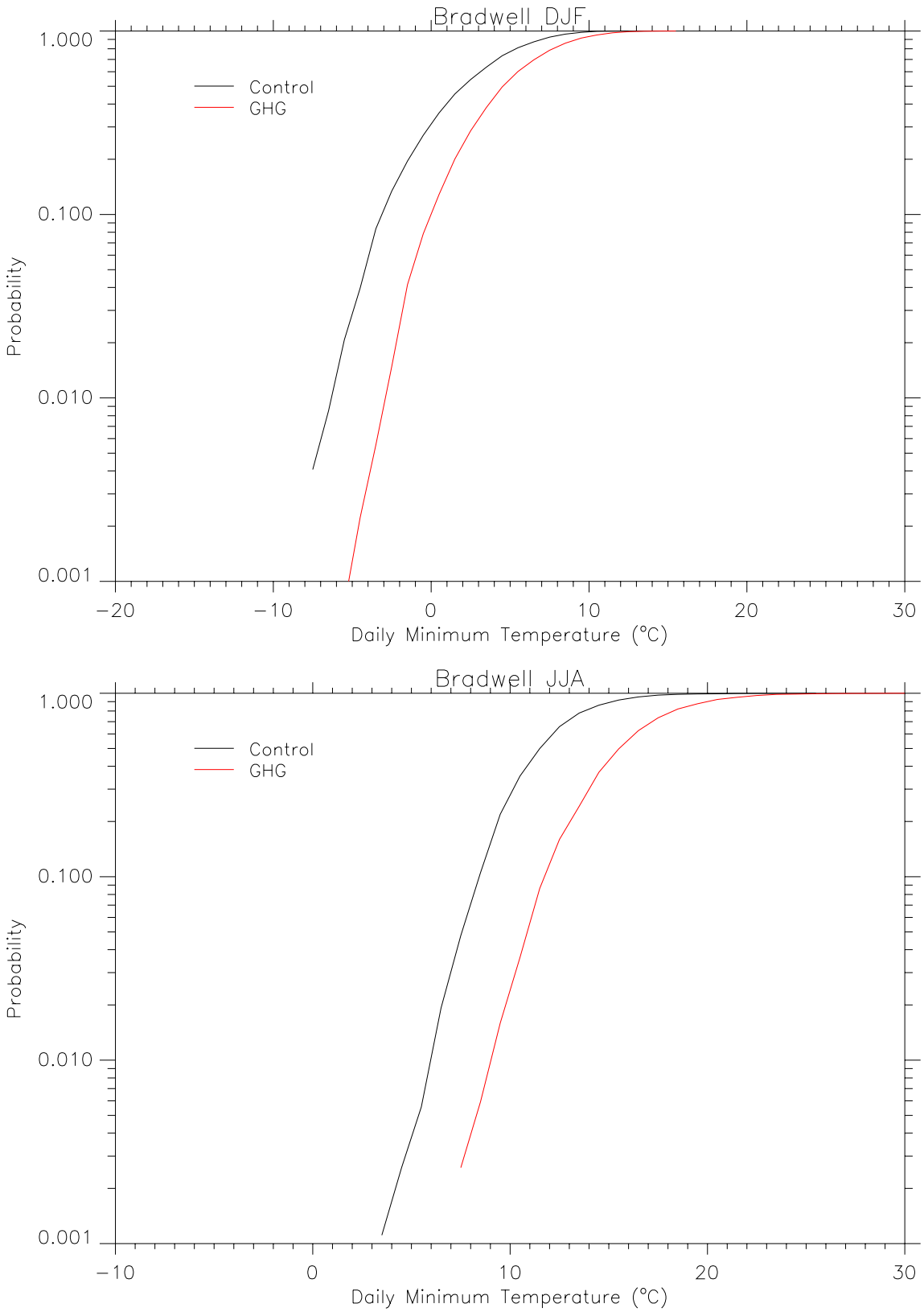

Figure A4.3 Probability of daily minimum temperature falling below given thresholds for Bradwell. Modelled current climate (black) and Medium High scenario 2080s climate (red) for winter (December – February, upper panel) and summer (June – August, lower panel)

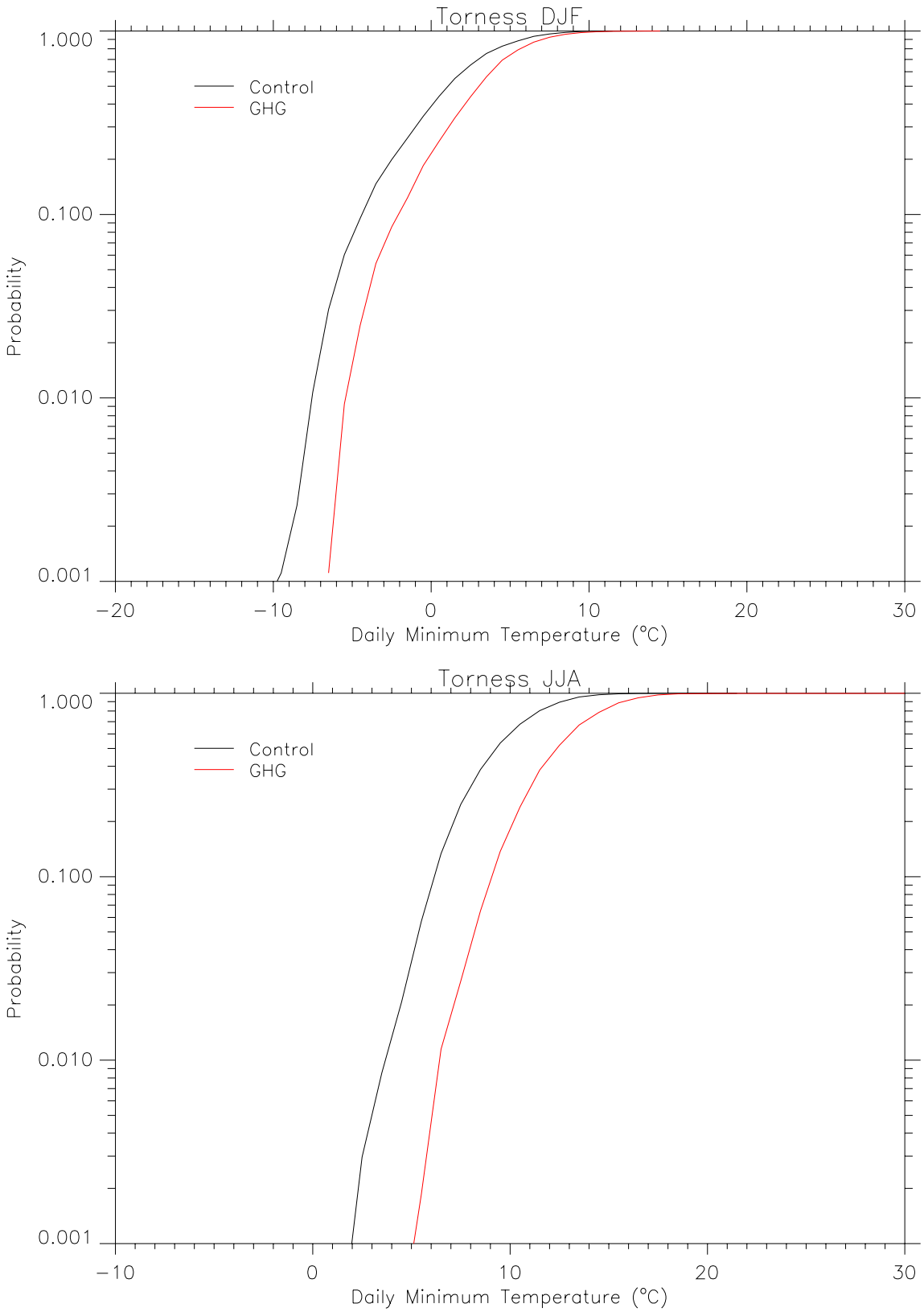

Figure A4.4 Probability of daily minimum temperature falling below given thresholds for Torness. Modelled current climate (black) and Medium High scenario 2080s climate (red) for winter (December – February, upper panel) and summer (June – August, lower panel)

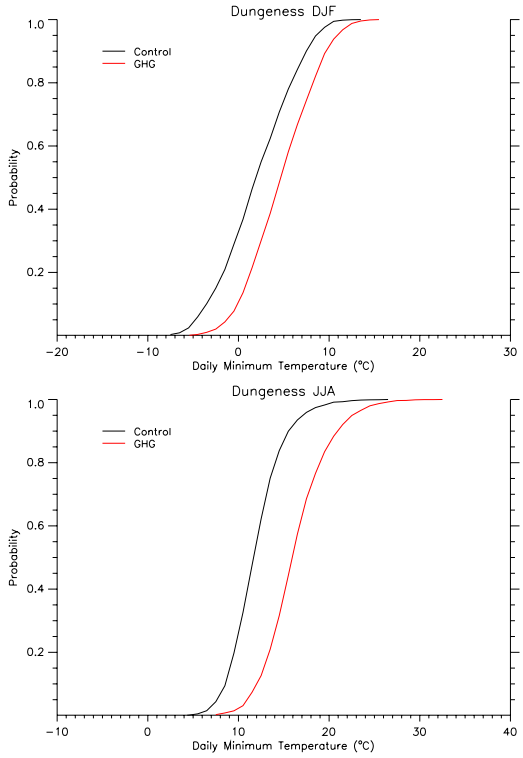

Figure A4.5 Probability of daily minimum temperature falling below given thresholds for Dungeness. Modelled current climate (black) and Medium High scenario 2080s climate (red) for winter (December – February, upper panel) and summer (June – August, lower panel)

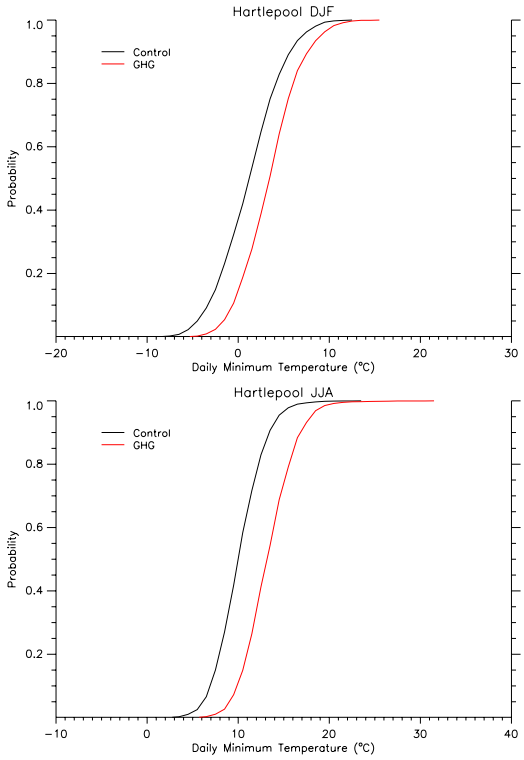

Figure A4.6 Probability of daily minimum temperature falling below given thresholds for Hartlepool. Modelled current climate (black) and Medium High scenario 2080s climate (red) for winter (December – February, upper panel) and summer (June – August, lower panel)

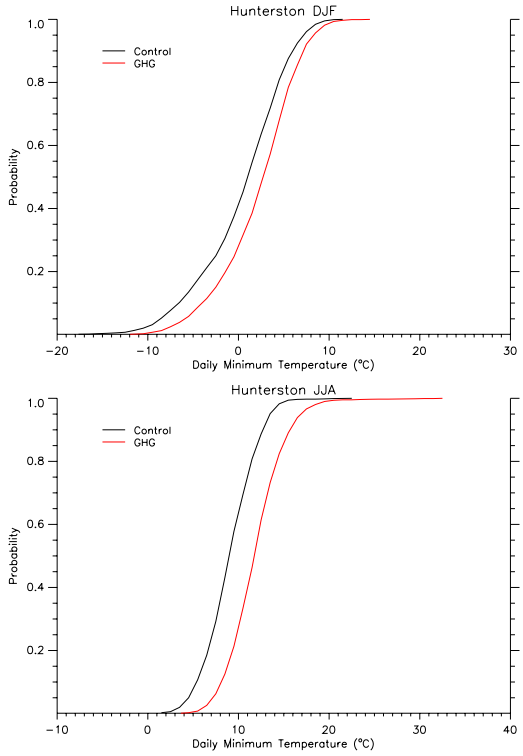

Figure A4.7 Probability of daily minimum temperature falling below given thresholds for Hunterston. Modelled current climate (black) and Medium High scenario 2080s climate (red) for winter (December – February, upper panel) and summer (June – August, lower panel)

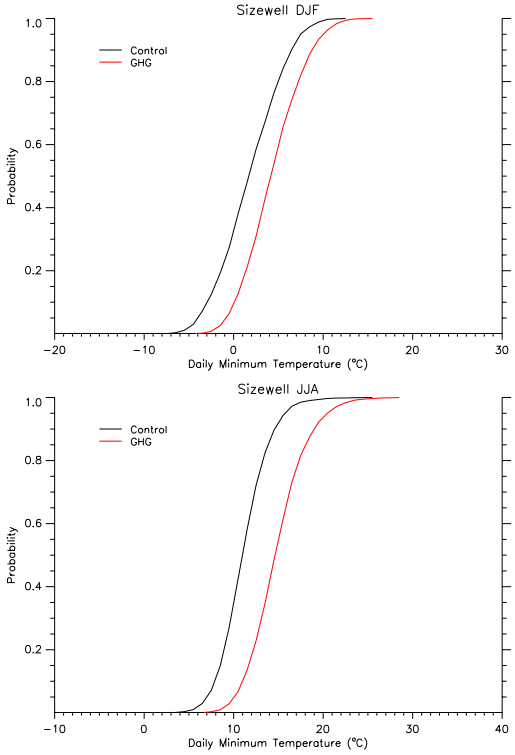

Figure A4.8 Probability of daily minimum temperature falling below given thresholds for Sizewell. Modelled current climate (black) and Medium High scenario 2080s climate (red) for winter (December – February, upper panel) and summer (June – August, lower panel)